P-158

ANNUAL REPORT

IN-32903

for

NASA GRANT NAG 5-501

entitled

SIMULTANEOUS SOLAR MAXIMUM MISSION (SMM) AND VERY LARGE ARRAY OBSERVATIONS OF SOLAR ACTIVE REGIONS

A NASA SMM GUEST INVESTIGATOR GRANT

for the period

1 September 1985 to 30 October 1986

(NASA-CR-177187) SIMULTANEOUS SOLAR MAXIMUM MISSION (SMM) AND VERY LARGE ARRAY OBSERVATIONS OF SOLAR ACTIVE REGIONS Annual Report, 1 Sep. 1985 - 30 Oct. 1986 (Tufts Univ.) 158 p CSCL 03B G3/92

N87-12522

Unclas 44710

Date of Submission: 30 October 1986

Kenneth R. Lang
Principal Investigator
NASA Grant NAG 5-501
Associate Professor of Astronomy
Department of Physics and Astronomy
Robinson Hall
Tufts University
Medford, MA 02155

TABLE OF CONTENTS

I. INTRODUCTION

This is an annual report for the SMM Guest Investigator Program entitled "Simultaneous Solar Maximum Mission and Very Large Array Observations of Solar Active Regions" during the period from 1 September 1985 to 30 August 1986. This program was allocated $28,245 from NASA Grant NAG 5-501 for the period 1 April 1986 to 31 March 1987. This allocation was a continuation of previous funding under NASA Grant NAG 5-501 from 1 February 1985 to 31 March 1986.

An account of the research done during the first half year of our SMM Guest Investigator Program may be found in the Semi-Annual Report mailed 23 August 1985. Additional details may be found in the Science review article by Mukul R. Kundu and Kenneth R. Lang entitled "The Sun and Nearby Stars: Microwave Observations at High Resolution" [Science 228, 9-15 (1985)].

Here we will present a progress report on the work done between 1 September 1985 and 30 August 1986. During that period we published three papers that are reproduced in Section II. We also wrote five papers that have been accepted for publication; these are reproduced in Section III.

Our research deals mainly with VLA and SMM observations of the ubiquitous coronal loops that dominate the structure of the low corona. As illustrated in Sections II and III, the observations of thermal cyclotron lines at microwave wavelengths provide a powerful new method of accurately specifying the coronal magnetic field strength. We also delineate processes that trigger solar eruptions from coronal loops, including preburst heating and the magnetic interaction of coronal loops. Evidence for coherent burst mechanisms is provided for both the Sun and nearby stars, while other observations suggest the presence of currents that may amplify the coronal magnetic field to unexpectedly high levels. Here we also report the existence of a new class of compact, variable moving sources in regions of apparently-weak photospheric field.

Section IV describes three papers in progress. Two of these papers involve ongoing comparisons of simultaneous SMM-XRP and VLA-20 cm emission from solar active regions. In some cases the soft X-ray and 20 cm data describe the same plasma; the soft X-ray spectral lines are used to determine the electron density and electron temperature while the 20 cm thermal cyclotron line specifies the magnetic field strength. There are other instances when there is intense 20 cm emission without detectable X-ray radiation. In this event, the 20 cm emission is attributed to gyroresonance radiation of thermal electrons, and the magnetic field strength is also specified. In other cases, the 20 cm emission is more extensive than the X-ray radiation, and the microwave brightness temperature is slightly less than the electron temperature inferred from the X-ray data. Yet, the coronal loop plasma ought to be optically thick at 20 cm wavelength. This paradox is explained by a cool plasma that envelops the hotter one detected at X-ray wavelengths.

The last paper in Section IV describes the first VLA observations of the Sun at the longer 92 cm wavelength. A highly-polarized (90%) noise storm was resolved, and its outward velocity inferred from the time and angular displacements of the X-ray and 92 cm bursts.

In Section V we mention lectures given by the Principal Investigator at professional meetings. These include the NASA workshop on Coronal and Prominence Plasmas, the European Workshop on Radio Continua During Solar Flares, and Symposium 5 on Synopsis of the Solar Maximum Analysis, a part of the XXVI meeting of the Committee on Space Research (COSPAR).

Our final Section VI discusses funding and future prospects. Here we mention our plans to submit a proposal for the next round of the SMM Guest Investigator Program. This proposal will include the analysis of existing simultaneous observations with the SMM-XRP and the VLA-20 cm, while also including future simultaneous observations of the low corona at 20 cm, 92 cm and soft X-ray wavelengths.

FLARE STARS AND SOLAR BURSTS: HIGH RESOLUTION IN TIME AND FREQUENCY*

KENNETH R. LANG

Department of Physics and Astronomy, Tufts University, Medford, MA 02155, U.S.A.

Abstract. Coronal loops on the Sun and nearby stars are investigated using observations at 20 cm wavelength with high resolution in time and frequency. Observations of the dwarf M star AD Leonis with high time resolution using the Arecibo Observatory have resulted in the discovery of a quasi-periodic train of circularly polarized spikes with a mean periodicity of 32 ± 5 ms and a total duration of 150 ms. The individual spikes had rise times of ≤ 5 ms, leading to an upper limit to the linear size $L \leq 1.5 \times 10^8$ cm for the spike emitter. This size is only 0.005 of the estimated radius of AD Leonis. Provided that the emitter is symmetric, it has a brightness temperature of $T_B \geq 10^{16}$ K, suggesting a coherent burst mechanism such as an electron–cyclotron maser. Coronal oscillations might modulate the maser output, producing the quasi-periodic spikes. Observations at closely spaced wavelengths, or high frequency resolution, using the Very Large Array have revealed narrow-band structure ($\Delta\nu/\nu \leq 0.01$) in solar bursts and in the slowly-varying radiation of the dwarf M star YZ Canis Minoris. The narrow-band emission cannot be explained by continuum emission processes, but it might be attributed to electron–cyclotron maser radiation. Maser action at the second or first harmonic of the gyrofrequency implies magnetic field strengths of 250 and 500 G, respectively. Thus, observations with high resolution in time and frequency suggest coherent processes in the coronae of the Sun and dwarf M stars. The scientific potential of these discoveries may be best fulfilled by the construction of a solar-stellar synthesis radiotelescope.

1. Introduction

Very Large Array (VLA) observations at widely spaced wavelengths refer to different levels within the ubiquitous coronal loops that are the dominant structural element of solar active regions. The slowly-varying 6 cm emission often originates in the legs of coronal loops, while the slowly-varying 20 cm emission comes from the hot dense plasma trapped within the legs and apex of coronal loops (Lang *et al.*, 1982; Lang and Willson, 1983, 1984; Lang *et al.*, 1983; McConnell and Kundu, 1983; Kundu and Lang, 1985). VLA snapshot maps indicate that the impulsive component of microwave bursts is usually located near the apex of coronal loops (Marsh and Hurford, 1981; Lang and Willson, 1983, 1984; Willson and Lang, 1984; Kundu and Lang, 1985). These bursts may be triggered by temperature enhancements within coronal loops or by changes in the configuration of coronal magnetic fields.

The solar analogy suggests that coronal loops may also play a dominant role in the microwave emission from dwarf M flare stars. These stars exhibit slowly-varying microwave radiation that may be similar to the quiescent, or nonflaring, slowly-varying radiation of solar active regions. These stars also exhibit microwave bursts that are similar to those emitted by the Sun (Linsky and Gary, 1983; Pallavicini *et al.*, 1985).

Recent investigations have revealed two new approaches to the study of coronal loops on the Sun and nearby stars. They involve observations at 20 cm wavelength with high

* Proceedings of the Workshop on Radio Continua during Solar flares, held at Duino (Trieste), Italy, 27–31 May, 1985.

Solar Physics **104** (1986) 227–233.
© 1986 *by D. Reidel Publishing Company*

resolution in time and frequency. Observations with high time resolution using the Arecibo Observatory have led to the discovery of quasi-periodic spiked emission from the dwarf M star AD Leonis (Section 2). Observations at closely spaced wavelengths, or high frequency resolution, reveal narrow-band structure during solar bursts and in the slowly-varying radiation of the dwarf M star YZ Canis Minoris (Section 3). This paper highlights these recent results that seem to require coherent radiation mechanisms. It also draws attention to their possible implications for a solar-stellar synthesis radiotelescope.

2. Quasi-Periodic Spikes from AD Leonis

If the solar analogy is applicable, slowly-varying emission and stellar bursts from nearby stars ought to be emitted from coronal loops that are a fraction of a stellar radius in linear extent. Thermal bremsstrahlung from coronal loops on nearby stars would, however, be too weak to be detected, and thermal gyroresonant radiation would require impossibly large coronal loops for this radiation to be detected at 20 cm wavelength.

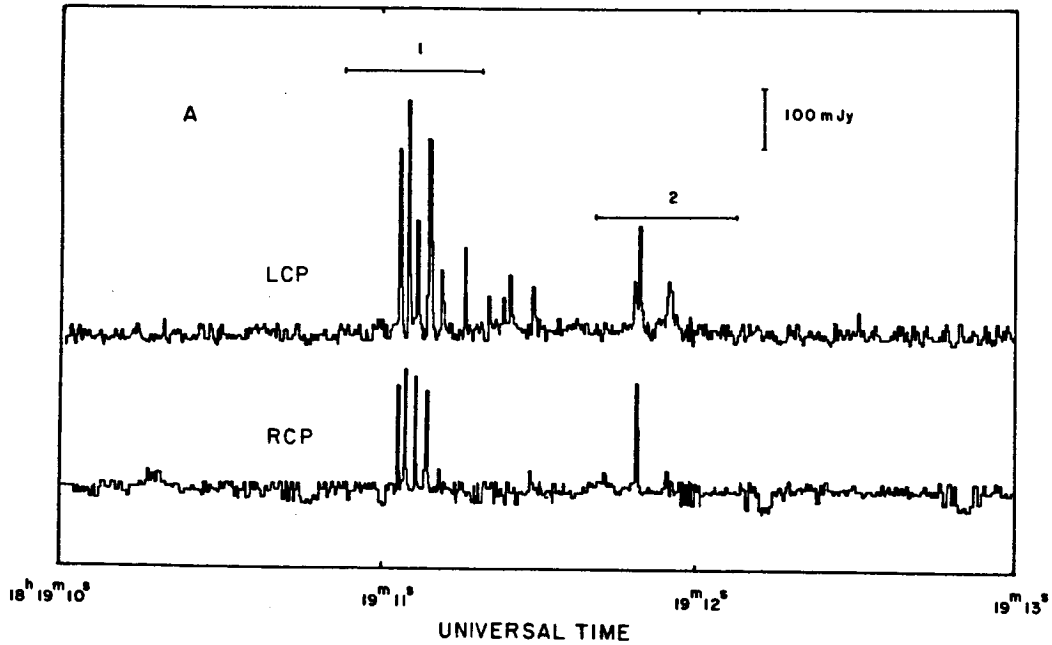

Fig. 1. The total power detected at a frequency of 1415 MHz (21.2 cm) while tracking the dwarf M star AD Leonis. Both the left-hand circularly polarized (LCP-top) and the right-hand circularly polarized (RCP-bottom) signals are shown. Here the integration time is 5 ms. The data exhibit a train of five quasi-periodic spikes with a mean periodicity of $\tau_P = 32 \pm 5$ ms, a total duration of $\tau_D = 150$ ms (horizontal bar 1), and circular polarizations of about 33%. The data also include individual spikes that are 100% left-hand circularly polarized. Each of the spikes had a rise time of $\tau_R \leq 5$ ms, leading to an upper limit to the linear size $L \leq 1.5 \times 10^8$ cm and a brightness temperature of $T_B \geq 10^{16}$ K if the spike emitter is symmetric.

Non-thermal and/or coherent emission processes are required if the slowly-varying or burst emission originates from stellar loops or star spots that are similar in size to their counterparts on the Sun.

As illustrated in Figure 1, observations of AD Leonis at 1415 MHz (21.2 cm) indicate a train of quasi-periodic spikes that suggest a coherent burst emitter that is modulated by coronal oscillations. The quasi-periodic spikes have a mean periodicity of 32 ± 5 ms and a total duration of 150 ms. They have a maximum flux density of 300 mJy and circular polarizations of about 33%. Each of the spikes have rise times of ≤ 5 ms, the integration time employed.

An upper limit to the linear size of the emitting region is $L \leq 1.5 \times 10^8$ cm, the distance that light travels in 5 ms. This is only 0.005 of the estimated radius of AD Leonis ($R = 3.0 \times 10^{10}$ cm). Provided that the spike emitter is symmetric, it has an area that is less than 2.5×10^{-5} of the surface area of the star's visible disk. The maximum flux density and linear size can be combined with the star's distance (4.85 pc) to infer a brightness temperature of $T_B \geq 10^{16}$ K from the Rayleigh–Jeans expression.

The high circular polarization of the spikes indicates an intimate connection with strong stellar magnetic fields, whereas the high brightness temperatures suggest a coherent emission mechanism. Similar highly circularly polarized spikes with high brightness temperatures ($T_B \geq 10^{12}$ K) have been observed during solar bursts (Dröge, 1977; Slottje, 1978). The spikes emitted from both the Sun and AD Leonis may be explained by electron–cyclotron maser emission (Melrose and Dulk, 1982). Magnetic field strengths of $H = 250$ and 500 G are inferred if the radiation is at the second or first harmonic of the gyrofrequency, respectively.

But what accounts for the quasi-periodic spikes? Some process must modulate the coherent burst emitter in a quasi-periodic manner. One possibility is coronal oscillations that provide a currently-popular explanation for longer (50 ms to 5 s) quasi-periodic pulsations during some solar bursts (Roberts *et al.*, 1984). An inhomogeneity of size $a = 2 \times 10^7$ cm might account for the quasi-periodic spikes with an Alfvén velocity corresponding to $H = 250$ G and plausible values of density.

3. Narrow-Band Structure in Solar Bursts and in the Slowly-Varying Radiation from YZ Canis Minoris

Recent VLA observations at closely spaced wavelengths near 20 cm have provided evidence for coherent emission processes during solar bursts (Lang and Willson, 1984). One highly circularly polarized (100%) burst exhibited a factor of two difference in brightness temperature (1.5×10^8 K and 0.8×10^8 K) at two wavelengths separated by only 32 MHz (burst 7 of Figure 2 at 1658 and 1690 MHz). The high circular polarization and narrow bandwidth ($\Delta\nu/\nu \leq 0.01$) of this burst are comparable to those expected from electron–cyclotron masers. Although the burst source was apparently resolved, the 10 s integration time of the VLA may have integrated several briefer, spatially-separated coherent spikes.

Narrow-band, slowly-varying microwave radiation has been detected from the dwarf

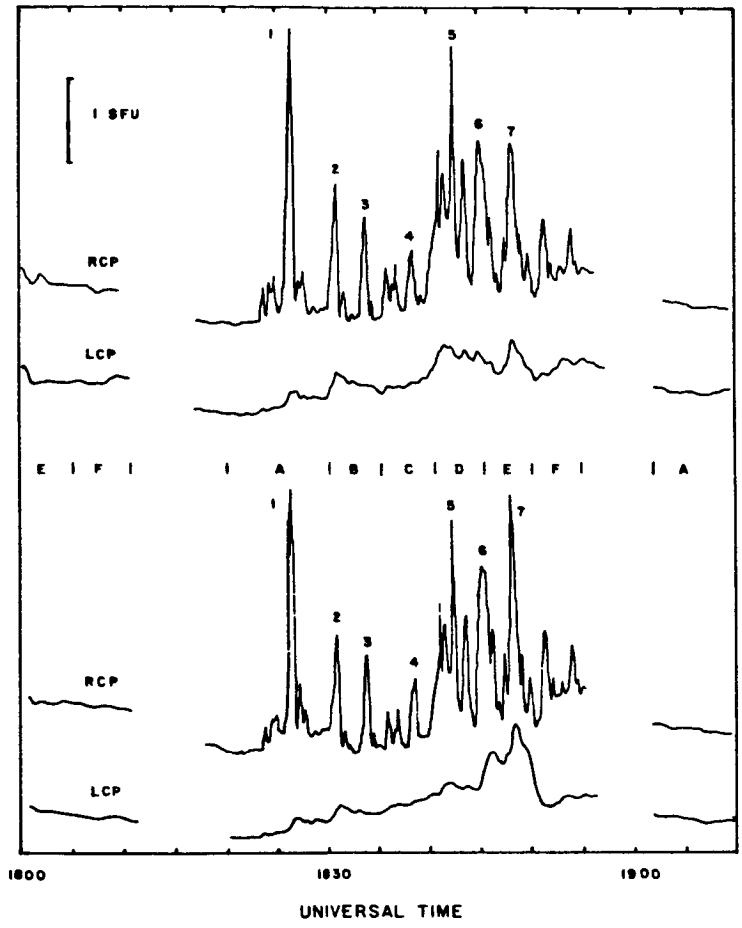

Fig. 2. A sequence of right circularly polarized (RCP) impulsive bursts from a solar active region observed at wavelengths near 20 cm (1400 MHz). The top and bottom profiles are separated by only 30 MHz; burst 7 has a factor of two difference in brightness temperature over this narrow frequency interval, suggesting coherent burst emission. This figure originally appeared in Lang and Willson (1984).

M star YZ Canis Minoris at frequencies near 1465 MHz. Slow variations over time-scales of an hour and as much as 20 mJy in strength peak at different times for frequencies ν = 1415 and 1515 MHz (Figures 3 and 4), indicating narrow-band structure of bandwidth $\Delta\nu \leq 100$ MHz, or $\Delta\nu/\nu \leq 0.1$. Cyclotron line structure from gyroresonant radiation can be ruled out because the high flux density and large observing frequency would require coronal loops that are more than one hundred times larger than the star.

We might speculate that the slowly-varying radiation from YZ Canis Minoris is due to continuous low-level, coherent burst activity. High circular polarization would be expected to be occasionally observed if the coherent mechanism is associated with

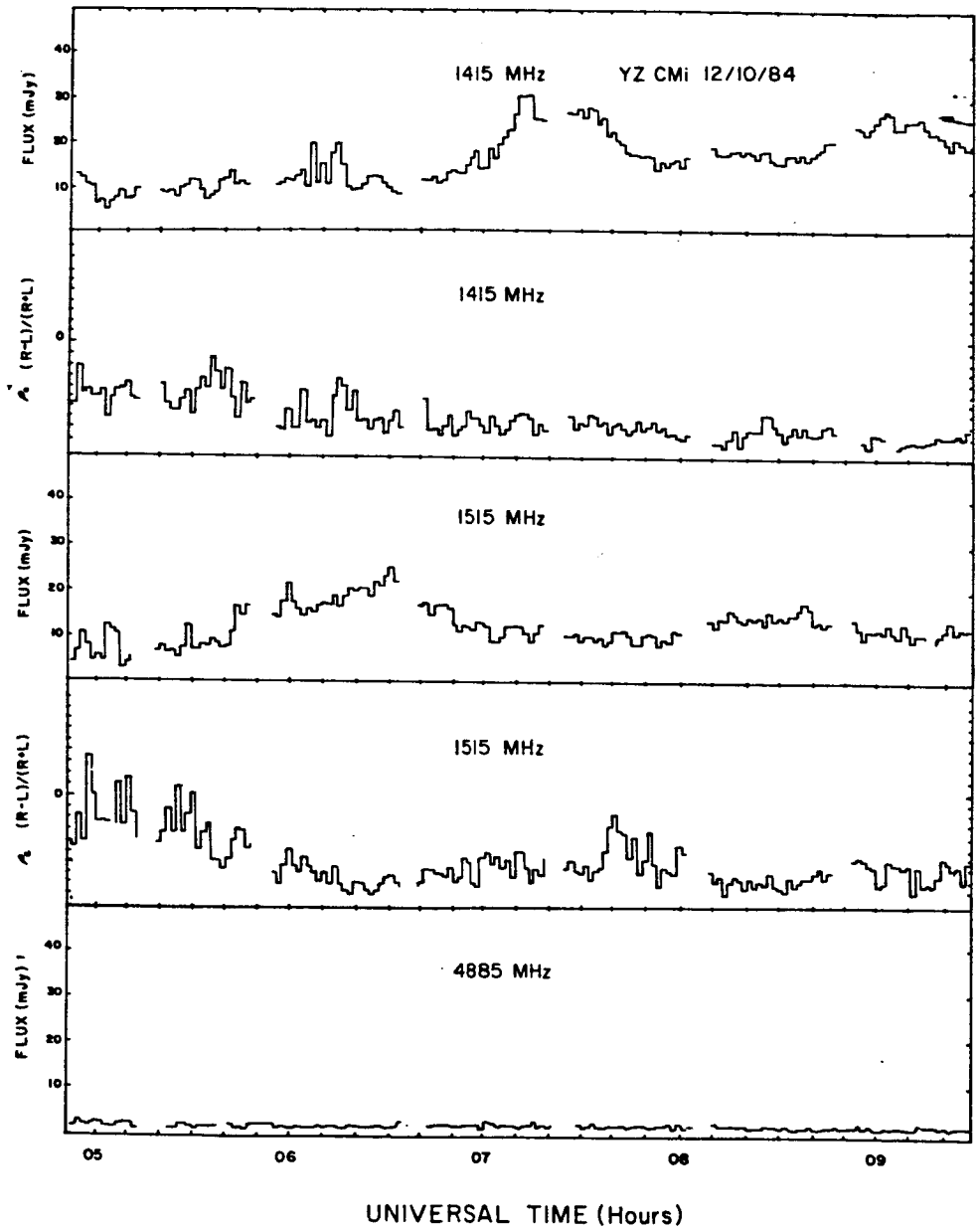

Fig. 3. Slowly-varying emission from the dwarf M flare star YZ Canis Minoris at two closely spaced frequencies of 1415 and 1515 MHz and at 4885 MHz. The emission at the two frequencies peaks at different times, suggesting a coherent emission mechanism with a bandwidth of less than 100 MHz. There are no detectable fluctuations at 4885 MHz.

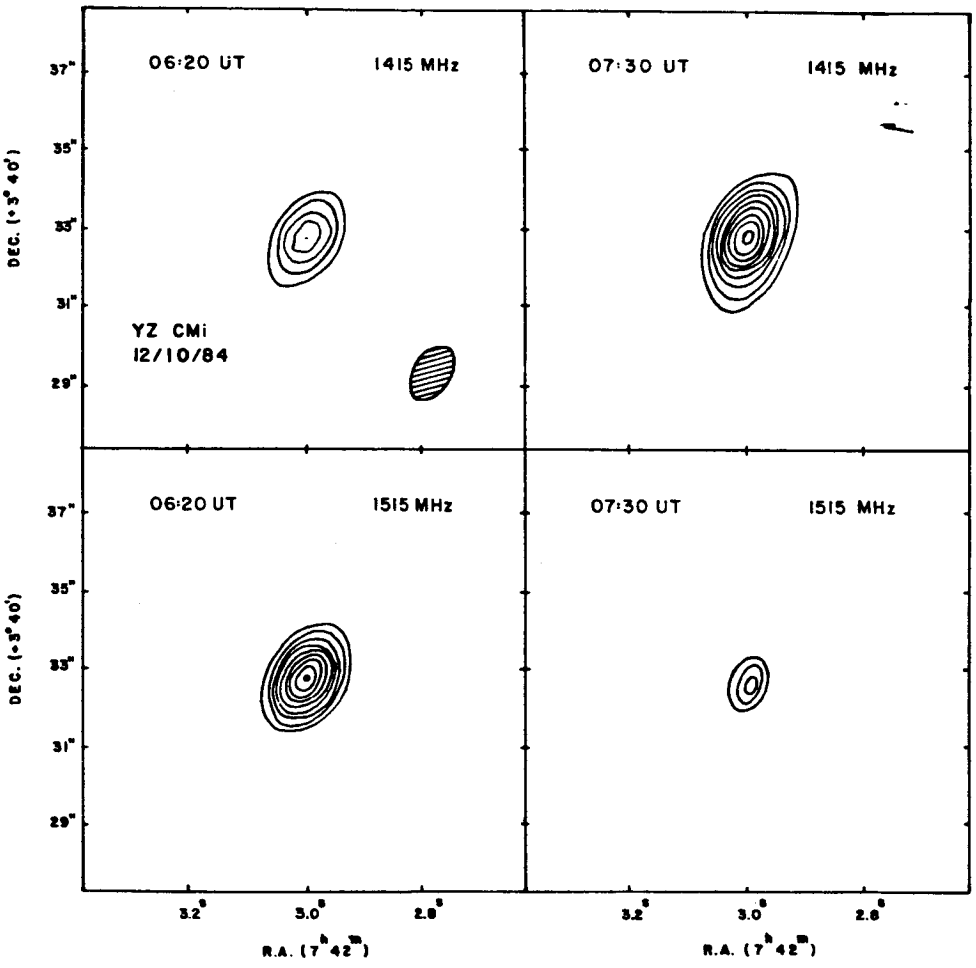

Fig. 4. VLA snapshot maps of the emission from the dwarf M flare star YZ Canis Minoris. The unresolved emission peaks at different times at two frequencies separated by only 100 MHz, suggesting a coherent burst mechanism. The contours are at intervals of 6, 8, 10, 12,... Jy/beam area, with maximum values of 14 and 22 Jy/beam area at 06 : 20 UT and 1415 and 1515 MHz, respectively, and 25 and 10 Jy/beam area at 07 : 30 UT for the same respective frequencies.

intense magnetic fields, and the stochastic nature of continued bursts might explain the variability of the observed microwave radiation.

4. Conclusions

Observations at 20 cm wavelength with high resolution in time and frequency have provided evidence for coherent emission mechanisms on the Sun and nearby stars. However, observations are limited by infrequent use of the Arecibo Observatory and the Very Large Array for solar and stellar observations. The scientific potential suggested

by the data presented here can only be fully realized by the development of a solar-stellar synthesis radiotelescope. Such an instrument would be dedicated to solar and stellar observations with high angular, temporal and frequency resolution.

Acknowledgements

Radio astronomical studies of the Sun at Tufts University are supported under Air Force Office of Scientific Research grant AFOSR–83–0019 and contract N0014-86-K-0068 with the Office of Naval Research. Investigations of flare stars at Tufts University are also supported by NASA grant NAG 5–477, and our simultaneous VLA and Solar Maximum Mission observations of the Sun are supported by NASA grant NAG 5–501.

References

Drōge, F.: 1977, *Astron. Astrophys.* **57**, 285.
Kundu, M. R. and Lang, K. R.: 1985, *Science* **228**, 9.
Lang, K. R. and Willson, R. F.: 1983, *Adv. Space Res.* **2**, 91.
Lang, K. R. and Willson, R. F.: 1984, *Adv. Space Res.* **4**, 105.
Lang, K. R., Willson, R. F., and Gaizauskas, V.: 1983, *Astrophys. J.* **267**, 455.
Lang, K. R., Willson, R. F., and Rayrole, J.: 1982, *Astrophys. J.* **258**, 384.
Linsky, J. L. and Gary, D. E.: 1982, *Astrophys. J.* **274**, 776.
Marsh, K. A. and Hurford, G. J.: 1980, *Astrophys. J.* **240**, L111.
McConnell, D. and Kundu, M. R.: 1983, *Astrophys. J.* **269**, 698.
Melrose, D. B. and Dulk, G.: 1982, *Astrophys. J.* **259**, 844.
Pallavicini, R., Willson, R. F., and Lang, K. R.: 1985, *Astron. Astrophys.* **149**, 95.
Roberts, B., Edwin, P. M., and Benz, A. O.: 1984, *Astrophys. J.* **279**, 857.
Slottje, C.: 1978, *Nature* **275**, 520.
Willson, R. F. and Lang, K. R.: 1984, *Astrophys. J.* **279**, 427.

THE ASTROPHYSICAL JOURNAL, 298:911–917, 1985 November 15
© 1985. The American Astronomical Society. All rights reserved. Printed in U.S.A.

VLA OBSERVATIONS OF SOLAR ACTIVE REGIONS AT CLOSELY SPACED FREQUENCIES: EVIDENCE FOR THERMAL CYCLOTRON LINE EMISSION

ROBERT F. WILLSON
Department of Physics, Tufts University
Received 1984 August 10; accepted 1985 May 20

ABSTRACT

VLA observations of a solar active region at 10 closely spaced frequencies between 1440 and 1720 MHz are presented. The synthesis maps show, on two successive days, significant changes in the brightness temperature within this narrow frequency range. We show that these changes cannot be due to either thermal bremsstrahlung or gyroresonance emission from a coronal loop in which the temperature, density, or magnetic field varies monotonically with height. Instead, we attribute the brightness spectrum to cyclotron line emission from a narrow layer where the temperature is elevated above the surrounding part of the loop.

Subject headings: interferometry — radiation mechanisms — Sun: radio radiation

I. INTRODUCTION

Very Large Array (VLA)[1] observations of solar active regions near 20 cm wavelength delineate looplike structures that appear to connect lower lying areas of opposite magnetic polarity (Lang, Willson, and Rayrole 1982; Dulk and Gary 1983; Lang, Willson, and Gaizauskas 1983; McConnell and Kundu 1983). These sources have peak brightness temperatures of between 1.5×10^6 and 4.0×10^6 K, suggesting that they are the radio wavelength counterparts of coronal loops seen at soft X-ray wavelengths.

The radiation mechanism responsible for this emission is, however, the subject of some controversy. Lang, Willson, and Rayrole (1983) and Dulk and Gary (1983) have, for example, attributed 20 cm emission to optically thick thermal bremsstrahlung of a hot plasma trapped within magnetic arches connecting underlying sunspots. There is no detectable polarization near the magnetic neutral lines, and this has been attributed to optically thick emission or to magnetic fields that are transverse to the line of sight. A few 20 cm loops exhibit small circular polarization ($\rho_c \leq 20\%$) near their legs, and this has been attributed ot the effects of bremsstrahlung propagating in longitudinal magnetic fields of strength $H_l \approx 20$–70 G (Dulk and Gary 1983).

Other VLA observations suggest that low-harmonic gyroresonance absorption may provide the bulk of the opacity in 20 cm loops. McConnell and Kundu (1983) have, for example, found that the brightness of one loop could be best explained by gyroemission near the loop top and thermal bremsstrahlung near the feet. Velusamy and Kundu (1981) also compared radio and X-ray observations of systems of postflare loops, and found that gyroresonance emission was the most likely mechanism in these sources.

Both competing processes of bremsstrahlung and gyroresonance emission predict a smoothly varying continuum spectrum that decreases slowly with increasing frequency. The theory of cyclotron absorption, for example, indicates that observations at a given frequency, ν, refer to a narrow layer in the solar atmosphere at which $\nu = s\nu_H$, where $s = 2, 3, 4$ is the harmonic number and ν_H is the gyrofrequency. If the magnetic field in a coronal loop decreases uniformly with height, then it was thought that the individual cyclotron lines would merge to form a smooth continuum. Theoretical work has shown however, that individual cyclotron lines might also be detected as narrow-band enhancements in the radio-frequency spectra of solar active regions if the radiation were emitted from relatively thin layers in the corona where the magnetic field is relatively constant (Syrovatskii and Kuznetsov 1980; Kuznetsov and Syrovatskii 1981). The presence of neutral current sheets, in which the temperature and density are higher than in the surrounding parts of the loop, might also lead to abrupt changes in the brightness temperature over a small frequency range (Syrovatskii 1977; Syrovatskii and Kuznetsov 1980). Recently, Willson (1983) mapped several active regions at three closely spaced frequencies near 1446 MHz and found that two of the sources showed striking changes in brightness within these narrow frequency ranges. These changes could not be explained by either thermal bremsstrahlung or gyroresonance emission from a loop in which the temperature, density, or magnetic field varied uniformly with height. They could, however, be explained by individual cyclotron lines emitted in small regions (10″–30″) where the magnetic field was relatively constant with $H \approx 125$–180 G.

Observations of cyclotron line emission are potentially important because they provide a means of specifying the physical conditions within coronal loops and current sheets. We have now tried to confirm the presence of cyclotron lines on the Sun by using the VLA to map an active region on two successive days at 10 different frequences between 1440 and 1720 MHz. In this paper we present these observations and compare them with theoretical spectra of cyclotron line emission from coronal loops.

II. OBSERVATIONS

The VLA (B-configuration) was used to observe the active region AR 4398 on 1984 January 28 and 29. The position of AR 4398 at 1300 UT on January 28 and 29 was 14°N 11°W and 14°N 24°W, respectively. The active region was observed at 10 different frequencies between 1440 MHz (21.8 cm) and 1720 MHz (17.4 cm) with bandwidths of 12.5 MHz during a 10 hr period between 1300 UT and 2300 UT on each day. At these frequencies the half-power beamwidth of the individual antennas ranges between 26.0 and 31.2 and the synthesized

[1] The VLA is a facility of the National Radio Astronomy Observatory, which is operated by Associated Universities, Inc., under contract with the National Science Foundation.

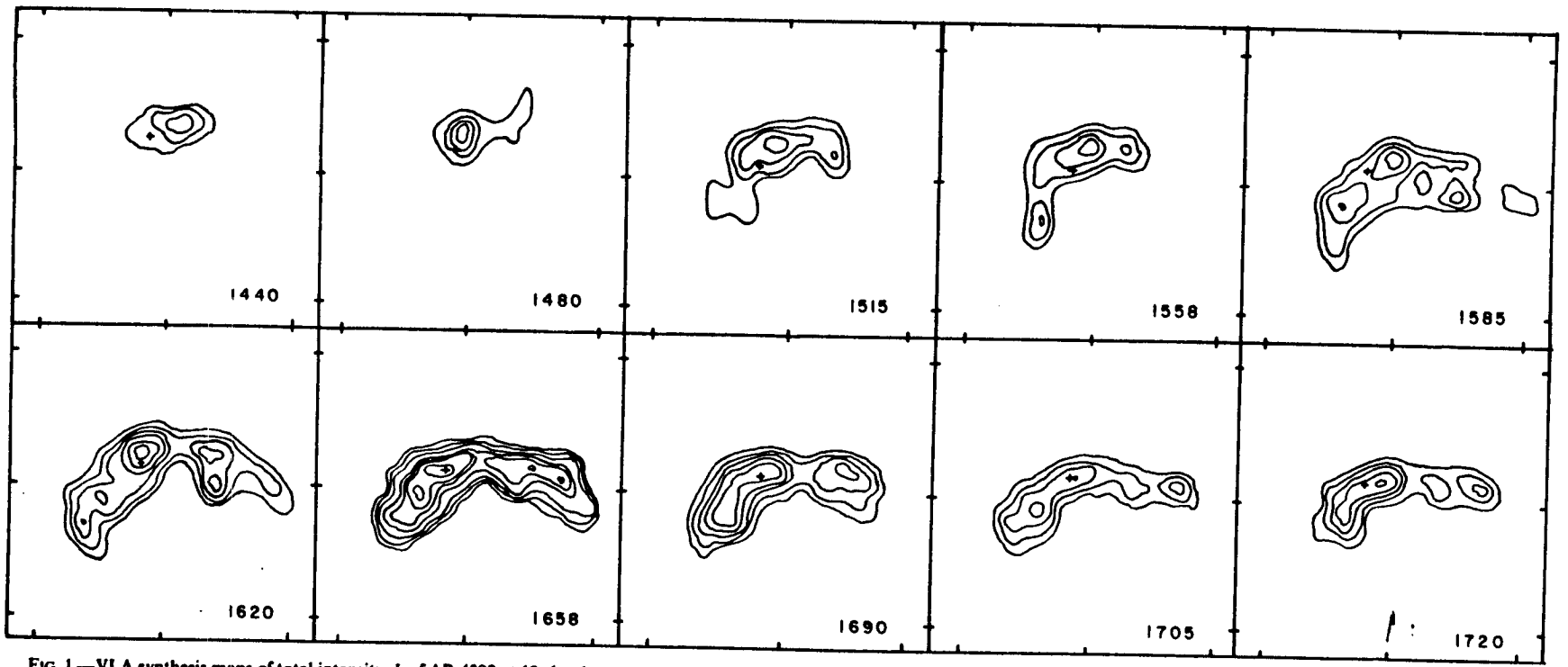

FIG. 1.—VLA synthesis maps of total intensity, I, of AR 4398 at 10 closely spaced frequencies during a 10 hr period on 1984 January 28. Synthesized beamwidth is $\theta \approx 3'' \times 4''$. Contours of the maps mark levels of equal brightness temperature. Outermost contour and contour interval are equal to 1.1×10^6 and 4.0×10^5 K, respectively. Angular scale can be determined from the 60" spacing between fiducial marks on the area.

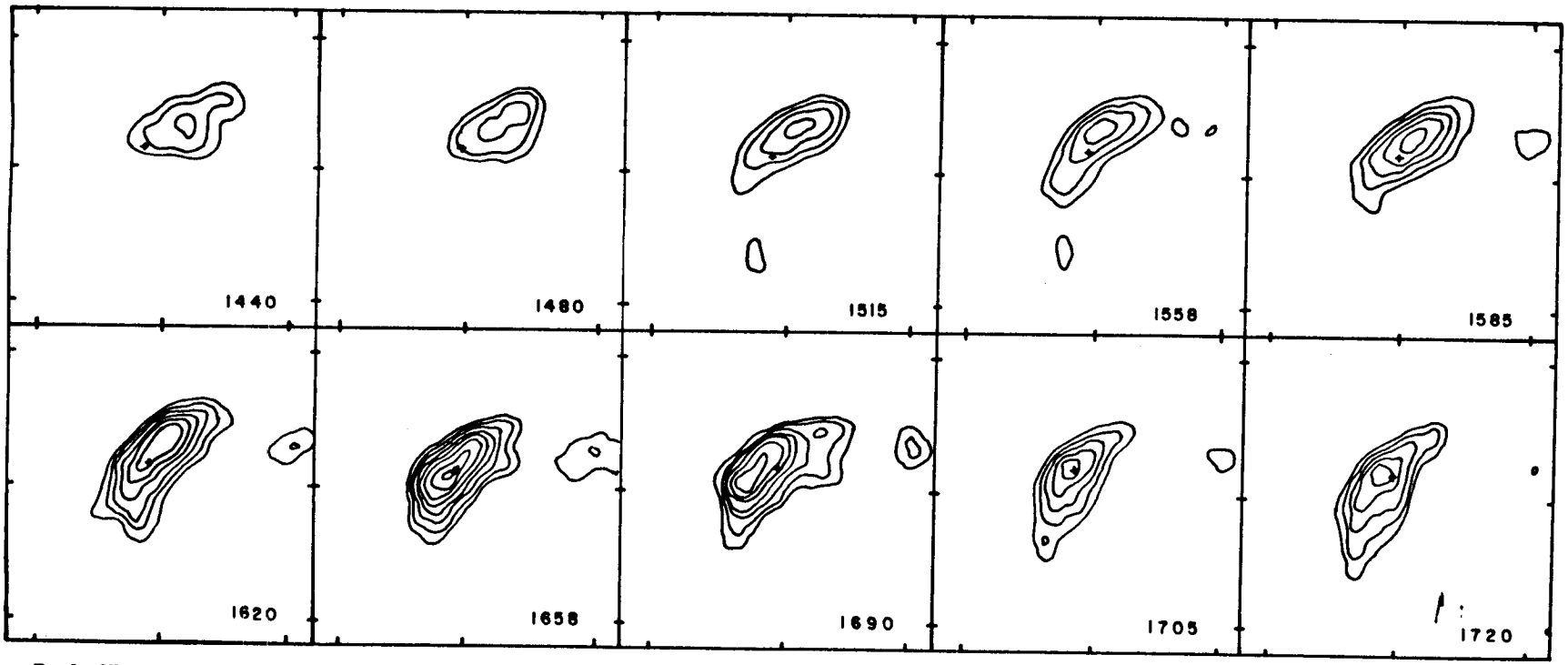

FIG. 2.—VLA synthesis maps of total intensity, I, of AR 4398 at 10 closely spaced frequencies using data obtained during a 10 hr interval on 1984 January 29. Contour levels and angular scale are same as in Fig. 1.

beamwidth varies between 3.'0 × 3.'5 and 3.'6 × 4.'2. The four independent intermediate frequency channels now available at the VLA made it possible to record the left and right circularly polarized signals of two different frequencies at once. The active region was observed at successive pairs of frequencies for a period of 5 minutes, so that all 10 frequencies could be observed in 25 minutes. This sequence of observations was followed by successive 2 minute observations of the calibrator source 3C 48. The data were calibrated using 3C 48 together with a correction for the difference in the signals from high-temperature noise sources located on four of the antennas. The temperatures of these sources were measured at each frequency and polarization prior to the solar observations and are believed to be accurate to $\lesssim 5\%$. The flux of 3C 48 at each frequency was determined from its flux of 15.37 Jy at 1465 MHz and its spectral index of $\alpha = -0.81$. Since some of the observations were made outside of the nominal protected radio band near 1421 MHz, the total power signal from two of the antennas was monitored for the presence of interference. No interference was detected during these observations, however. We also examined the data for the presence of solar bursts which could have corrupted the maps at one or more frequencies. Only one burst was detected, between 1820 and 1950 UT on January 29, and these data were edited before maps were made. The calibrated data were edited and used together with the standard CLEAN procedure to make synthesis maps of both total intensity, I, and circular polarization, V.

The maps of total intensity are shown in Figures 1 and 2. There was no detectable circular polarization ($V/I \leq 15\%$) on either day, suggesting that the regions were optically thick to both the ordinary and extraordinary modes of wave propagation. On both days the region shows a looplike structure of 1.'0 to 1.'5 in length, whose peak brightness temperature first increases systematically from $\sim 1.5 \times 10^6$ K at 1440 MHz to $\sim 4.0 \times 10^6$ K at 1658 MHz, and then begins to decrease at the highest frequencies. In Table 1 we give the brightness temperatures at a point denoted by a cross on the peak intensity at 1658 MHz, and in Figure 3 we plot these temperatures as a function of frequency. The error bars in Figure 3 represent 3 σ uncertainties determined from the residual noise left on the CLEANed maps.

As a check on the integrity of the solar calibration procedure, we have also plotted the brightness temperatures observed in a loop within the active region AR 4399, located $\sim 6.'5$ to the east of AR 4398. This was the only other major active region on the Sun during these 2 days. In contrast to AR 4398, the brightness spectrum of AR 4399 is nearly constant on both days, with an average brightness temperature of $T_B \approx 1.5 \times 10^6$ K. This result seems to indicate that the changes in brightness temperature observed from AR 4398 are not common to all sources, and therefore not due to an artifact of the calibration or CLEANing procedure.

In Figure 4 we compare the radio maps at the peak frequency of 1658 MHz with Kitt Peak magnetograms taken on the same day. The radio emission appears to connect regions of opposite magnetic polarity, suggesting that the sources are dipolar loops which join the underlying sunspots. Observations made at Mount Wilson Observatory (R. Howard, private communication) indicate that the two dominant spots have magnetic field strengths of $|H| \approx 2000$ G, and that the morphology and surface fields of these spots did not change appreciably from one day to the next. As we will argue in the next section, this may explain why the spectrum and morphology of the radio loops were also similar on the two days.

III. DISCUSSION

In this section we will show that the observed changes in brightness temperature of about a factor of 2.5 over a frequency range of ~ 300 MHz are difficult to explain by either thermal bremsstrahlung or gyroresonance emission from a loop in which the temperature, density, and magnetic field vary uniformly with height. These radio results, then, appear to conflict with the results of numerical models of quasi-static coronal loops which predict smooth gradients in both temperature and density along the loop (e.g., Rosner, Tucker, and Vaiana 1978; Vesecky, Antiochos, and Underwood 1979). On the other hand, these sharp changes in brightness temperature are consistent with the existence of neutral current sheets or thin inhomogeneous layers in the coronal loop where the temperature or density are thought to be higher than in their surroundings (Syrovatskii 1977).

As a starting point in our analysis, we assume that the magnetic field strength $B(Z)$ in the loop can be represented by a dipole function, $B(Z) = B_0 R_D^3/(Z + R_D)^3$, where Z is the height above the photosphere, B_0 (~ 2000 G) is the magnetic field at the solar surface, and R_D is the depth of the dipole below the loop base. If R_D is taken to be equal to one-half the distance, D, between the two footpoints, then Mount Wilson sunspot observations indicate $D \approx 8.0 \times 10^9$ cm and $R_D \approx 4 \times 10^9$ cm. We next divide the loop into thin layers of thickness 1.0×10^8 cm and compute the optical depth due to thermal bremsstrahlung and gyroresonance emission with assumed values of temperature and density at each height, Z, in the loop. In the simplest models, we assume that the loop has a constant temperature and density between $Z = 2 \times 10^9$ cm and 5×10^9 cm, the approximate height of 20 burst centimeter loop emission (Willson and Lang 1984). The equation of transfer for the emergent brightness temperature and circular polarization as a function of frequency was then solved for temperatures between 1.5×10^6 and 4.0×10^6 K, and densities between 1.0×10^9 and 5.0×10^9 cm^{-3}, using the equations for the thermal bremsstrahlung and gyroresonance optical depth given by Willson (1983). Models were also computed for different values of the parameter θ ($20° < \theta < 90°$), the angle between the magnetic field and the line of sight.

The results of these calculations indicate that for this range of temperatures and densities, and for $\theta > 60°$, gyroresonance absorption would render the loop optically thick with a nearly

TABLE 1

MAXIMUM BRIGHTNESS TEMPERATURES, T_b(max), WITHIN AR 4398 AT DIFFERENT FREQUENCIES

Date	1440*	1480	1515	1558	1585	1620	1658	1690	1705	1724
1984 Jan 28.....	1.4×10^6	1.4×10^6	1.6×10^6	1.8×10^6	2.2×10^6	3.0×10^6	3.7×10^6	3.2×10^6	2.5×10^6	2.6×10^6
1984 Jan 29.....	1.3×10^6	1.7×10^6	1.8×10^6	2.0×10^6	2.2×10^6	3.2×10^6	4.0×10^6	2.8×10^6	2.7×10^6	2.3×10^6

* All frequencies are in megahertz, all temperatures are in kelvins.

ORIGINAL PAGE IS
OF POOR QUALITY

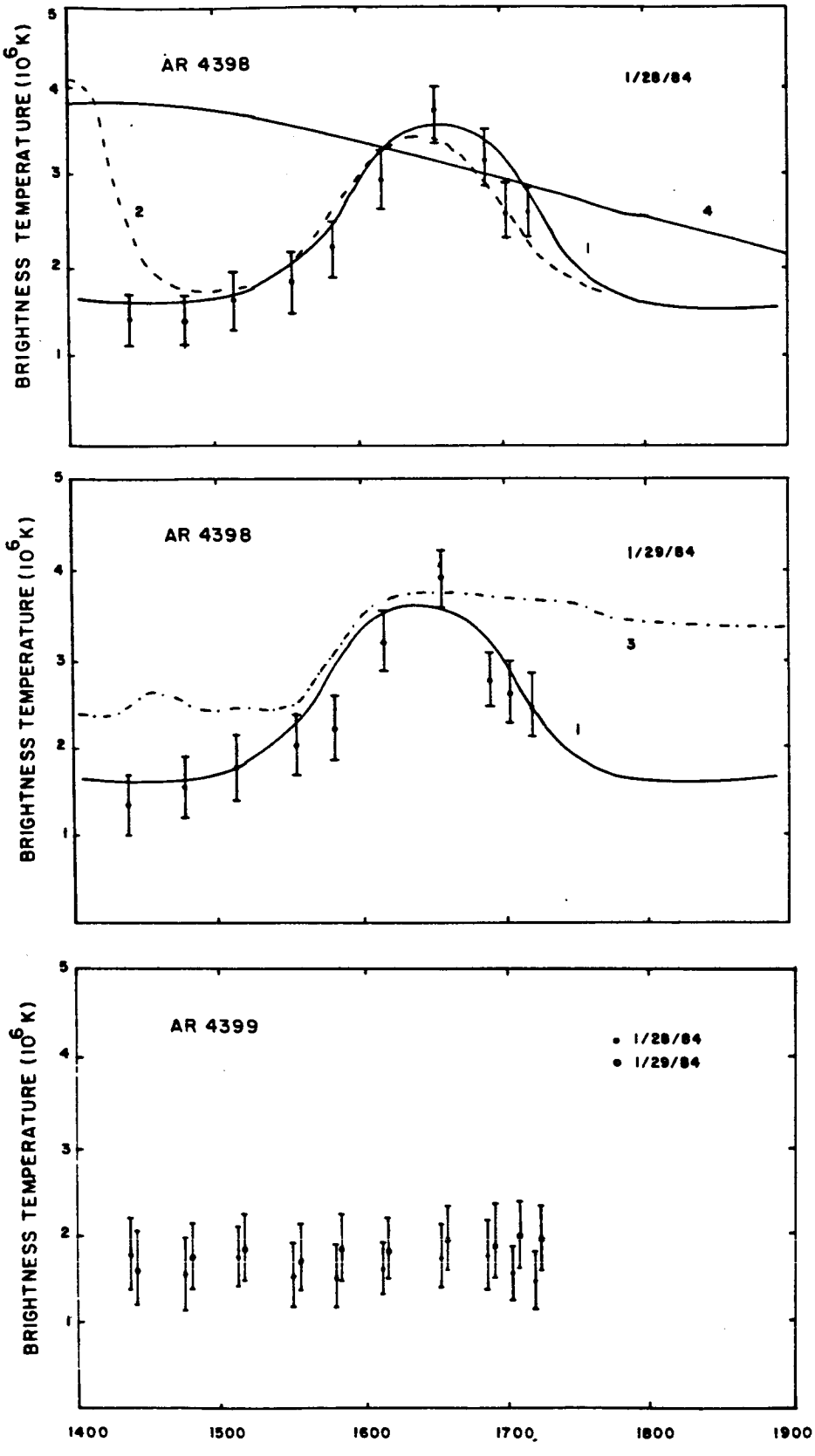

FIG. 3.—Theoretical plots of brightness temperature for different values of temperature density, and magnetic field strength in a coronal loop (*top, middle*). Maximum brightness temperatures of the loops in AR 4398 (*top, middle*) and AR 4399 (*bottom*) are also plotted with error bars corresponding to peak-to-peak fluctuations in background temperature of the synthesis maps. Curves 1 and 2 correspond to a coronal loop model that contains a thin ($\Delta L = 1.0 \times 10^8$ cm) layer where the magnetic field is $H = 145$ and 119 G, respectively, and where the temperature and density at $T_e = 3.8 \times 10^6$ K and $N_e = 1.0 \times 10^9$ cm^{-3}. The temperature and density in the rest of the loop are taken to be equal to $T_e = 1.5 \times 10^6$ K and $N_e = 1.0 \times 10^9$ cm^{-3}. Curve 3 corresponds to the same parameters as model 1, except that $N_e = 2.0 \times 10^{10}$ cm^{-3}. Curve 4 corresponds to a loop in which electron temperature increases monotonically from $T_e = 1.5 \times 10^6$ at $z = 5 \times 10^9$ cm to $T_e = 3.8 \times 10^6$ K at $z = 6 \times 10^9$ cm. In all cases, the angle θ between magnetic field and line of sight was taken to be equal to $\theta = 70°$.

Brightness temperature of active region AR 4399, located ~6.5 east of AR 4398, together with typical error bars, is plotted on bottom panel of figure.

ORIGINAL PAGE IS
OF POOR QUALITY

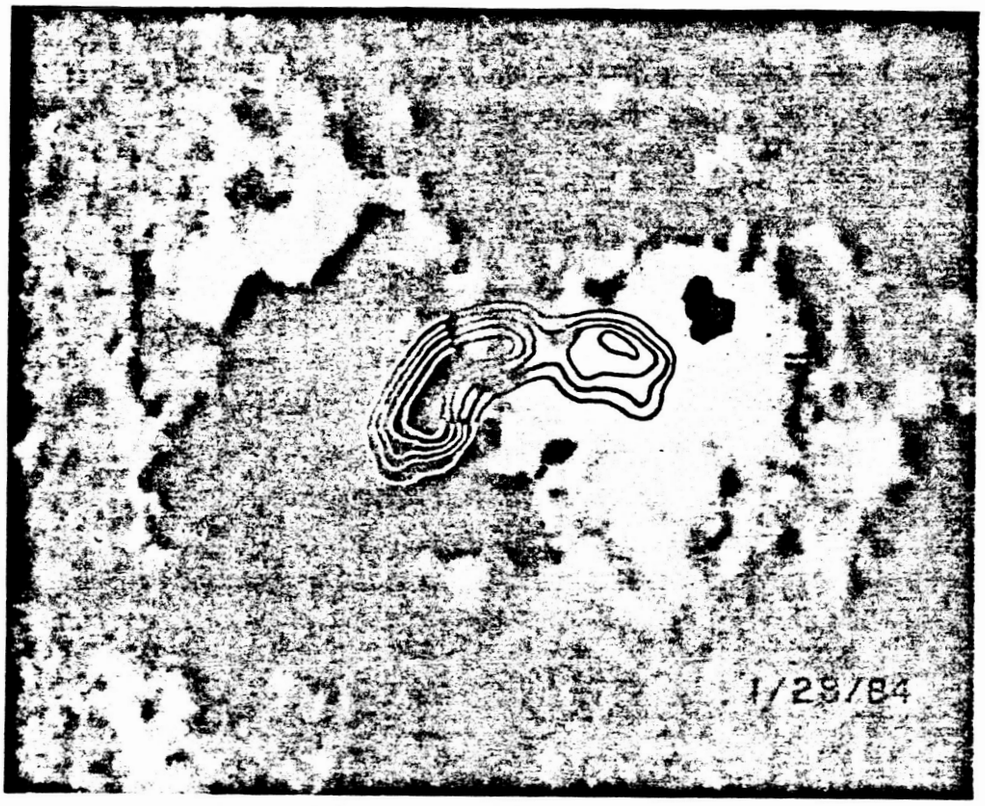

FIG. 4.—VLA synthesis maps of total intensity at 1658 MHz on 1984 January 28 (*top*) and 29 January (*bottom*), superposed on Kitt Peak magnetograms taken on the same day. Note that radio emission appears to connect areas of opposite magnetic polarity, and that peak brightness temperature occurs nearly along magnetic neutral line.

constant brightness temperature between 1.5×10^6 and 4×10^6 K, and a low degree of circular polarization ($\rho_c < 20\%$) throughout the range of frequencies observed. This is because the individual cyclotron lines at different harmonics that are emitted from a layer with constant temperature would merge to form a continuum. These results are in agreement with those of McConnell and Kundu (1983) who found that 20 cm coronal loops would be optically thick to gyroresonance emission at the third harmonic of the gyrofrequency for magnetic fields $H \approx 130$–170 G, temperatures $T \approx 1.5 \times 10^6$ K, and densities of $N_e \approx 5 \times 10^8$ cm^{-3}. We also found that these results are unchanged if the temperature and density are allowed to vary monotonically with height. In Figure 3 we show one such model in which the temperature varied from $T_e = 1.5 \times 10^6$ K at $Z = 5 \times 10^9$ cm to $T_e = 3.8 \times 10^6$ K at $Z = 6 \times 10^9$ cm.

Instead, we find that the peak in brightness temperature can be produced if the temperature, say T_c, in *one* of the layers with constant magnetic field is assumed to be higher than in the other layers. In this case, the individual cyclotron line with peak brightness temperature T_c will appear above the continuum spectrum produced by the other layers in the loop. The results of these model calculations are shown in Figure 3 for different values of the magnetic field strength, temperature, and density for which the peak at ~ 1658 MHz is a harmonic of the gyrofrequency. We find that the spectrum can be satisfactorily fit if the loop contains a thin layer in which $T_c = 3.5$–4.0×10^6 K, where the magnetic field is $H \approx 145$ G ($n = 4$), or possibly $H = 119$ G ($n = 5$). For $n = 3$ ($H = 197$ G), the line profile is too wide and flat-topped, while for $n > 6$ ($H > 100$ G) the lines are optically thin. That is, one explanation of these brightness temperature variations is the existence of a thin layer in which the temperature is ~ 3 times higher than in the rest of the loop where $T_e \approx 1.5 \times 10^6$ K. For an electron density of $N_e = 10^9$ cm^{-3}, we obtain good fits for 1×10^7 cm $< \Delta L < 1 \times 10^8$ cm. For narrower layers, the lines become optically thin and do not give a good fit to the data. The data also constrain the angle θ to $\theta \approx 65°$–$80°$, since smaller values would yield unacceptably high circular polarization ($\rho_c > 30\%$), and higher values would result in cyclotron line profiles that are too wide and flat-topped. We also find that these results are relatively insensitive to the assumed density in the heated layer, up to $N_e \approx 2 \times 10^{10}$ cm^{-3}. For higher densities, thermal bremsstrahlung becomes dominant in the layer, resulting in a sharp step in brightness temperature above ~ 1600 MHz (Fig. 3).

The fact that the brightness spectrum is nearly identical on both days suggests that the physical conditions in the loop were similar on these days. As noted earlier, the magnetic fields of underlying sunspots were relatively constant, so that one might also expect the coronal extension of these photospheric fields to be also relatively unchanged. The frequency of the cyclotron line emission would, under these conditions be relatively unaffected, and this might explain the similarity of the microwave spectrum from one day to the next.

The physical mechanism that gives rise to a thin, apparently stable, hot layer in the corona is uncertain. We note, however, that EUV observations of coronal loops have revealed the presence of temperature inhomogeneities in a number of sources (Foukal 1975, 1976; Raymond and Foukal 1982; Pye *et al.* 1978). These inhomogeneities cannot be explained by quasi-static loop models in which the pressure is assumed to be uniform (e.g., Rosner, Tucker, and Vaiana 1978), but they may be accommodated in more sophisticated models in which the pressure and heat deposition are allowed to vary with height and distance in the loop (Serio *et al.* 1981). Whether these structures represent current sheets or regions where the heating rate is higher than in the surrounding parts of the loop is also an open question at this time. Future observations with the VLA and other multifrequency radio interferometers, together with observations at ultraviolet and X-ray wavelength with the repaired *SMM*, may provide a more complete description of the magnetic field temperature and density stratification of active region coronal loops.

The author wishes to thank Kenneth R. Lang for useful discussions and an anonymous referee for helpful suggestions. Solar radio interferometric studies at Tufts University are supported under grant AFSOR-83-0019 with the Air Force Office of Scientific Research. Comparisons of VLA and *Solar Maximum Mission* satellite data are supported under NASA Guest Investigator grant NAG 5-501.

REFERENCES

Dulk, G. A., and Gary, D. E. 1983, *Astr. Ap.*, **124**, 103.
Foukal, P. 1975, *Solar Phys.*, **43**, 327.
———. 1976, *Ap. J.*, **210**, 575.
Kuznetsov, V. D., and Syrovatskii, S. I. 1981, *Solar Phys.*, **69**, 361.
Lang, K. R., Willson, R. F., and Gaizauskas, V. 1983, *Ap. J.*, **267**, 455.
Lang, K. R., Willson, R. F., and Rayrole, J. 1982, *Ap. J.*, **258**, 384.
McConnell, D., and Kundu, M. R. 1983, *Ap. J.*, **269**, 698.
Pye, J. P., Evans, K. D., Hutcheon, R. J., Gerassimenko, M., Davis, J. M., Krieger, A. S., and Vesecky, J. F. 1978, *Astr. Ap.* **65**, 123.
Raymond, J. C., and Foukal, P. 1982, *Ap. J.*, **253**, 323.
Rosner, R., Tucker, W. H., and Vaiana, G. S. 1978, *Ap. J.*, **220**, 643.
Serio, S., Peres, G., Vaiana, G. S., Golub, L., and Rosner, R. 1981, *Ap. J.*, **243**, 288.
Syrovatskii, S. I., and Kuznetsov, V. D. 1980, in *IAU Symposium 86, Radio Physics of the Sun*, ed. M. R. Kundu and T. E. Gergeley (Dordrecht: Reidel), p. 109.
Syrovatskii, V. D. 1977, *Astr. Zh. (Letters)*, **3**, 133.
Velusamy, T., and Kundu, M. R. 1981, *Ap. J. (Letters)*, **243**, L103.
Vesecky, J. F., Antiochos, S. K., and Underwood, J. H. 1979, *Ap. J.*, **233**, 987.
Willson, R. F. 1983, *Solar Phys.*, **89**, 103.
Willson, R. F., and Lang, K. R. 1984, *Ap. J.*, **279**, 427.

ROBERT F. WILLSON: Department of Physics, Tufts University, Medford, MA 02155

ORIGINAL PAGE IS
OF POOR QUALITY

THE ASTROPHYSICAL JOURNAL, 301:460–464, 1986 February 1
© 1986. The American Astronomical Society. All rights reserved. Printed in U.S.A.

STRUCTURE OF A SOLAR ACTIVE REGION FROM RATAN 600 AND VERY LARGE ARRAY[1] OBSERVATIONS

SH. B. AKHMEDOV, V. N. BOROVIK, AND G. B. GELFREIKH
Main Astronomical Observatory, Academy of Science of the USSR, Leningrad
V. M. BOGOD, A. N. KORZHAVIN, AND Z. E. PETROV
Special Astrophysical Observatory of the USSR, Academy of Science, Leningrad Branch
V. N. DIKIJ
Leningrad Polytechnical Institute
AND
KENNETH R. LANG AND ROBERT F. WILLSON
Department of Physics and Astronomy, Tufts University
Received 1985 February 19; accepted 1985 June 12

ABSTRACT

Solar active region AR 3804 was observed on the same days with the RATAN 600 and the VLA in 1982 July. The emission at wavelengths between 2 and 4 cm consisted of narrow ($\phi < 40''$), bright ($T_B \approx 0.2$ to 6×10^6 K) core sources surrounded by a weaker ($T_B \approx 10^4$–10^5 K), extended ($\phi \approx 200''$) halo. The brightest core sources are associated with sunspots and are interpreted in terms of the gyroradiation of thermal electrons at the second and third harmonics of the gyrofrequency. Two of the core sources were associated with a filament that lies above the magnetic neutral line in the photosphere. One of these filament-associated sources has a flat spectrum and is attributed to thermal bremsstrahlung. Relatively high magnetic field strengths of $H \approx 536$ G are inferred if the circular polarization of this source is due to propagation of the bremsstrahlung in the presence of a magnetic field, and even higher magnetic field strengths are required if the radiation is thermal gyroemission. Lower magnetic fields can be obtained if the radiation propagates through a region of transverse magnetic fields higher in the corona where polarization inversion occurs. The other filament-associated source had a high brightness temperature and steep radiation spectrum that cannot be attributed to either thermal bremsstrahlung or thermal gyroradiation. The weak magnetic field strengths at photospheric levels require implausibly high electron temperatures if the high brightness temperatures are to be explained. This source might be attributed to currents that enhance coronal magnetic fields. In this event gyroemission might account for the radiation. Alternatively, it may be due to nonthermal radiation such as the gyrosynchrotron radiation of subrelativistic electrons. VLA synthesis maps at 20 cm reveal hot ($T_B \approx 10^6$ K) coronal loops that connect underlying sunspots of opposite magnetic polarity, but RATAN 600 observations reveal the presence of a much more extended source that accounts for the vast majority of the flux detected at this wavelength. This extended source may also be attributed to the gyrosynchrotron radiation of subrelativistic electrons.

Subject headings: radiation mechanisms — Sun: radio radiation — Sun: sunspots

I. INTRODUCTION

Very Large Array (VLA) observations with high angular resolution ($\theta \gtrsim 1''$) at different microwave wavelengths ($\lambda = 2$, 6, and 20 cm) have been used to specify the temperature and magnetic structure at different heights in solar active regions. These multiple-wavelength observations specify the three-dimensional structure of active regions in the transition region and the low solar corona (Lang and Willson 1983, 1984; Lang, Willson, and Gaizauskas 1983; Shevgaonkar and Kundu 1984; Kundu and Lang 1985). However, active regions often have a complex structure with local sources that have different emission mechanisms (Gelfreikh *et al.* 1970; Kundu 1982).

Measurements of the spectrum and polarization of the local sources can help specify their emission mechanisms, while also supplementing the interpretation of the VLA observations. We have therefore begun collaborative observations in which the same active region is observed by the VLA and the Soviet RATAN 600 (Radio Astronomy Telescope of the Academy of Sciences [Nauk]). The RATAN 600 observations provide high angular resolution in the east-west direction at five wavelengths between 2 and 4 cm, thereby determining the radiation spectra of the local sources. Accurate polarization measurements (to 0.5%) are also made at these wavelengths, while more extended structures are detected at decimetric wavelengths (see Table 1).

The VLA and RATAN 600 observations complement each other. The VLA provides high angular resolution in two dimensions at three wavelengths, but the wavelengths are not close enough to determine the spectra of the local sources, and the polarization accuracy is only $\sim 10\%$. The RATAN 600 provides information on extended sources that are not detected with the VLA because of incomplete UV coverage. On the other hand, confusion arising because of the poor angular resolution (in one dimension) of the RATAN 600 can be overcome by VLA observations.

In this paper we will emphasize the unique capabilities of the

[1] The Very Large Array (VLA) is a facility of the National Radio Astronomy Observatory, which is operated by Associated Universities, Inc., under contract with the National Science Foundation.

ORIGINAL PAGE IS
OF POOR QUALITY

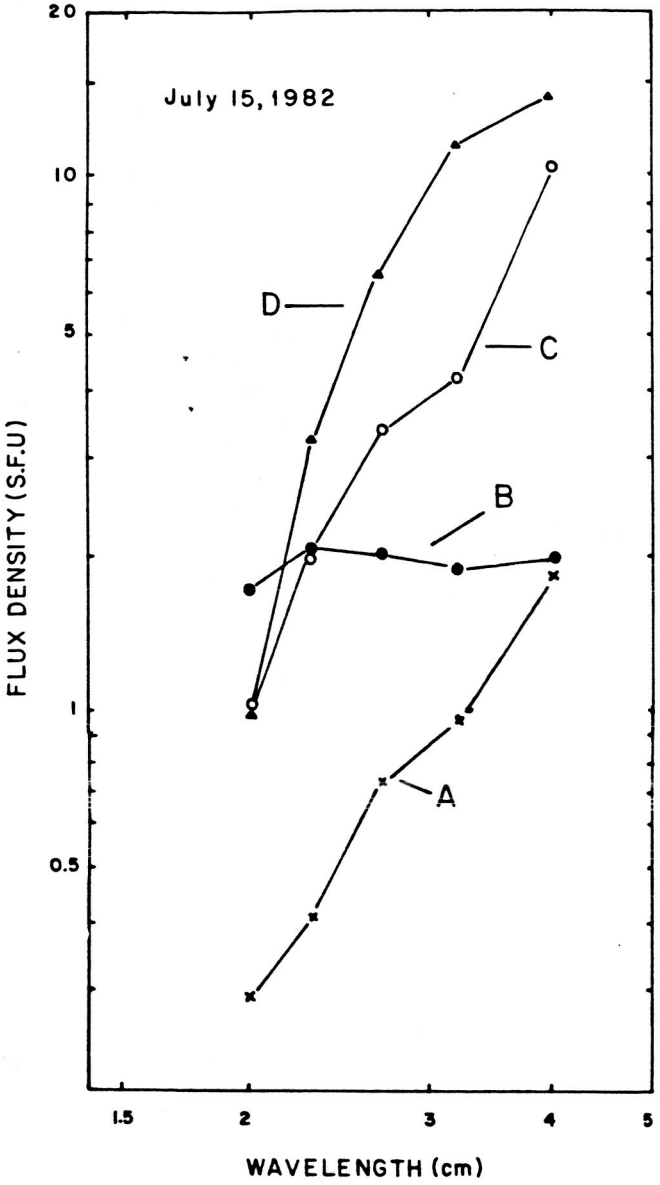

FIG. 2.—Radiation spectrum of four core sources. Here the flux density in solar flux units (sfu) has been plotted as a function of wavelength. For comparison purposes, 1 sfu = 10^4 fu = 10^4 Jy = 10^{-19} ergs cm^{-2} s^{-1} Hz^{-1}.

cm emission consists of two components: one elongated component that connects underlying sunspots of opposite magnetic polarity, and a more compact source that also lies between oppositely polarized sunspots. The radiation at 20 cm wavelength is therefore attributed to the hot ($T_B \approx 10^6$ K), dense plasma that is trapped within magnetic loops that connect underlying sunspots of opposite magnetic polarity. The linear extent of the 20 cm coronal loops is 10^9–10^{10} cm. These results confirm previous work indicating that 20 cm VLA observations delineate the structure of the ubiquitous coronal loops that had previously only been detected at X-ray wavelengths (Lang, Willson, and Rayrole 1982; Dulk and Gary 1983; McConnell and Kundu 1983).

The RATAN 600 observations at 13 and 21 cm indicate an extended source whose angular size $\phi \approx 4'$ is comparable to that of the entire active region. Such extended sources are often

TABLE 2

PARAMETERS FOR FOUR CORE RADIO SOURCES

Core	Wavelength (cm)	I (Jy per arcsec)	ϕ	ρ_c (%)	T_B (10^6 K)
A.....	2.0	≥315	≤8″	...	≥0.23
	2.3	360	10	53	0.28
	2.7	535	13	100	0.43
	3.2	560	17	100	0.49
	4.0	765	23	...	0.77
B.....	2.0	941	17	...	0.32
	2.3	1374	14	8	0.75
	2.7	1162	16	30	0.77
	3.2	972	18	40	0.80
	4.0	1024	18	...	1.32
C.....	2.0	807	12	...	0.39
	2.3	1356	14	7	0.74
	2.7	2080	15	19	1.46
	3.2	1944	20	11	1.44
	4.0	4012	24	...	3.88
D.....	2.0	315	30	...	0.06
	2.3	1308	23	28	0.44
	2.7	2648	23	45	1.22
	3.2	4212	25	33	2.50
	4.0	6675	24	...	6.45

undetectable on VLA synthesis maps. The total flux density of the 21 cm extended source detected with the RATAN 600 is 1.5×10^5 Jy, whereas the total flux density of the 20 cm loops detected with the VLA is 3.0×10^3 Jy. This indicates that the flux of the 20 cm coronal loops detected with the VLA is only ~2% of the total flux of the entire active region at 21 cm. Thus, the coronal loops may be superposed upon much more extended sources that account for most of the active region flux at these wavelengths.

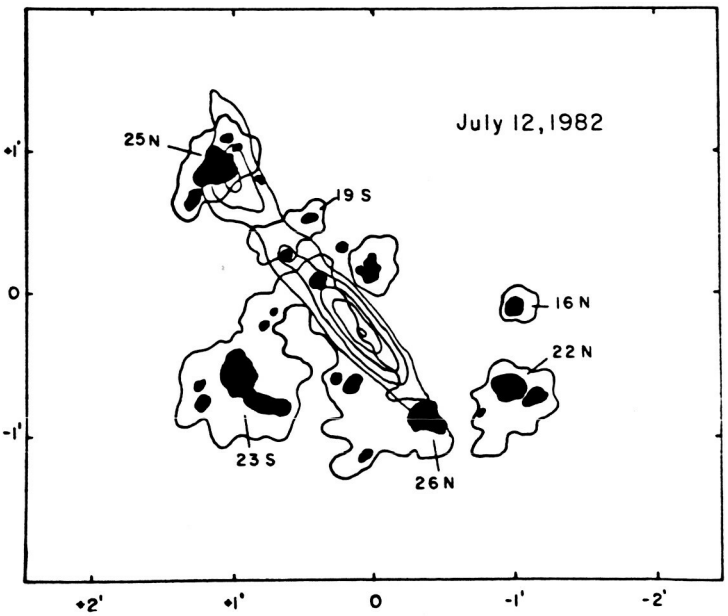

FIG. 3.—VLA synthesis map of the 20 cm emission from AR 3084 on 1982 July 12 is superposed upon the sunspot picture provided by M. N. Gnevyshev. The sunspots (*black*) have numbers corresponding to the longitudinal magnetic field strength in hundreds of gauss and letters denoting the magnetic polarity ("N" or "S"). The 20 cm contours are of equal brightness temperature corresponding to 0.2, 0.4, 0.6, 0.8, and 1.0 times the peak brightness temperature of 1.8×10^6 K.

III. DISCUSSION

The sunspot-associated core sources A and C may be attributed to gyroradiation of thermal electrons at the second and third harmonic of the gyrofrequency. Strong evidence for gyroresonance absorption at coronal levels in solar active regions was provided by Kundu, Schmahl, and Gerassimenko (1980) through a comparison of microwave, EUV, and X-ray observations. The near equality of the microwave brightness and electron temperatures indicated that the microwave emission was thermal. The measured electron densities and temperatures indicated that free-free absorption is inadequate and that gyroresonance absorption at the second or third harmonic of the gyrofrequency provides sufficient optical depth at microwave wavelengths. Thermal gyroradiation at coronal levels above sunspots was additionally confirmed by the detection of circularly polarized ring-shaped or horseshoe structures (Alissandrakis and Kundu 1982; Lang and Willson 1982) that were predicted using the theory of gyroresonant emission from individual sunspots (Gelfreikh and Lubyshev 1979). It is also consistent with the 100% circular polarization observed for the core source A.

The magnetic field intensity, H_c, at the bottom of the corona may be inferred from the short wavelength limit, λ_c, of the polarized gyroresonant emission through the relation (Akhmedov *et al.* 1982)

$$H_c = \frac{3570}{\lambda_c} \text{ gauss}, \quad (1)$$

for the third harmonic. For core source A, a value of $H_c = 1690$ gauss is obtained. This may be compared with the magnetic field strength $H = 2100$–2600 gauss for the sunspots in the underlying photosphere.

The filament-associated core source B has the flat spectrum of optically thin thermal bremsstrahlung. A lower estimate to the emission measure, $\int N_e^2 dl$, can be obtained by assuming that the electron temperature, T_e is equal to the brightness temperature, T_B, at longer wavelength $\lambda = 4.0$ cm. The relevant formulae (Lang 1974) then give $\int N_e^2 dl = 5.6 \times 10^{29}$ cm^{-5} and an electron density $N_e \approx 2.1 \times 10^{10}$ cm^{-3} for core source B.

The observed circular polarization of the filament-associated source B might be explained in terms of a propagation effect in which the optical depths of the ordinary and extraordinary waves differ. In the quasi-longitudinal (Q-L) approximation for wave propagation in the direction of an external magnetic field, the degree of circular polarization $\rho_c \approx 2\nu_H \cos\theta/\nu$, where the gyrofrequency $\nu_H = 2.8 \times 10^6 H$ Hz in a longitudinal magnetic field strength of H, the angle between the line of sight and the direction of the magnetic field is θ, and ν is the frequency of the radiation. At our observing wavelength of $\lambda \approx 3$ cm where the circular polarization $\rho_c \approx 30\%$ we obtain $H = 536$ gauss for Q-L propagation. Although this longitudinal magnetic field strength may be large for a filament associated source, it cannot be avoided by an appeal to the alternative gyroresonant emission process.

The optical thickness due to gyroresonant absorption increases with increasing angle, θ, between the line of sight and the direction of the magnetic field, and we might expect a large θ near the magnetic neutral line. However, even with $\theta = 85°$, plausible values for the electron temperature, $T_e \approx 2 \times 10^6$ K, electron density $N_e \approx 10^{10}$ cm^{-3}, and extent $L \approx 10^9$ cm indicate that the highest harmonic, s, of the gyrofrequency that is consistent with the observed brightness temperature of $T_B = 1.0 \times 10^6$ K is $s = 5$ (see McConnell and Kundu 1983, for the relevant formulae). This harmonic corresponds to a longitudinal magnetic field strength of $H \approx 714$ gauss if the gyrofrequency is at $\lambda = 3$ cm. Higher harmonics that correspond to weaker magnetic fields require implausibly high electron temperatures to produce the observed brightness temperature.

One method of accounting for circular polarization with lower magnetic field strengths involves a polarization inversion in a region of quasi-transverse (Q-T) magnetic field (Cohen 1960). The coupling of the ordinary and extraordinary modes as the radiation passes through the Q-T region will cause an inversion in the sense of circular polarization if the frequency ν is less than the critical frequency, ν_T, given by $\nu_T^4 = 10^{17} N_e L_H H^3$. Assuming $N_e = 10^{10}$ cm^{-3}, a magnetic scale length of $L_H = 10^9$ cm and $\nu_T \geq 10^{10}$ Hz, we find $H \geq 46$ gauss. This inversion occurs high in the corona above the region where the radiation is formed. However, because source B is located above a magnetic neutral line, we have no evidence for whether or not a polarization inversion has taken place.

Kundu *et al.* (1977) and Kundu and Alissandrakis (1984) have provided evidence for polarization inversion in the regions of bright 6 cm sources ($T_B \approx 2 \times 10^6$ K) associated with magnetic neutral lines. Their observations led to an estimate of $H \sim 20$ gauss for the Q-T region. Similar values of magnetic field strength in the Q-T region have been inferred from centimeter-wavelength polarization inversions by Peterova and Akhmedov (1973).

Of special interest is the filament-associated core source D. This source has a large brightness temperature of $T_B \approx 7 \times 10^6$ K at $\lambda = 4$ cm and an exceptionally rapid increase of flux density with wavelength. Because the optical depth must be less than unity in order to account for the observed circular polarization, the electron temperature must be greater than 7×10^6 K. This unusually high electron temperature argues against thermal emission processes. Moreover, the steep radiation spectrum rules out thermal bremsstrahlung.

Although one can obtain a steep spectrum from thermal gyroemission as the result of an exponential term in the optical depth (see McConnell and Kundu 1983), the region must have an implausibly high magnetic field strength. If the radiation were due to gyroemission at the second harmonic of the gyrofrequency, then a magnetic field strength of $H = 1800$ gauss is implied. This is inconsistent with the fact that the source lies above a magnetic neutral line in the solar photosphere where much weaker magnetic fields prevail. When more plausible magnetic field strengths of $H \sim 140$ gauss are assumed for the regions where $T_e \approx 10^6$ K, then the observed radiation must occur at high harmonics of the gyrofrequency ($s = 26$ for $\lambda = 3$ cm). The optical depth due to gyroresonance absorption is then negligibly small, and implausibly high electron temperatures of $T_e \gg 10^7$ K are inferred. However, there is the possibility that strong currents produce higher magnetic fields in the low corona than those expected from current-free extrapolations from photospheric values. In this event thermal gyroemission might account for the radiation.

An alternative explanation for the radiation from the core source D may be some sort of nonthermal emission mechanism (Gelfreikh *et al.* 1970). Such a mechanism was suggested by observations of 6 cm sources of high brightness temperature in regions where the magnetic fields are weak (Webb *et al.* 1983). These sources have been attributed to the nonthermal synchrotron emission of mildly relativistic electrons (Chiuderi Drago and Melozzi 1984).

One possibility is that source D is the gyrosynchrotron radiation of subrelativistic electrons. The theoretical formulae describing gyrosynchrotron radiation have been given (Ramaty 1969; Takakura and Scalise 1970; Ramaty and Petrosian 1972; Petrosian 1981). Theoretical results of the gyrosynchrotron radiation from mildly relativistic electrons have been summarized by Dulk and Marsh (1982), who provide simplified expressions for nonthermal (power-law) and thermal (Maxwellian) distributions. Using their formulae, we find that a nonthermal electron energy distribution with a power-law index $\delta = -4.0$ and a magnetic field strength of $H = 40$ gauss describes the flux density spectrum of source D between 2.0 and 4.0 cm. The observed flux density can be accounted for with a magnetic field of strength $H = 40$ gauss and an electron density $N = 2 \times 10^9$ cm^{-3} for electrons with energies $E > 10$ keV. These values of H and N may plausibly account for the observed emission from source D.

The extended component of decimetric emission at 13 and 21 cm wavelength may be similarly accounted for by gyrosynchrotron radiation. Plausible magnetic field strengths of $H \approx 80$ gauss can be inferred from the observed circular polarization (15%–50%) and Takakura and Scalise's (1970) formulae for the volume emissivity of the ordinary and extraordinary waves. Because of the much larger volume of the extended emission, the required electron density $N_e \approx 10^2$ cm^{-3} may be relatively low.

One possible difficulty with this explanation is that some as yet unspecified mechanism must be continually accelerating the electrons. For example, the energy loss by synchrotron radiation (Lang 1974) with a power-law electron energy distribution has a half-time for the total emitted radiation (Chiuderi and Chiuderi-Drago 1967) of several hours for a magnetic field strength of $H = 40$ gauss.

We are especially grateful to Yu. N. Parijskij, the late D. V. Korolkov and V. K. Abalakin for their support of collaborative observations between the RATAN 600 and the VLA. We thank D. Rust, P. Simon, and V. E. Stepanov for the stimulus to international collaboration provided by support activities for the *Solar Maximum Mission* satellite. We also thank the staff of the RATAN 600 and VLA telescopes for their support and help. Travel support for use of a foreign telescope (the RATAN 600) was provided by the NSF. Radio astronomical studies of the Sun and other active stars at Tufts University are supported under grant AFOSR-83-0019 with the Air Force Office of Scientific Research.

REFERENCES

Akhmedov, Sh. B., Gelfriekh, G. B., Bogod, V. M., and Korshavin, A. N. 1982, *Solar Phys.*, **79**, 41.
Alissandrakis, C. E., and Kundu, M. R. 1982, *Ap. J. (Letters)*, **253**, L49.
Chiuderi, C., and Chiuderi-Drago, F. 1967, *Nuovo Cimento*, **48**, 186.
Chiuderi-Drago, F., and Melozzi, M. 1984, *Astr. Ap.*, **131**, 103.
Cohen, M. H. 1960, *Ap. J.*, **131**, 664.
Dulk, G. A., and Gary, D. E. 1983, *Astr. Ap.*, **124**, 103.
Dulk, G. A., and Marsh, K. A. 1982, *Ap. J.*, **259**, 350.
Felli, M., Lang, K. R., and Willson, R. F. 1981, *Ap. J.*, **247**, 325.
Gelfreikh, G. B., and Lubyshev, B. I. 1979, *Soviet Astr.*, **23**, 316.
Gelfreikh, G. B., Akhmedov, Sh. B., Borovic, V. N., Golnev, V. Ja., Korshavin, A. N., Nagnibeda, V. G., and Peterova, N. G. 1970, *Izvestia GAO*, N185, 167.
Kundu, M. R. 1982, *Rept. Progr. Phys.*, **45**, 1435.
Kundu, M. R., and Alissandrakis, C. E. 1984, *Solar Phys.*, **94**, 249.
Kundu, M. R., Alissandrakis, C. E., Bregman, J. D., and Hin, A. C. 1977, *Ap. J.*, **213**, 278.
Kundu, M. R., and Lang, K. R. 1985, *Science*, **228**, 9.
Kundu, M. R., Schmahl, E. J., and Gerassimenko, M. 1980, *Astr. Ap.*, **82**, 265.
Lang, K. R. 1974, *Astrophysical Formulae* (New York: Springer-Verlag).
Lang, K. R., and Willson, R. F. 1982, *Ap. J. (Letters)*, **255**, L111.
———. 1983, *Adv. Space Res.*, **2**, No. 11, 91.
———. 1984, *Adv. Space Res.*, **4**, No. 7, 105.
Lang, K. R., Willson, R. F., and Gaizauskas, V. 1983, *Ap. J.*, **267**, 455.
Lang, K. R., Willson, R. F., and Rayrole, J. 1982, *Ap. J.*, **258**, 384.
McConnell, D., and Kundu, M. R. 1983, *Ap. J.*, **269**, 698.
Parijskij, Yu. N., *et al.* 1976, *Soviet Astr.*, **53**, 1017.
Peterova, N. G., and Akhmedov, Sh. B. 1973, *Soviet Astr.*, **17**, 768.
Petrosian, V. 1981, *Ap. J.*, **251**, 727.
Ramaty, R. 1969, *Ap. J.*, **158**, 753.
Ramaty, R., and Petrosian, V. 1972, *Ap. J.*, **178**, 241.
Shevgaonkar, R. K., and Kundu, M. R. 1984, *Ap. J.*, **283**, 413.
Shivris, O. N. 1980, *Ap. Issledovanija (Izvestia SAO)*, **12**, 134.
Takakura, T., and Scalise, C. 1970, *Solar Phys.*, **11**, 434.
Webb, D. F., Davis, J. M., Kundu, M. R., and Velusamy, T. 1983, *Solar Phys.*, **85**, 267.

SH. B. AKHMEDOV, V. N. BOROVIK, and G. B. GELFREIKH: Main Astronomical Observatory, Academy of Science of the USSR, 196140 Leningrad M-140, USSR

V. M. BOGOD, A. N. KORZHAVIN, and Z. E. PETROV: Special Astrophysical Observatory of the USSR, Academy of Science, Leningrad Branch, 196140 Leningrad M-140, USSR

V. N. DIKIJ: Leningrad Polytechnical Institute, 196140 Leningrad M-140, USSR

KENNETH R. LANG and ROBERT F. WILLSON: Department of Physics and Astronomy, Tufts University, Medford, MA 02155

SOLAR BURST PRECURSORS AND ENERGY BUILD UP AT MICROWAVE WAVELENGTHS*

KENNETH R. LANG and ROBERT F. WILLSON

Department of Physics and Astronomy

Tufts University

Medford, MA 02155

U.S.A.

* To be published in Advances in Space Research, Proceedings of the XXVI Committee on Space Research (COSPAR), Pergamon Press, 1986.

SOLAR BURST PRECURSORS AND ENERGY BUILD UP AT MICROWAVE WAVELENGTHS

Kenneth R. Lang and Robert F. Willson

Department of Physics, Tufts University, Medford, MA 02155, U.S.A.

ORIGINAL PAGE IS
OF POOR QUALITY

ABSTRACT

We summarize high-resolution microwave observations (VLA) of heating and magnetic triggering in coronal loops. Magnetic changes that precede solar eruptions on time scales of tens of minutes involve primarily emerging coronal loops and the interaction of two or more loops. Thermal cyclotron lines have been detected in coronal loops, suggesting the presence of hot current sheets that enhance emission from relatively thin layers of enhanced temperature and constant magnetic field. These current sheets may play a role in the excitation of solar bursts. A filament-associated source with a high brightness temperature and steep radiation spectrum occurs above a region of apparently weak photospheric field. This source might be attributed to currents that enhance coronal magnetic fields. Compact (ϕ = 5") transient sources with lifetimes of 30 to 60 minutes have also been detected in regions of apparently weak photospheric field. We conclude by comparing VLA observations of coronal loops with simultaneous SMM-XRP observations.

MAGNETIC CHANGES AND PREBURST HEATING

The VLA has recently been used to detect changes in the configuration of coronal magnetic fields and temperature enhancements within coronal loops that are important in the excitation of solar bursts. It has long been known that solar eruptions are intimately connected with the magnetic fields in active regions, for the ultimate source of energy for these bursts must be magnetic energy. It has only recently been realized, however, that evolving magnetic fields in the solar corona may play a dominant role in triggering solar eruptions /1/.

Fig. 1. The ten second V.L.A. synthesis maps of the impulsive phase of two solar bursts at 20 cm wavelength superposed on Hα photographs of the optical flares taken at the same time at the Big Bear Solar Observatory. The 20 cm bursts originate near the tops of coronal loops that are about 40,000 kilometers above the flaring region seen at optical wavelengths. The western solar limb is visible in both photographs.

Preflare changes in active regions are detected as increases in the intensity and polarization of the microwave emission at centimeter wavelengths. These increases precede solar eruptions on time scales of 10 minutes to an hour. The high angular resolution provided by the Very Large Array (VLA) has shown that these increases are related to preburst heating in coronal loops and to changes in the coronal magnetic field topology /2/. The VLA snapshot maps have also made possible tests of flare models that could not be carried out at optical wavelengths. For instance, the region of microwave energy release occurs at the apex of coronal loops, while the optical flares occur at the loop footpoints (See Fig. 1).

The VLA results indicate that preburst changes can be ordered into three major categories: (I) changes within a single coronal loop, (II) the emergence of coronal loops, and (III) interaction between coronal loops. As illustrated in Figure 2, coronal loops or arcades of loops often begin to heat up and change structure about 15 minutes before the eruption of impulsive bursts. Examples of the other types of magnetic interaction detected by the University of Maryland and Tufts groups are given in the review by Kundu and Lang /2/.

ORIGINAL PAGE IS
OF POOR QUALITY

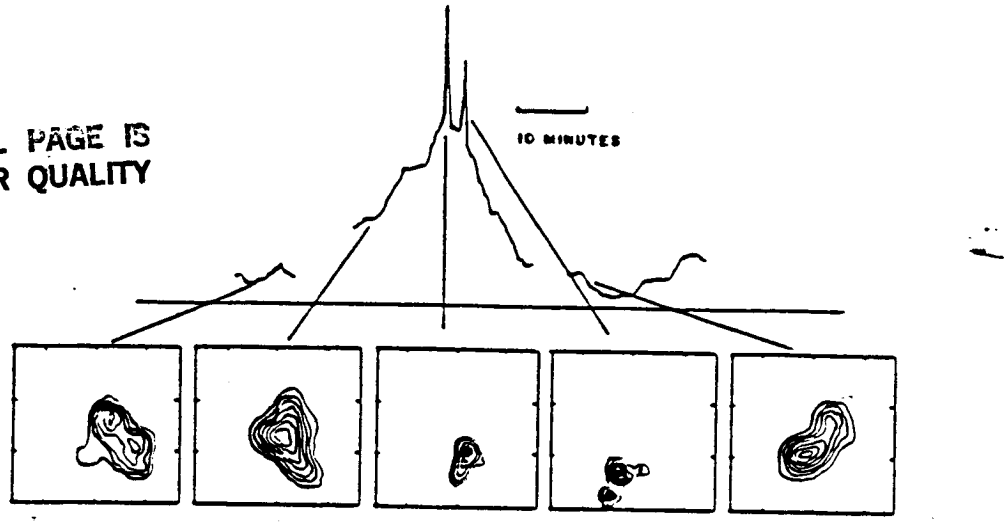

Fig. 2. The time profile of a solar burst at 20 cm wavelength suggests heating within a coronal loop prior to the emission of two impulsive microwave bursts. Radio and X-ray data have been combined to derive a peak electron temperature T_e of 2.5×10^7 K and an average electron density N_e of 10^{10} cm^{-3} during the heating phase. The changing orientation illustrated in the 10 second VLA snapshot maps could be related to the shear of photospheric fields.

THERMAL CYCLOTRON LINES AND EVIDENCE FOR CURRENTS

Theoretical work has shown that individual cyclotron lines might be detected as narrow-band enhancements in the radio-frequency spectra of solar active regions /3/. The spectra of individual cyclotron lines have subsequently been observed at wavelengths near 20 cm when the apex of a coronal loop is resolved /4/ - see Figure 3. This is because the magnetic field strength is relatively constant near the loop apex; the cyclotron lines would merge into a continuum along the loop legs where the magnetic field strength decreases uniformly with height. Neutral current sheets might also play a role, leading to intense radio emission from a thin layer near the loop apex. Both a uniform field and a steep temperature gradient in the uniform region are probably required to detect the cyclotron lines. In any event, observations of individual cyclotron lines indicate magnetic field strengths of $H = 145 \pm 5$ G at the apex of some coronal loops. Observations of individual cyclotron lines provide an unusually accurate method of specifying the coronal magnetic field strength, while also suggesting the presence of currents.

Evidence for current amplification of the coronal magnetic field may be provided by sources of high brightness temperature and steep radiation spectrum above regions of apparently-weak magnetic field /5/. An example is the filament associated source D whose spectrum is shown in Figure 4. If this emission is due to thermal gyroradiation, strong magnetic fields are required to produce gyroradiation at the first few harmonics of the gyrofrequency. Higher harmonics produce insufficient optical depth to account for the high brightness temperatures. The strong magnetic fields could be obtained if currents amplify the magnetic field in the low corona to values greater than those expected from extrapolations from the photosphere. The emission could alternatively be due to nonthermal radiation in weak magnetic fields. Nonthermal synchrotron radiation from mildly relativistic electrons is one possibility, but some as yet unspecified mechanism must be continuously accelerating the electrons.

COMPACT VARIABLE SOURCES

We have recently discovered compact, variable highly-polarized sources in regions of apparently-weak photospheric magnetic field /6/. Our subsequent VLA observations have confirmed the existence of compact, variable 2 cm sources that are not associated with active regions, but these sources had no detectable circular polarization.

The 2 cm maps showed two compact ($\theta \approx 5''$), highly circularly polarized ($P_c \approx 80$ to 90%) sources that vary on time scales of 30 to 60 minutes. The left circularly polarized source varied in maximum brightness temperature from $T_B \approx 2.0 \times 10^5$ K to $T_B < 0.5 \times 10^5$ K.

ORIGINAL PAGE IS
OF POOR QUALITY

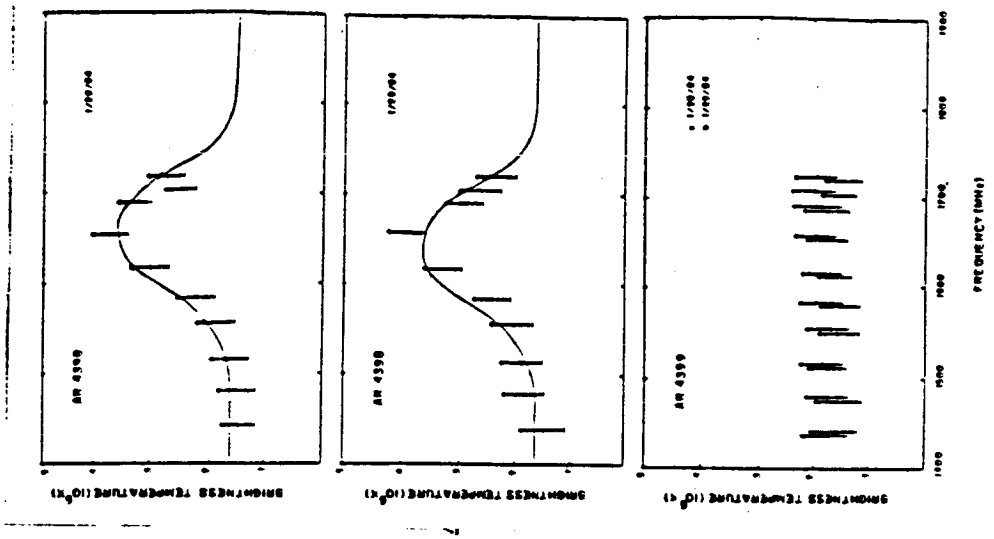

Fig. 3. VLA data at ten closely-spaced frequencies near 1440 MHz (20 cm) showing thermal cyclotron line spectra from active region AR 4398 on successive days, together with optically-thick thermal bremsstrahlung spectra from active region AR 4399 on the same days.

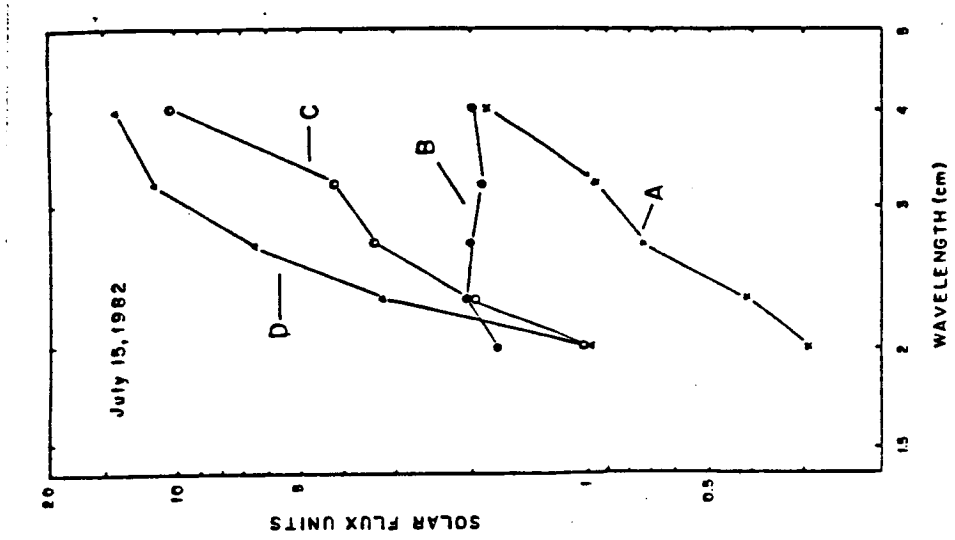

Fig. 4. The radiation spectra for the three types of sources usually detected at short centimeter wavelengths. The most common type of source is the sunspot-associated component (A and C) that is attributed to thermal gryoresonance radiation in the legs of coronal loops that are connected to the underlying sunspots. Source D is a filament-associated component located above a magnetic neutral line in regions of apparently-weak magnetic field. It may be due to thermal gyroradiation in current-amplified magnetic fields. The filament-associated source B has the flat spectrum of optically-thin thermal bremsstrahlung.

Comparisons with Mr. Wilson magnetograms indicate that the two compact, variable sources were located in regions of apparently-weak photospheric magnetic field ($H < 80$ G), and that they did not overlie sunspots. The high polarization of these sources is therefore somewhat enigmatic, for the polarization of thermal radiation requires strong magnetic fields of $H \approx 2{,}000$ G.

The enigmatic presence of highly polarized sources in regions of apparently-weak photospheric magnetic field may be explained by any one of three hypothesis. First, the photospheric field may have strengths of up to 2,000 G in compact regions that are not readily detected by the photospheric magnetograms. Alternatively, the magnetic field in the transition region or the low corona may be amplified by currents to a strength above that in the underlying photosphere. If either of these hypothesis is true, then the high circular polarization of the 2 cm sources can be attributed to either thermal gyroradiation or the propagation of thermal bremsstrahlung in the presence of a magnetic field of strength $H \approx 2{,}000$ G. A third hypothesis is that the compact 2 cm sources are due to non-thermal gyrosynchrotron radiation of mildly relativistic electrons in relatively weak magnetic fields of strength $H \approx 50$ G.

ONGOING COMPARISONS OF VLA AND SMM-XRP DATA

We are continuing with a comparison of 20 cm coronal loop data (VLA) with soft X-ray data obtained with the SMM satellite. In some instances, there is radiation at 20 centimeters

wavelength near sunspots where no X-ray radiation is detected /7/. In other cases, the 20 centimeter radiation appears at the apex of coronal loops, but with a slightly lower brightness temperature, $T_B \approx 1.4$ to 1.7×10^6 K, than the electron temperature, $Te \approx 3.0 \times 10^6$ K, inferred from the X-ray data. This may be explained by a low temperature plasma with $T_e \approx 10^5$ K that lowers the effective brightness temperature of the radio bremsstrahlung while not affecting the X-ray data that only detects the 10^6 K plasma /8/.

ORIGINAL PAGE IS
OF POOR QUALITY

Fig. 5. A comparison of the 20 cm emission (V.L.A.-left), soft X-ray (S.M.M.-middle) and Hα (SOON-right) emission of an active region on the same day. The angular spacing between fiducial marks on the axes is 60 arc-seconds.

As illustrated in Figure 5, there are other instances in which the 20-cm radiation and the soft X-ray emission have the same angular extent. In this case, the maximum brightness temperature of the radio emission has the same value as the electron temperature, $T_e = 3 \times 10^6$ K, inferred from the X-ray data. At first sight it would seem that the 20-cm emission is the thermal bremsstrahlung of the X-ray emitting plasma (electron density $N_e = 2 \times 10^{10}$ cm^{-3}), but in this instance we have also detected a cyclotron line. Preliminary modeling indicates a thin layer of $T_e \approx 4 \times 10^6$ K with a magnetic field strength of H = 145 or 187 G (harmonic n = 4 or 3). The thermal electrons that give r se to the X-ray radiation therefore also seem to produce strong gyroresonant radiation at 20 centimeters wavelength.

ACKNOWLEDGEMENTS

Radio astronomical studies of the Sun at Tufts University are supported under grant AFOSR-83-0019 with the Air Force Office of Scientific Research and by contract N00014-86-K-0068 with the Office of Naval Research (ONR). Comparisons of VLA and Solar Maximum Mission satellite data are supported under NASA Guest Investigator grant NAG 5-501.

REFERENCES

1. K.R. Lang and R.F. Willson, V.L.A. observations of flare build-up in coronal loops, Advances in Space Research 4, No. 7, 105 (1984).

2. M.R. Kundu and Kenneth R. Lang, The Sun and nearby stars: microwave observations at high resolution, Science, 228, 9 (1985).

3. V.S. Kuznetsov and S.I. Syrovatskii, On the possibility of observations of current sheets in the radio band, Solar Physics, 69, 361 (1981).

4. R.F. Willson, V.L.A. observations of solar active regions at closely spaced frequencies: evidence for thermal cyclotron line emission, Astrophysical Journal, 298, 911 (1985).

5. S.B. Akmedov, et al., Structure of a solar active region from RATAN 600 and Very Large Array observations, Astrophysical Journal, 301, 460 (1986).

6. R.F. Willson and K.R. Lang, VLA observations of compact, variable sources on the Sun, Astrophysical Journal (1986) - to be published.

7. K.R. Lang, R.F. Willson, K.T. Strong and K.L. Smith, Simultaneous Solar Maximum Mission and Very Large Array observations of solar active regions, Astrophysical Journal (1986) - to be submitted.

8. K.R. Lang, R.F. Willson, K.T. Strong and K.L. Smith, Physical parameters of solar active regions inferred from thermal cyclotron lines and soft X-ray spectral lines, Astrophysical Journal (1986) - to be submitted.

CORONAL DIAGNOSTICS*

KENNETH R. LANG

Department of Physics and Astronomy

Tufts University

Medford, MA 02155

* To be published in Coronal and Prominence Plasmas, a NASA Workshop Proceedings, U.S. Government Printing Office, Washington, D.C., 1986.

CORONAL DIAGNOSTICS

KENNETH R. LANG

Department of Physics and Astronomy
Tufts University
Medford, MA 02155

INTRODUCTION

The relatively recent development of satellite-bourne X-ray telescopes and ground-based aperture synthesis radio telescopes has led to an examination of the solar corona with unprecendented resolution in space, time and frequency. The high spatial and spectral resolution of the X-ray instruments aboard Skylab and the Solar Maximum Mission (SMM) satellite have, for instance, showed that coronal loops dominate the structure of the Sun's lower corona [see Vaiana and Rosner (1978) for a review]. Strong magnetic fields hold a hot, dense plasma within the ubiquitous coronal loops.

Observations of soft X-ray spectral lines indicate that the quiescent, or non-flaring, coronal loops have electron temperatures $T_e \sim 2$ to 4×10^6 K and electron densities $N_e \sim 10^9$ to 10^{11} cm $^{-3}$ with total extents $L \sim 10^9$ to 10^{10} cm. Similar temperatures are inferred from radio-wavelength brightness temperatures that are comparable to the local electron temperatures.

The detailed temperature and magnetic structure of the quiescent, or non-flaring, coronal loops has been inferred from radio wavelength synthesis observations. Synthesis maps describe the two-dimensional distribution of source brightness and the two-dimensional structure of the magnetic field [see Kundu and Lang (1985) for a review]. The unique ability to specify the strength and structure of the coronal magnetic fields is an important aspect of the radio wavelength synthesis maps.

Our current understanding of coronal loops is summarized in this chapter. It includes observations from ground-based radio telescopes and from X-ray telescopes lofted above the atmosphere, as well as theoretical interpretations of these observations.

The remaining sections of this introductory overview highlight both the observational and theoretical results that are discussed in greater detail in the following papers. We begin by discussing the three-dimensional structure of coronal loops. Alternative radiation mechanisms are then described within the context of both the radio and X-ray emission. Various methods of determining the strength and structure of the coronal magnetic field are then described. The final sections of

this introduction include the coronae of nearby stars and future prospects for radio diagnostics of coronal loops.

THREE DIMENSIONAL STRUCTURE OF CORONAL LOOPS

Observations at different radio wavelengths generally sample different levels within coronal loops, with longer wavelengths referring to higher levels. The heights of the radio structures can be inferred from their angular displacements from underlying photospheric features, and the two-dimensional maps at different radio wavelengths can be combined to specify the three-dimensional structure of coronal loops. The accuracy of these height determinations depends on the geometry of the magnetic field, and the accuracy is greatest near the limb.

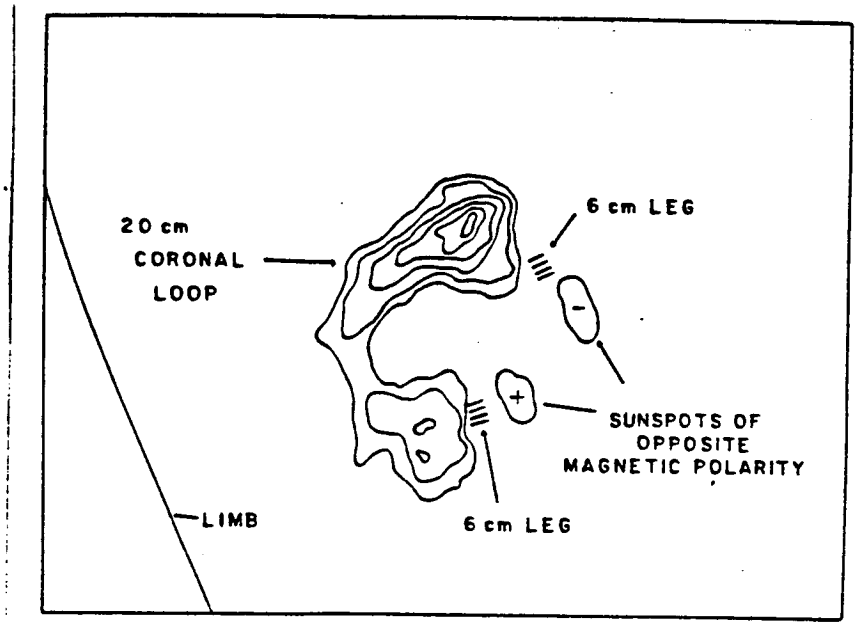

Figure 1. A VLA synthesis map of the total intensity, I, of the 20 cm emission from a coronal loop. The contours mark levels of equal brightness temperature corresponding to 0.2, 0.4, ...1.0 times the maximum brightness temperature of $T_B = 2 \times 10^6$ K. A schematic portrayal of the 6 cm emission, which comes from the legs of the magnetic loops, has been added together with the underlying sunspots that are detected at optical wavelengths.

Multiple-wavelength synthesis observations with the Very Large Array (VLA) have been carried out at wavelengths λ = 20, 6 and 2 cm (see Figure 1). The radiation at 20 cm can originate at both the apex and legs of coronal loops, and sometimes delineates the hot, dense plasma detected at X-ray wavelengths. The 20-cm coronal loops have brightness temperatures $T_B = 1 \times 10^6$ to 4×10^6 K and extents of $L = 10^9$ to 10^{10} cm. Magnetic field strengths of H 145 G have been inferred from cyclotron lines at the apex of the 20-cm loops. Bright, highly polarized 6-cm cores often mark the legs of dipolar loops with $T_B = 2 \times 10^6$ to 5×10^6 K and heights $h \approx 10^9$ cm above the underlying sunspots. Values of H of ~ 600 to 900 G are inferred from the fact that these cores emit gyroradiation at the second or third harmonic of the gyrofrequency. The 2-cm emission has brightness temperatures of $T_B \approx 10^5$ K and often overlies sunspots at heights $h \approx 5 \times 10^8$ cm where H is $\approx 10^3$ G.

The 20-cm coronal loops have been discussed by Velusamy and Kundu (1981), Lang, Willson and Rayrole (1982), Dulk and Gary (1983), and McConnell and Kundu (1984). Multiple-wavelength VLA observations at 2, 6 and 20 cm have been presented by Lang, Willson and Gaizauskas (1983), Shevgaonkar and Kundu(1984), Kundu and Lang (1985) and Kundu (1986 - this proceedings). Most recently, Gary and Hurford (1986) have used microwave spectroscopy during a solar eclipse to delineate the physical conditions at a variety of levels within the legs and apex of a coronal loop (see Figure 2.

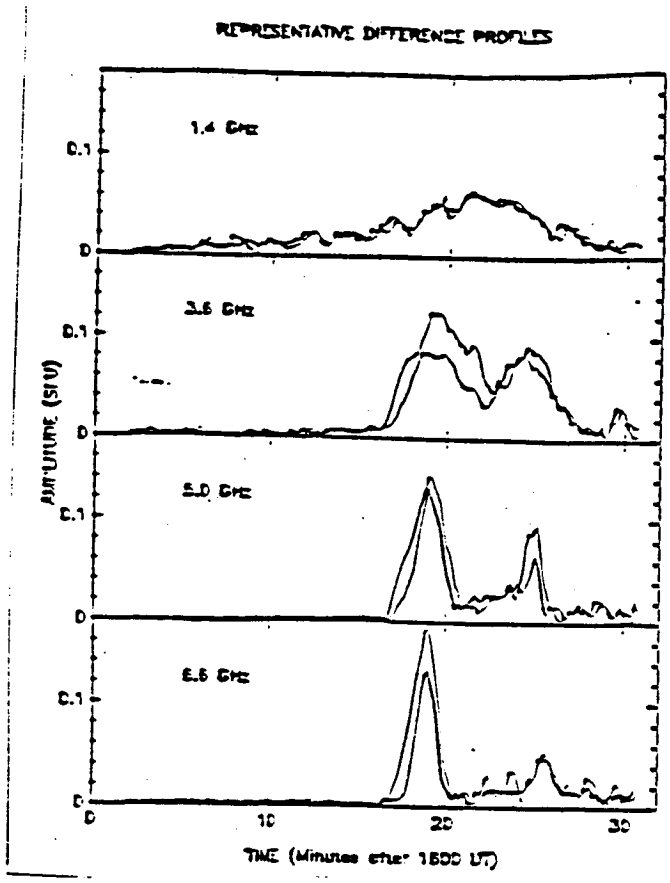

Figure 2. Differenced OVRO time profiles at four representative frequencies. Right hand circular (RH) polarization is shown by the heavy lines, and left hand (LH) polarization by the light lines. Below 3 GHz, the active region appears as a single board source. At higher frequencies, the region bifurcates into two main sources, becoming more localized to the sunspots as the observing frequency increases. The sense of polarization in the two spot sources is consistent with gyroresonance emission.

RADIATION MECHANISMS OF CORONAL LOOPS

The quiescent, or non-flaring, radiation of coronal loops is usually thermal in nature. The soft X-ray radiation is, for example, attributed to the thermal bremsstrahlung of hot million-degree electrons. However, at centimeter wavelengths there are two different thermal mechanisms: the bremsstrahlung of thermal electrons accelerated in the electric field of ions and the gyroresonant radiation of thermal electrons accelerated by magnetic fields can contribute to the emission. While the thermal bremsstrahlung emission is sensitive to the electron temperature and emission measure, gyroresonant emission is sensitive to the local magnetic field and electron temperature. It is this gyroresonant radiation which provides a sensitive measure of coronal magnetic field strength. Thus, it is important to distinguish which of these mechanisms is responsible for the emission from any given source at these wavelengths.

Strong evidence for thermal gyroradiation at coronal levels above sunspots has been provided by comparing the soft X-ray and centimeter-wavelength radiation of active regions [Kundu, Schmahl and Gerassimenko (1980); Pallavicini, Sakurai and Vaiana (1981); Schmahl et al. (1982)]. Although there is intense X-ray emission from the apex of coronal loops, the X-ray radiation often falls to undetectable levels in the legs of coronal loops above sunspots. Yet, intense radio radiation has sometimes been observed from both the apex and the legs of coronal loops. At other times radio emission has been detected from just the apex or just the legs of the loops, depending on the wavelength and observing conditions.

The near equality of the radio brightness and electron temperatures indicates that the radio emission from coronal loops is usually thermal. But the low electron densities inferred from the X-ray data above sunspots indicate that thermal bremsstrahlung is too weak to account for the intense radio radiation. The extra source of opacity has been attributed to gyroresonance absorption at the second or third harmonic of the gyrofrequency.

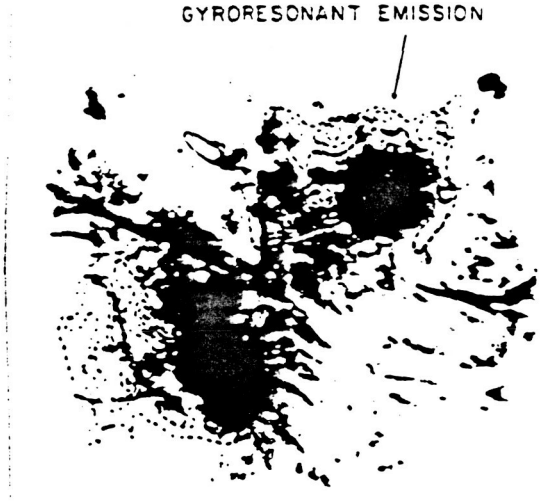

ORIGINAL PAGE IS
OF POOR QUALITY

Figure 3. A Westerbork Synthesis Radio Telescope synthesis map of circular polarization at $\lambda = 6$ cm overlaid on an Hα photograph obtained from the observatory at Athens. The contours are in steps of 1.5×10^5 K. The circularly polarized horseshoe structure that rings the sunspot umbra is due to gyroresonant emission in the curved magnetic fields of the sunspot penumbra.

Thermal gyroradiation at coronal levels above sunspots has been additionally confirmed by the detection of circularly polarized ring-shaped or horseshoe structures at 6 cm wavelength [Alissandrakis and Kundu (1982); Lang and Willson (1982)]. The highly-polarized (up to 100 percent) structures were precicted by the theory of gyroradiation in the curved magnetic fields above sunspot penumbrae [Gel'freikh and Lubyshev (1979)]. There is no detectable circular polarization above the central sunspot umbrae where the magnetic fields project radially upward into the hot coronal regions (see Figure 3). Depressions in the radio brightness temperature above sunspot umbrae have been attributed to cool material in these regions [Strong, Allisandrakis and Kundu(1984)].

At the longer, 20 cm, wavelength, emission is detected sometimes from both the apex and the legs of coronal loops (Lang, Willson, Strong, and Smith, 1986, and see Figure 4), and sometimes from just the apex (Webb et al., 1986). In the latter case, the electron densities and temperatures inferred from the X-ray spectral lines indica that the plasma is optically thick at 20 cm, and hence that the observed brightness temperature should be equal to the electron temperature. However, the observed brightness temperature is a factor of 2 - 3 lower than the local electron temperature Brosius and Holman (1986--this proceedings) and Holman (1986--this proceedings) expla this low brightness temperature in terms of a relatively cool, $<10^5$ K external plasma around the hot 2.5×10^6 K loops. Such material absorbs emissions primarily from the loop footpoints, where the optical depth along the line of sight is greatest. The loops and the external plasma are separated by a thin transition zone. The emission measure distributions for such models have been calculated, and have been found not only to agree well with recent observational emission measure curves for solar active region loops, but also to rise on both the cool and the hot side of the emission measure minimum. This is the first time that a theoretical emission measure curve fo a single active region loop has been found to do this (cf. Antiochos and Noci, 1986).

Figure 4. A comparison of the soft X-ray (S.M.M.-left), H (SOON-middle) and 20 cm (V.L.A.-right) emission of an active region on the same day. The most intense soft X-ray emission is well correlated with intense 20 cm and H emission; but the 20 cm emission also extends across the areas near the sunspots where it is also intense. The angular spacing between fiducial marks on the axes is 60 arc-seconds.

ORIGINAL PAGE IS
OF POOR QUALITY

Alternative radiation mechanisms may be required for intense radio emission from regions overlying weak photospheric magnetic fields. Observations of these regions have been reported by Akmedov et al. (1986), Lang (1986a-this prodeedings), Lang and Willson (1986a-this proceedings), Webb, Davis, Kundu and Velusamy (1983), and Willson and Lang(1986). A possible explanation, first studied in detail by Chiuderi, Drago a Melozzi (1984), is the nonthermal synchrotron emission of mildly relativistic electrons; but some currently-unspecified mechanism must be accelerating the electrons. An equally plausible explanation is that currents amplify the magnetic field in the low solar corona to strengths that are a factor of ten larger than those inferred from magnetograms of the underlying photosphere. The observed radio emission might then be attributed to the gyroradiation of thermal electrons at the second and third harmonic of the gyrofrequency.

SPECIFYING THE CORONAL MAGNETIC FIELD

Measurements of the spectrum, polarization and angular size of active region sources at centimeter wavelengths have been pioneered by Soviet astronomers using the RATAN 600 [Radio Astronomy Telescope of the Academy of Sciences (Nauk)-see Akmedov et al. (1986)], and further developed and extended using the frequency-agile interferometer at the OVRO [Owens Valley Radio Observatory-see Hurford and Gary (198 this proceedings)]. By measuring both the angular size and the flux density at a variety of wavelengths, one can uniquely determine the brightness temperature spectru of the sources. Circular polarization data can additionally be used to specify the magnetic field strength. Hurford and Gary (1986-this proceedings) have used this technique of microwave spectroscopy to measure the field distribution in the lower corona above sunspots.

In fact, both the strength and structure of the coronal magnetic field can be specified along the legs of coronal loops where gyroradiation dominates. The observations indicate that the magnetic fields systematically diverge and decrease in strength at higher heights (longer wavelengths) above single sunspots [see Hurford and Gary (1986) - this proceedings].

The magnetic field strength can also be inferred from individual cyclotron lines when gyroradiation dominates the emission. The observations at a single wavelength refer to a predetermined height where the radiation frequency is at one of the low harmonics of the gyrofrequency. Multiple-frequency observations provide information at a fixed height, regardless of field strength.

Holman and Kundu (1985) and Holman (1986 - proceedings) have pointed out that the emitting layers might be spatially resolved when a thin loop is observed. The magnetic field strength within each layer can then be inferred from the observing wavelength and the relevant harmonic. However, the cyclotron lines may overlap when the loop is thick or when a thin loop is observed along its legs.

ORIGINAL PAGE IS
OF POOR QUALITY

The spectrum of an individual cyclotron line may also be obtained when observing at several wavelengths. For example, the spectra of individual cyclotron lines have been observed at wavelengths near 20 cm when the apex of a coronal loop is resolved [Willson (1985), Lang (1986a-this proceedings), Lang, Willson, Strong and Smith (1986)]. This is because the magnetic field strength is relatively constant near the loop apex; the cyclotron lines would merge into a continuum along the loop legs where the magnetic field strength decreases uniformly with height. Neutral current sheets might also play a role, leading to intense radio emission from a thin layer near the loop apex. Both a uniform field and a steep temperature gradient in the uniform region are probably required to detect the cyclotron lines. In any event observations of individual cyclotron lines indicate magnetic field strengths of $H = 145 \pm 5$ G at the apex of some coronal loops.

Solar bursts might also be used to infer the strength and configuration of coronal magnetic fields. Roberts, Edwin and Benz (1984) and Roberts (1984, 1986 - proceedings) have shown that bursts can impulsively generate magneto-acoustic oscillations in a coronal loop. These oscillations may be observed as quasi-periodic radio variations whose onset, duration and periodicity can be used to infer the height, size and magnetic field strength of the emitting region.

THE CORONAE OF NEARBY STARS

Nearby main-sequence stars of late spectral type exhibit quiescent, or non-flaring, X-ray emission whose absolute luminosity may be as much as 100 times that of the Sun [Vaiana et al. (1981)]. This suggests that these stars have hot stellar coronae with large-scale coronal loops and strong magnetic fields. The solar analogy suggests that these coronae might also be detected at radio wavelengths.

Nearby dwarf M flare stars do, in fact, exhibit slowly varying radio emission at 6 and 20 cm wavelength that is analogous to that of solar active regions. However, the X-ray observations rule out detectable thermal bremsstrahlung at radio wavelengths; the temperatures and emission measures inferred from the X-ray data indicate that the radio bremsstrahlung would be at least two orders of magnitude below detection thresholds. Moreover, thermal gyroradiation is an unlikely source of the intense 20 cm radiation from some of these stars; implausibly large coronal loops would have to be up to 10 times larger than the star with magnetic field strengths larger than 100 G at these remote distances. The most likely source of this slowly varying radiation in M-dwarf stars is gyrosynchrotron radiation from nonthermal electrons (Holman, 1986; Lang and Willson, 1986b).

In other words, the fact that we detect radio emission from these stars means that something unusual is happening on them. As an example, radio bursts from the dwarf M, stars have been attributed to coherent emission mechanisms like electron-cyclotron masers or coherent plasma radiation [Melrose and Dulk (1982); Dulk (1985)].

Quasi-periodic and individual spikes have been detected from the dwarf M star AD Leonis at 20 cm wavelength [Lang et al. (1983), Lang and Willson (1986a), Lang (1986a)-this proceedings)]. These spikes are up to 100% circularly polarized with rise times less than 5 milliseconds. The rapid rise time indicates that the emitter's size is less than 0.005 of the star's radius, and that a symmetric emitter has a brightness temperature in excess of 10^{16} K. Such a high brightness temperature requires a coherent radiation mechanism. Similar high brightness temperature spikes

ORIGINAL PAGE IS
OF POOR QUALITY

have been observed during solar flares. Unlike solar flares, however, the underlying nonspiky emission from the AD Leonis flare is probably also coherent [Holman, Bookbinder and Golub (1985)].

Coherent emission is also suggested by the narrow-band, slowly varying, 20-cm emission from the dwarf M star YZ Canis Minoris [Lang and Willson (1986)], as well as narrow-band 20 cm flares from the red dwarf stars AD Leo and UV Ceti [White, Kundu and Jackson (1986)]. The narrow-band structure cannot be explained by continuum emission processes such as thermal bremsstrahlung, thermal gyroradiation, or nonthermal gyrosynchrotron radiation. Coherent radiation processes seem to be required.

If the radiation is emitted by an electron-cyclotron maser at the second harmonic of the gyrofrequency, then the magnetic field strength is H = 250 G, and constraints on the plasma frequency imply an electron density of $N_e \approx 6 \times 10^9$ cm^{-3}. Coherent plasma radiation at the first or second harmonic of the plasma frequency respectively require $N_e = 2 \times 10^{10}$ cm^{-3} and H << 500 G or $N_e = 6 \times 10^9$ cm^{-3} and H << 250 G. Thus, the coherent burst mechanisms suggest that the coronae of dwarf M stars have physical parameters similar to those of solar active regions.

FUTURE PROSPECTS FOR CORONAL DIAGNOSTICS

Probable observations of coherent radiation processes on nearby stars are stimulating further searches for coherent signatures in the Sun's radio radiation. In fact, narrow-band structure has been observed in a solar burst [Lang and Willson (1984): Lang (1986b)], and rapid spikes during some solar bursts have been interpreted in terms of electron-cyclotron masers [Holman, Eichler and Kundu (1980); Holman (1983)] Future observations with high resolution in time and frequency at the VLA, OVRO and Nancay will help determine the role that coherent radiation processes play in solar active regions.

The next decade will also include detailed comparisons of radio and X-ray observations with model coronal loops that include both thermal bremsstrahlung and thermal gyroradiation. Coronal magnetic fields may be directly inferred from observations and models in which the expected radio emission is computed as a function of wavelength, polarization and viewing angle. A comparison of the observed radiation with theoretical expectations will determine magnetic field strengths, electron densities and electron temperatures.

The evolution of coronal loops has strong future potential. Of special interest are the preheating and magnetic changes that trigger solar bursts [see Kundu and Lang (1985) for a review]. Emerging coronal loops and the magnetic interaction of existing coronal loops will be particularly interesting topics.

Future studies of the evolution of the three-dimensional magnetic and plasma structure of coronal loops will lead to valuable new insights to the nature of solar active regions and eruptions on the Sun and nearby stars. Such insights can only be fully realized by the development of a solar-stellar synthesis radiotelescope. Such an instrument would be dedicated to solar and stellar observations with high angular, temporal and frequency resolution.

ACKNOWLEDGEMENTS

Radio astronomical studies of the Sun at Tufts University are supported under Air Force Office of Scientific Research grant AFOSR-83-0019 and contract N0014-86-K-0068 with the Office of Naval Research. Our simultaneous VLA and Solar Maximum Mission satellite observations of the Sun are supported under NASA grant NAG 5-501.

REFERENCES

Akhmedov, S.B., et al., 1986, "Structure of a Solar Active Region from RATAN 600 and Very Large Array Observations," Astrophys. J., 301, 460-464.

Alissandrakis, C.E. and M.R. Kundu, 1982, "Observations of Ring Structure in a Sunspot Associated Source at 6 Centimeter Wavelength," Astrophys. J. (Letters), 253, L49-L52.

Alissandrakis, C.E. and M.R. Kundu, 1984, "Center-to-Limb Variation of a Sunspot-Associated Microwave Source," Astron. Astrophys., 139, 271-284.

Antiochos, S.K. and G. Noci, 1986 "The Structure of the Static Corona and Transition Region," Astrophys. J., 301, 440-447

Brosius, J.W. and G.D. Holman, 1986, "Theoretical Models of Free-Free Microwave Emission from Solar Magnetic Loops," this Proceedings.

Chiuderi-Drago, F. and M. Melozzi, 1984, "Non-Thermal Radio Sources in Solar Active Regions," Astron. Astrophys. 131, 103-110.

Dulk, G.A., 1985, "Radio Emission from the Sun and Stars," Ann. Rev. Astron. Ap., 23, 169-180.

Dulk, G.A. and D.E. Gary, 1983, "The Sun at 1.4 GHz: Intensity and Polarization," Astron. Astrophys. 124, 103-107.

Gary, D.E. and G.J. Hurford, 1986, "Multi-Frequency Observations of a Solar Active Region During a Partial Eclipse, BBSO 259, submitted to Astrophys. J.

Gel'friekh, G.B. and B.I. Lubyshev, 1979, "Structure of Local Sources of the S Component of Solar Radio Emission," Sov. Astron. A.J., 23, 316-322.

Holman, G.D., 1983, "Some Recent Results in the Interpretation of High Brightness Temperature Microwave Spike Emission," Adv.Space Res., 2, No.11, 181-183

Holman, G.D., 1986, "Coronal Heating and the X-ray and Micorwave Emission from M-Dwarf Flare Stars," in Proceedings of the Fourth Cambridge Workshop on Cool Stars, Stellar Systems, and the Sun, eds. M. Zeilik and D.M. Gibson (Springer-Verlag), in press.

Holman, G.D., 1986, " High-Spatial-Resolution Microwaveand Related Observations as Diagnostics of Coronal Loops," - this Proceedings.

Holman, G.D., J. Bookbinder and L. Golub, 1985, "Implications of the 1400 MHz Flare Emission from AD Leo for the Emission Mechanism and Flare Environment," in Radio Stars, ed. R.M. Hjellming and D.M. Gibson, (Dordrecht: Reidel), 35-37.

Holman, G.D., D. Eichler and M.R. Kundu, 1980, "An Interpretation of Solar Flare Microspikes as Gyrosynchrotron Masering," in Radio Physics of the Sun - I.A.U. Symposium No. 86, ed. M.R. Kundu and T.E. Gergely, (Dordrecht: Reidel), 457-459.

Holman, G.D. and M.R. Kundu, 1985, "The Microwave Structure of Hot Coronal Loops," Astrophys. J., 292, 291-296.

Hurford, G.J. and D.E. Gary, 1986, "Measurement of Coronal Fields Using Spatially Resolved Microwave Spectroscopy," - this Proceedings.

Kundu, M.R., 1986, "Three Dimensional Structures of Solar Active Regions," this Proceedings."

Kundu, M.R. and C.E. Alissandrakis, 1984, "Structure and Polarization of Active Region Microwave Emission," Solar Phys., 94, 249-283.
Kundu, M.R. and K.R. Lang, 1985, "The Sun and Nearby Stars," Science, 228, 9-15.
Kundu, M.R., E.J. Schmahl and M. Gerassimenko, 1980, "Microwave, EUV and X-ray Observations of Active Region Loops: Evidence for Gyroresonance Absorption in the Corona," Astron. Astrophys. 82, 265-271.
Kundu, M.R. and T. Velusamy, 1980, "Observation with the VLA of a Stationary Loop Structure in the Sun at 6 cm Wavelength," Astrophys. J. (Letters), 240, L63-L65.
Lang, K.R., 1986a, "Coronal Plasmas on the Sun and Nearby Stars," this Proceedings.
Lang, K.R., 1986b, "Flare Stars and Solar Bursts: High Resolution in Time and Frequency," Solar Phys., in press.
Lang, K.R., J. Bookbinder, L. Golub and M. Davis, 1983, "Bright, Rapid, Highly Polarized Radio Spikes from the M Dwarf AD Leo," Astrophys. J. (Letters), 272, L15-L18.
Lang, K.R. and R.F. Willson, 1982, "Polarized Horseshoes Around Sunspots at 6 Centimeter Wavelength," Astrophys. J. (Letters), 255, L111-L117.
Lang, K.R. and R.F. Willson, 1983, "Multiple Wavelength Observations of Flaring Active Regions," Adv. Space Res. 2, No. 11, 91-100.
Lang, K.R. and R.F. Willson, 1984, "V.L.A. Observations of Flare Build-Up in Coronal Loops," Adv. Space Res. 4, No. 7, 105-110.
Lang, K.R. and R.F. Willson, 1986a, "Compact, Variable, Moving Sources on the Sun at 2 Centimeters Wavelength," this Proceedings.
Lang, K.R. and R.F. Willson, 1986b, "Narrow-Band, Slowly Varying Decimetric Radiation from the Dwarf M Flare Star YZ Canis Minoris," Astrophys. J. (Letters), 302, L17-L21.
Lang, K.R. and R.F. Willson, 1986c, "Millisecond Radio Spikes from the Dwarf M Flare Star AD Leonis," Astrophys. J., in press.
Lang, K.R., R.F. Willson and V. Gaizauskas, 1983, "Very Large Array Observations of Solar Active Regions III. Multiple Wavelength Observations," Astrophys. J., 267, 455-464.
Lang, K.R., R.F. Willson and J. Rayrole, 1982, "Very Large Array Observations of Coronal Loops at 20 Centimeter Wavelength," Astrophys. J., 258, 384-387.
Lang, K.R., R.F. Willson, K.T. Strong and K.L. Smith, 1986a, "Physical Parameters of a Solar Active Region Inferred from Thermal Cyclotron Lines and Soft X-Ray Spectral Lines, Astrophys. J., to be submitted.
Lang, K.R., R.F. Willson, K.T. Strong and K. L. Smith, 1986b, "Simultaneous Solar Maximum Mission and Very Large Array Observations of Solar Active Regions," Astrophys. J., to be submitted.
McConnell, D. and M.R. Kundu, 1983, "VLA Observations of a Solar Active Region and Coronal Loops," Astrophys. J., 269, 698-705.
Melrose, D.B. and G.A. Dulk, 1982, "Electron-Cyclotron Masers as the Source of Certain Solar and Stellar Bursts," Astrophys. J., 259, 844-858.
Pallavicini, R., T. Sakurai and G.S. Vaiana, 1981, "X-Ray, EUV and Centimetric Observations of Solar Active Regions: an Empirical Model for Bright Radio Sources," Astron. Astrophys., 98, 316-327.
Roberts, B., 1984, "Waves in Inhomogeneous Media," in The Hydrodynamics of the Sun, ESA SP-220, November.
Roberts, B., 1986, "Guided MHD Waves as a Coronal Diagnostic Tools," this Proceedings
Roberts, B., P.M. Edwin and A.O. Benz, 1984, "On Coronal Oscillations," Astrophys. J., 279, 857-865.
Schmahl, E.J., et al., 1982, "Active Region Magnetic Fields Inferred from Simultaneous VLA Microwave Maps, X-Ray Spectroheliograms, and Magnetograms," Solar Physics 80, 233-249.

Shevgaonkar, R.K. and M.R. Kundu, 1984, "Three-Dimensional Structures of Two Solar Active Regions from VLA Observations at 2, 6 and 20 Centimeter Wavelengths" Astrophys. J., 283, 413-420.

Strong, K.T., C.E. Alissandrakis and M.R. Kundu, 1984, "Interpretation of Microwave Active Region Structures Using SMM Soft X-Ray Observations," Astrophys. J., 277, 865-873.

Vaiana, G.S. and R. Rosner, 1978, "Recent Advances in Coronal Physics," Ann. Rev. Astron. Ap. 16, 393-405.

Vaiana, G.S., et al., 1981, "Results From An Extensive Einstein Stellar Survey," Astrophys. J., 245, 163-182.

Velusamy, T. and M.R. Kundu, 1981, "VLA Observations of Postflare Loops at 20 Centimeter Wavelength," Astrophys. J. (Letters), 243, L103-L107.

Webb, D.F., J.M. Davis, M.R. Kundu and T. Velusamy, 1983, "X-Ray and Microwave Observations of Active Regions," Solar Phys. 85, 267-283.

Webb, D.F., G.D. Holman, J.M. Davis, M.R. Kundu and R.K. Shevgaonkar, 1986, "The Plasma and Magnetic Field Properties of Coronal Loops Observed At High Spatial Resolution," submitted to Astrophys. J.

White, S.M., M.R. Kundu and P.D. Jackson, 1986, "Narrowband Radio Flares from Red Dwarf Stars," Astrophys. J., submitted.

Willson, R.F., 1983, "Possible Detection of Thermal Cyclotron Lines from Small Sources Within Solar Active Regions," Solar Phys., 89, 103-113.

Willson, R.F., 1985, "VLA Observations of Solar Active Regions at Closely Spaced Frequencies: Evidence for Thermal Cyclotron Line Emission," Astrophys. J., 298, 911-917.

CORONAL PLASMAS ON THE SUN AND NEARBY STARS*

KENNETH R. LANG

Department of Physics and Astronomy

Tufts University

Medford, MA 02155

* To be published in Coronal and Prominence Plasmas, a NASA Workshop Proceedings, U.S. Government Printing Office, Washington, D.C. 1986.

CORONAL PLASMAS ON THE SUN AND NEARBY STARS

KENNETH R. LANG

Department of Physics and Astronomy
Tufts University
Medford, MA 02155

INTRODUCTION

The Very Large Array (VLA) has been used to observe solar microwave sources with second-of-arc angular resolution. Both the quiescent, or non-flaring, microwave sources and the flaring ones are usually resolved. They are often associated with the apex and/or legs of the ubiquitous coronal loops, which heretofore have been observable only with X-ray telescopes sent above the atmosphere. Multiple-wavelength VLA observations can specify the strength, evolution and structure of the magnetic fields in coronal loops, while also providing constraints on the electron density and electron temperature of the plasma trapped within the coronal loops.

VLA observations are providing new insights to the preburst heating and magnetic interaction that precede eruptions from solar active regions [Lang and Willson, (1983, 1984)]; but these interesting studies are not discussed here [see Kundu and Lang (1985) for a review]. We instead summarize our current understanding of the quiescent, or non-flaring, microwave emission from solar active regions. The next section briefly reviews the thermal radiation mechanisms that account for most of the quiescent emission, while also pointing out that current-amplified magnetic fields or non-thermal radiation may be required in some instances. This is followed by a discussion of the 20 cm radiation of coronal loops and the thermal cyclotron lines that accurately specify their magnetic field strength. The 20 cm and X-ray emission of the coronal plasma are then compared. We next discuss the coronae of nearby stars, where coherent radiation processes seem to prevail, and then conclude our summary with promising research opportunities for the future.

THERMAL RADIATION, CURRENTS AND NON-THERMAL RADIATION

The quiescent microwave emission of solar active regions has been attributed to the thermal radiation of hot electrons trapped within the strong magnetic fields of coronal loops. The microwave brightness temperature is then on the order of the million-degree electron temperature, and either thermal bremsstrahlung or thermal gyroresonant radiation dominate the emission. Bremsstrahlung, or braking radiation, is emitted when the thermal electrons are accelerated in the electric fields of ions and gyroresonant radiation is emitted when the thermal electrons are accelerated by magnetic fields.

Strong evidence for gyroresonant radiation at coronal levels above sunspots was provided by a comparison of microwave, EUV and X-ray observations [Kundu, Schmahl and Gerassimenko (1980); Pallavicini, Sakurai and Vaiana (1981)]. The near equality of the microwave brightness and electron temperatures indicated that the microwave emission was thermal, but the absence of detectable X-ray radiation above sunspots indicated a relatively low electron density there. This meant that the high microwave brightness temperature above sunspots could not be due to bremsstrahlung, but it could be explained by thermal gyroresonant radiation at the second or third harmonic of the gyrofrequency.

Thermal gyroradiation at coronal levels above sunspots was fully confirmed by the detection of circularly polarized ring-shaped or horseshoe structures [Allisandrakis and Kundu (1982); Lang and Willson (1982)] that were predicted using the theory of gyroresonant radiation in the curved magnetic fields above individual sunspots [Gel'freikh and Lubyshev(1979]. These structures were observed at 6 cm wavelength where circular polarizations as high as 100% were detected. Bright sunspot-associated sources observed at 2 to 6 centimeters wavelength are now widely believed to be due to the gyroradiation of million-degree electrons spiralling about strong magnetic fields above sunspots.

But there is another class of compact, bright microwave sources in this wavelength range that are not associated with sunspots. They occur above regions of apparently-weak photospheric magnetic fields. For instance observations at 6 cm wavelength revealed sources with coronal brightness temperatures $T_B > 10^6$ K in regions away from sunspots [Schmahl et al. (1982); Webb, Davis, Kundu and Velusamy (1983)]. Force-free (potential) magnetic field extrapolations from the known photospheric values indicate that the magnetic field in the low solar corona is too weak to account for the observed emission by gyroradiation.

The situation is even worse at shorter wavelengths where stronger magnetic fields are required to produce gyroradiation at the first few harmonies of the gyrofrequency. (Higher harmonics produce insufficient optical depth to account for the high brightness temperatures.) Lang and Willson (1986a-this proceedings) and Willson and Lang (1986) report the presence of compact, bright 2-cm sources that require magnetic field strengths of $H \approx 2{,}000$ G in the low solar corona at regions away from sunspots if they are attributed to gyroresonance radiation.

Bright microwave sources in regions of apparently-weak photospheric fields can be explained by two different hypotheses. First, the emission could be thermal gyroradiation at the second or third harmonic of the gyrofrequency in strong magnetic fields. Currents might amplify the magnetic field in the low corona to values greater than those expected from extrapolations from the photosphere. Alternatively the photospheric magnetograms could be misleading, and strong magnetic fields could exist in isolated regions away from sunspots. Secondly, the emission could be nonthermal radiation in weak magnetic fields. Nonthermal synchrotron radiation from midly relativistic electrons is one possibility, but some as yet unspecified mechanism must be continuously accelerating the electrons [Akhmedov et al. (1986), Chiuderi-Drago and Melozzi (1984); Willson and Lang (1986)].

Figure 1 provides the radiation spectra for the three types of sources usually detected at short centimeter wavelengths [see Akmedov et al. (1986) for greater details]. The most common type of source is the sunspot-associated component (A and C) that is attributed to thermal gyroresonance radiation in the legs of coronal loops that are connected to the underlying sunspots. Source D is a filament-associated component located above a magnetic neutral line in regions of apparently-weak magnetic field. Yet, this source has a steep radiation spectrum and high brightness temperature of $T_B > 7 \times 10^6$ K. It may be attributed to non-thermal radiation or to thermal gyroradiation in current-amplified magnetic fields. Then there is the filament-associated source B that has the flat spectrum of optically-thin thermal bremsstrahlung. Electron densities $N_e \approx 10^9$ to 10^{10} cm^{-3} are consistent with this interpretation, suggesting that in this case we are detecting the same thermal plasma that is observed at X-ray wavelengths from coronal loops. But this plasma is more commonly detected at the longer radio wavelength of 20 centimeters.

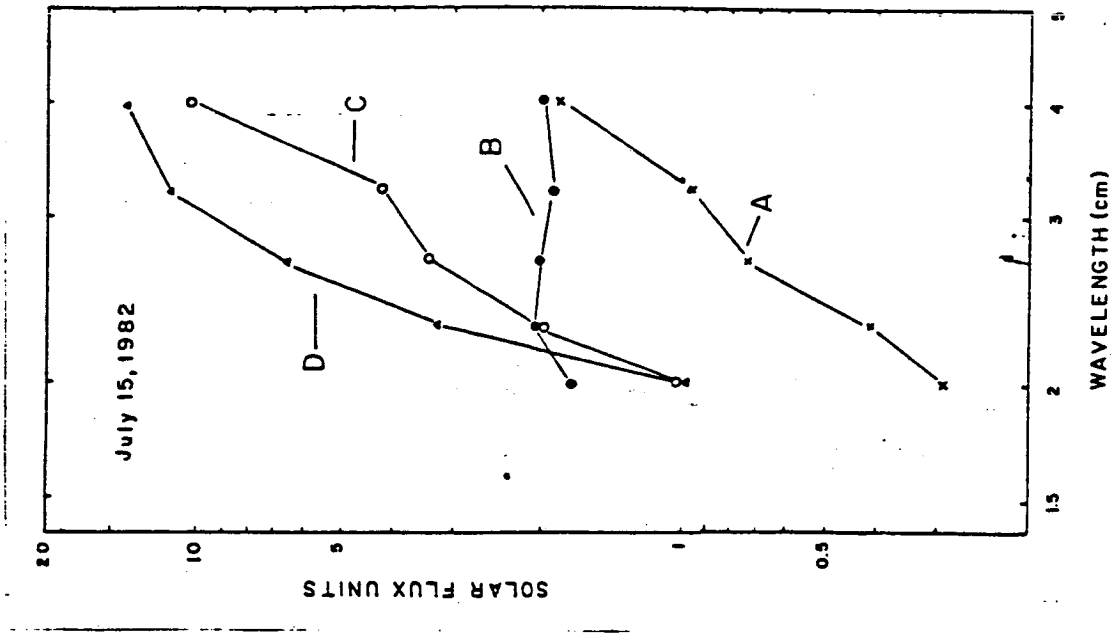

Figure 1. The radiation spectra of four sources associated with an active region. The steep spectrum of the filament-associated source D is attributed to the gryrosynchrotron radiation of mildly relativistic electrons whereas the flat spectrum of the source B is attributed to thermal bremsstrahlung. The sunspot-associated sources A and C are attributed to gyroresonance emission in the legs of coronal loops.

CORONAL LOOPS AT 20 CM WAVELENGTH AND THERMAL CYCLOTRON LINES

Radiation from a post-flare loop at 20 centimeters wavelength was reported by Velusamy and Kundu (1981); but there is a much more extensive literature regarding the quiescent 20-cm radiation of coronal loops [Lang, Willson and Rayrole (1982); Lang, Willson and Gaizauskas (1983); McConnell and Kundu (1983); Shevgaonkar and Kundu (1984); Kundu and Lang (1985); Kundu (1986 - this proceedings); Lang (1986 - this proceedings)]. The radiation at this longer wavelength often comes from the hot, dense plasma trapped within the coronal loop (see Figure 2 for a typical example). The 20-cm coronal loops have peak brightness temperatures of 1×10^6 to 4×10^6 K and extents of about 10^{10} cm. Their radio emission can be attributed to thermal bremsstrahlung or thermal gyroresonant radiation, or both.

Of special interest is the recent detection of thermal cyclotron lines near the apex of coronal loops at wavelengths near 20 centimeters [see Figure 3 and Willson (1985) for greater details]. These cyclotron lines are emitted at harmonics of the gyrofrequency, with a wavelength that depends only on the harmonic number and the magnetic field strength. However, because the magnetic field in the legs of coronal loops decrease uniformly with height, the individual cyclotron lines at short wavelengths will usually merge into a smooth continuum.

ORIGINAL PAGE IS
OF POOR QUALITY

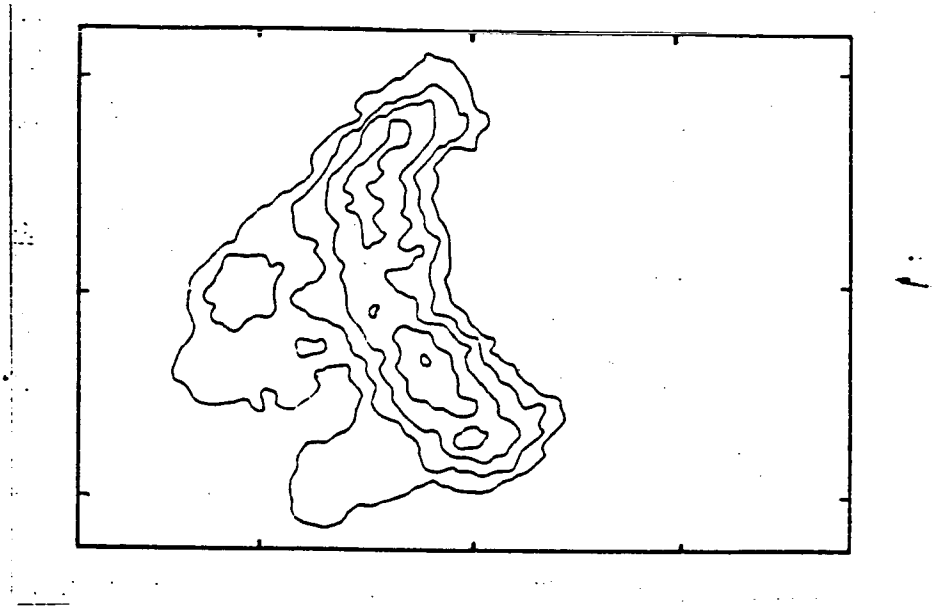

Figure 2. A typical radio wavelength (20 cm) V.L.A. map of the hot, million-degree plasma trapped in a coronal loop. The angular scale between fiducial marks on the axes is 60 arc-seconds.

At 20 centimeters wavelength we can observe the apex of coronal loops where the magnetic field is nearly constant and the spectrum of individual cyclotron lines can be resolved. This will be particularly true if currents or some other process confine the intense emission to a thin, hot layer within the loop apex.

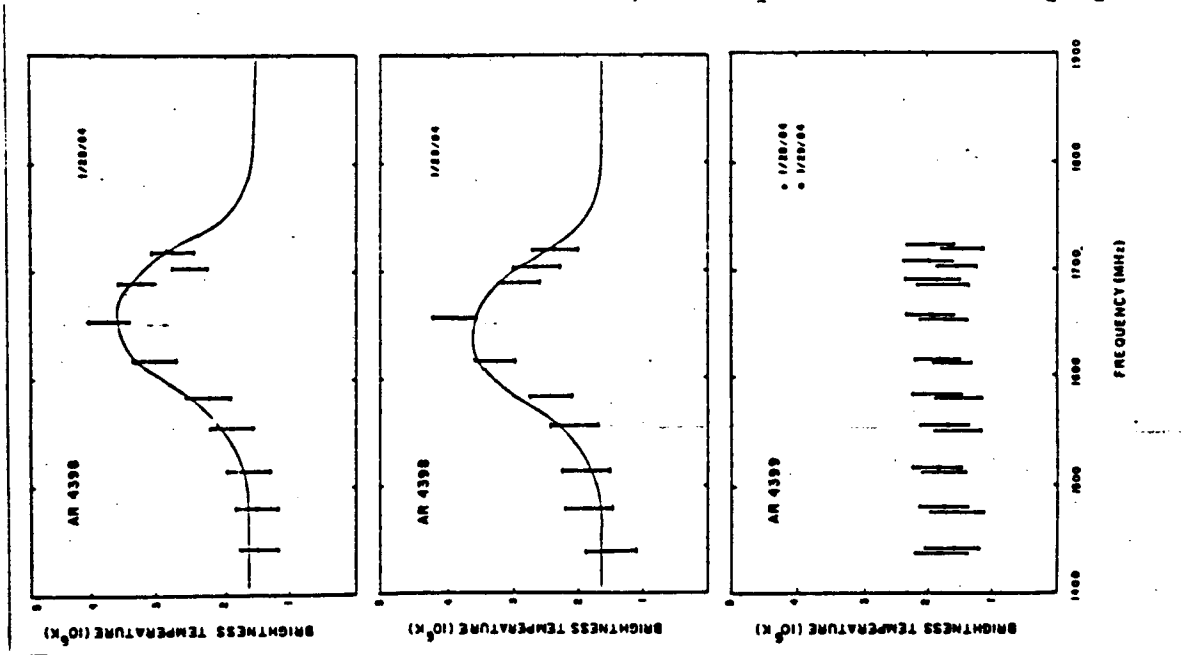

Figure 3. VLA data at ten closely-spaced frequencies near 1440 MHz (20 cm), showing thermal cyclotron line spectra from active region AR 4398 on successive days, together with optically-thick thermal bremsstrahlung spectra from active region AR 4399 on the same days.

Individual cyclotron lines from AR 4398 are shown in Figure 3 together with the flat spectrum of the nearby active region AR 4399. The flat spectrum of AR 4399 is attributed to thermal bremsstrahlung, whereas the spectrum of AR 4398 can be explained by cyclotron line emission from a narrow layer of width $\Delta L \approx 10^8$ cm, electron density $N_e \approx 10^9$ cm^{-3} and a relatively high electron temperature $T_e \approx 4 \times 10^6$ K (solid line). Here the harmonic number n = 4 and the magnetic field strength H = 145 G. A key aspect of this discovery is the extraordinary precision in measuring the magnetic field strength; a change of only $\Delta H = 20$ G shifts the central frequency of the line by 170 MHz.

COMPARISON OF THE 20 CM AND X-RAY EMISSION

As previously mentioned, comparisons between the X-ray and short microwave (3 to 6 cm) radiation from solar active regions provided evidence for a new source of opacity at microwave wavelengths above sunspots. It has been attributed to gyroresonance effects in the legs of coronal loops connecting with underlying sunspots. Recent comparisons of the 6 cm radiation from the apex of coronal loops indicates that its brightness temperature is less than the electron temperature measured at X-ray wavelengths; this has been explained by a cool ($\approx 10^5$ K) external plasma [Holman (1986 - this proceedings); Webb, Holman, Davis and Kundu (1986)].

However, there have been no published comparisons of X-ray data with the 20 cm emission of the coronal plasma. In some instances, there is radiation at 20 centimeters wavelength near sunspots where no X-ray radiation is detected. The radio emission may be attributed to gyroresonant radiation of a low density plasma in magnetic fields of strength H = 145 to 290 G (harmonic n = 4 to 2), [see Lang, Willson, Strong and Smith (1986a) for greater details].

In other cases, the 20 centimeter radiation appears at the apex of coronal loops, but with a slightly lower brightness temperature, $T_B \approx 1.4$ to 1.7×10^6 K, than the electron temperature, $T_e \approx 3.0 \times 10^6$ K, inferred from the X-ray data. This may be explained by a low temperature plasma with $T_e \approx 10^5$ K that lowers the effective brightness temperature of the radio bremsstrahlung while not affecting the X-ray data that only detects the 10^6 K plasma [see Holman (1986 - this proceedings); Lang (1986 - this proceedings); and Lang, Willson, Strong and Smith (1986a) for greater details]. Because the line of sight through the low temperature plasma is greatest along the legs of coronal loops, it can reduce the size of the radio source below that of the X-ray emission. That is, the low temperature plasma can, under the right circumstances, confine the detectable radio radiation to the apex of coronal loops.

As illustrated in Figure 4, there are other instances in which the 20-cm radiation and the soft X-ray emission have the same angular extent. In this case, the maximum brightness temperature of the radio emission has the same value as the electron temperature, $T_e = 3 \times 10^6$ K, inferred from the X-ray data. At first sight it would seem that the 20-cm emission is the thermal bremsstrahlung of the X-ray emitting plasma (electron density $N_e = 2 \times 10^{10}$ cm^{-3}), but in this instance we have also detected a cyclotron line. Preliminary modeling indicates a thin layer of $T_e \approx 4 \times 10^6$ K with a magnetic field strength of H = 145 or 187 G (harmonic n = 4 or 3). The thermal electrons that give rise to the X-ray radiation therefore also seem to produce strong gyroresonant radiation at 20 centimeters wavelength.

ORIGINAL PAGE IS
OF POOR QUALITY

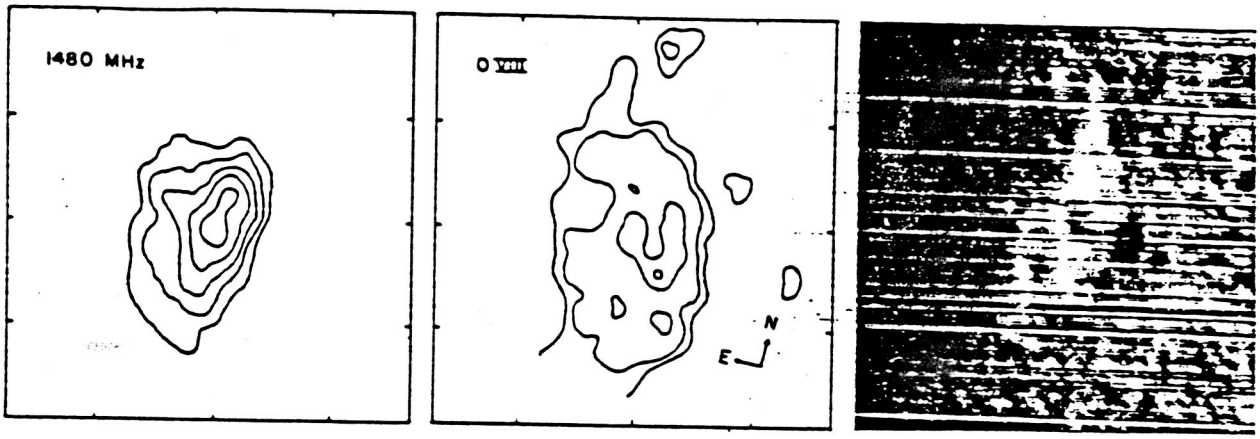

Figure 4. A comparison of the 20 cm emission (V.L.A-left), soft-X-ray (S.M.M.-middle) and Hα (SOON-right) emission of an active region on the same day. The angular spacing between fiducial marks on the axis is 60 arc-seconds.

CORONAE OF NEARBY STARS

Nearby dwarf M stars exhibit slowly-varying, quiescent microwave radiation and microwave bursts that have been detected with the Very Large Array (VLA) and the Arecibo Observatory. Observations with high resolution in frequency and time provide strong evidence for coherent radiation mechanisms in the coronae of these stars [Lang (1986b)]. Such mechanisms provide stringent constraints on the electron density and magnetic field strength in the stellar coronae.

Narrow-band, slowly varying radiation has been detected from the dwarf M star YZ Canis Minoris when using the VLA at wavelengths near 20 centimeters [Lang and Willson (1986b)]. White, Kundu and Jackson (1986) subsequently repeated this experiment, finding narrow-band bursts from the dwarf M stars AD Leonis and UV Ceti. The narrow-band structure cannot be explained by continuum emission processes such as thermal bremsstrahlung, thermal gyroresonant radiation or nonthermal gyrosynchrotron radiation. Although gyroresonant radiation can give rise to narrow-band cyclotron lines, it requires an implausibly large source that is hundreds of times larger than the star. The observations of narrow-band structure can apparently only be explained by coherent mechanisms like electron-cyclotron lines or coherent plasma radiation.

Independent evidence for coherent radiation mechanisms is provided by high-time-resolution observations of the dwarf M star AD Leonis at the Arecibo Observatory [Lang, Bookbinder and Golub (1983), Lang and Willson (1986c)]. As illustrated in Figure 5, quasi-periodic, highly polarized spikes are observed at 20 centimeters wavelength with rise times of less than 5 milliseconds. An upper limit to the linear size of the spike emitting region is $L < 1.5 \times 10^8$ cm, the distance

that light travels in 5 milliseconds. This size is only five hundredths of the estimated radius of AD Leonis. Provided that the emitter is symmetric, it has a brightness temperature greater than 10^{16} K. The high degrees of circular

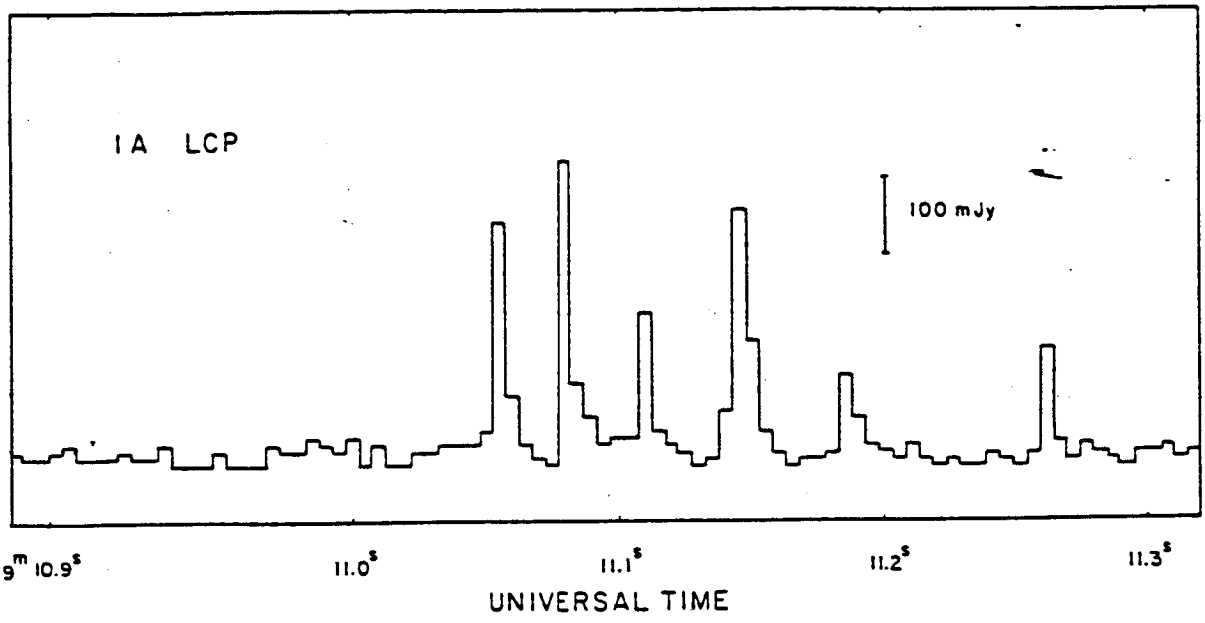

Figure 5. The total power detected at a frequency of 1415 MHz (21.2 cm) while tracking the dwarf M star AD Leonis. The left-hand circularly polarized (LCP) signal has been displayed with a 5 ms integration time. There are five quasi-periodic spikes with a mean periodicity of $T_p = 32 \pm 5$ ms and a total duration of $\tau_D = 150$ ms. Each of these spikes had a rise time of $\tau_R \leq 5$ ms, leading to an upper limit to the linear size $L \leq 1.5 \times 10^8$ cm for the spike emitter. A symmetric source of this size would have a brightness temperature of $T_B > 10^{16}$ K, requiring a coherent radiation mechanism.

polarization (up to 100%) indicate an intimate connection with the star's magnetic field, and the high brightness temperatures suggest a coherent radiation mechanism such as an electron-cyclotron maser or coherent plasma radiation.

The coherent process provides constraints on the electron density, N_e, and the magnetic field strength, H, in the stellar coronae [see Dulk (1985) for the relevant formulae]. If the electron-cyclotron maser emits at the second harmonic of the gyrofrequency, the longitudinal magnetic field strength H = 250 G and constraints on the plasma frequency imply an electron density of $N_e = 6 \times 10^9$ cm^{-3}. Coherent plasma radiation at the first or second harmonic of the plasma frequency respectively require $N_e = 2 \times 10^{10}$ cm^{-3} and and $H \ll 500$ G or $N_e = 6 \times 10^9$ cm^{-3} and $H \ll 250$ G.

PROMISING DIRECTIONS FOR THE FUTURE

Future VLA observations at 20 centimeters wavelength will continue to provide diagnostic tools for the solar corona. Observations of thermal cyclotron lines offer a promising method of accurately determining the coronal magnetic field strength. Comparisons with soft X-ray spectral lines will help delineate the

electron density and temperature, while also specifying the radiation mechanisms. One promising approach that grew out of this conference involves simultaneous observations with the VLA and the Owens Valley Radio Observatory (OVRO). The OVRO will provide spectral information that is not obtainable with the VLA, whereas the high angular resolution of the VLA will remove ambiguities in the OVRO data. Future collaborations between the Tufts University group and the Observatoire de Paris - Nancay Radio Heliograph will provide new perspectives to coherent radiation processes on the Sun. The rapidly growing studies of the microwave radiation from dwarf M and RS CVn stars will continue to provide new insights to physical processes in stellar coronae. The full potential of these studies of the Sun and nearby stars will only be realized by the development of a solar-stellar synthesis radiotelescope. Such an instrument would be dedicated to solar and stellar observations with high angular, temporal and frequency resolution.

ACKNOWLEDGEMENTS

Radio astronomical studies of the Sun at Tufts University are supported under Air Force of Scientific Research grant AFOSR-83-0019 and contract N0014-86-K-0068 with the Office of Naval Research. Simultaneous VLA and Solar Maximum Mission observations of the Sun are supported by NASA grant NAG 5-501.

REFERENCES

Akhmedov, S.B., et al., 1986, "Structure of a Solar Active Region from RATAN 600 and Very Large Array Observations," Astrophys. J., 301, 460-464.

Alissandrakis, C.E. and M.R. Kundu, 1982, "Observations of Ring Structure in a Sunspot Associated Source at 6 centimeter Wavelength", Astrophys. J. (Letters), 253, L49-L52.

Chiuderi-Drago, F. and M. Melozzi, 1984, "Non-Thermal Radio Sources in Solar Active Regions," Astrophys. 131, 103-110.

Dulk, G.A., 1985 "Radio Emission from the Sun and Stars," Ann, Rev. Astron. Ap., 23 169-180

Dulk, G.A. and D.E. Gary, 1983, "The Sun at 1.4 GHz: Intensity and Polarization," Astron. Astrophys., 124, 103-107

Gel'friekh, G.B. and B.I. Lubyshev, 1979, "Structure of Local Sources of the S Component of Solar Radio Emission " Sov. Astron. A.J., 23, 316.

Holman, G.D., 1986, "Determining Magnetic and Plasma Structure of Coronal Loops from Microwave and Soft X-ray Observations",: this Proceedings.

Kundu, M.R., 1986, "Three Dimensional Structure of Solar Active Regions," this Proceedings.

Kundu, M.R. and K.R. Lang, 1985, "The Sun and Nearby Stars,"Science, 228, 9-15.

Kundu, M.R., E.J. Schmahl and M. Gerassimenko, 1980, "Microwave, EUV and X-ray Observations of Active Region Loops: Evidence for Gyroresonance Absorption in the Corona,"Astron. Astrophys. 82, 265-271.

Kundu, M.R. and T. Velusamy, 1980, " Observation with the VLA of a Stationary Loop Structure in the Sun at 6 cm Wavelength," Astrophys. J. (Letters), 240, L62-L65.

Lang, K.R., 1986a, "Coronal Diagnostics "-this Proceedings.

Lang, K.R., 1986b, "Flare Stars and Solar Bursts: High Resolution in Time and Frequency," Solar Phys., in press.

Lang, K.R., J. Bookbinder, L. Golub and M. Davis, 1983, "Bright, Rapid, Highly Polarized Radio Spikes from the Dwarf AD Leo," Astrophys. J. (Letters), 272, L15-L18.

Lang, K.R. and R.F. Willson, 1982, "Polarized Horseshoes Around Sunspots at 6 Centimeter Wavelength.", Astrophys. J. (Letters), 255 L111-L117.
Lang, K.R. and R.F. Willson, 1983, "Multiple Wavelength Observations of Flaring Active Regions," Adv.Space Res. 2, No. 11, 91-100.
Lang, K.R. and R.F. Willson, 1984, "V.L.A. Observations of Flare Build-Up in Coronal Loops," Adv. Space Res. 4, no. 7, 105-110.
Lang, K.R. and R.F. Willson, 1986a, "Compact, Variable, Moving Sources on the Sun at 2 Centimeters Wavelength," this Proceedings.
Lang, K.R. and R.F. Willson, 1986b, "Narrow-Band, Slowly Varying Decimetric Radiation from the Dwarf M Flare Star YZ Canis Minoris," Astrophys. J. (Letters), 302, L17-L21.
Lang, K.R. and R.F. Willson, 1986c, "Millisecond Radio Spikes from the Dwarf M Flare Star AD Leonis," Astrophys. J., in press.
Lang, K.R., R.F. Willson and V. Gaizauskas, 1983, "Very Large Array Observations of Solar Active Regions III. Multiple Wavelengths Observations," Astrophys. J. 267, 455-464.
Lang, K.R., R.F. Willson and J. Rayrole, 1982, "Very Large Array Observations of Coronal Loops at 20 Centimeter Wavelength," Astrophys. J., 258, 384-387.
Lang, K.R., R.F. Willson, K.T. Strong and K.L. Simth, 1986a, "Simultaneous Solar Maximum Mission and Very Large Array Observations of Solar Active Regions", Astrophys. J., to be submitted.
Lang, K.R., R.F. Willson, K.T. Strong and K.L. Smith, 1986b, "Physical Parameters of Solar Active Regions Inferred from Thermal Cyclotron Lines and Soft X-ray Spectral Lines, Astrophys, J., to be submitted.
McConnell, D. and M.R. Kundu, 1983, "VLA Observations of a Solar Active Region and Coronal Loops," Astrophys. J., 269, 698-705.
Schmahl, E.J., et al., 1982, "Active Region Magnetic Fields Inferred from Simultaneous VLA Microwave Maps, X-ray Spectroheliongrams, and Magnetograms", Solar Phys. 80, 233-249.
Shevgaonkar, R.K. and M.R. Kundu, 1984, "Three-Dimensional Structures of Two Solar Active Regions from VLA Observations at 2, 6 and 20 Centimeter Wavelengths," Astrophys. J., 283, 413-420.
Strong, K.T., C.E. Alissandrakis and M.R. Kundu, 1984, "Interpretation of Microwave Active Region Structures Using SMM Soft X-ray Observations," Astrophys. J. 277, 865-873.
Velusamy, T. and M.R. Kundu, 1981, "VLA Observations of Postflare Loops at 20 Centimeter Wavelength," Astrophs. J. (Letters), 243, L103-L107.
Webb, D.M. J.M. Davis, M.R. Kundu and T. Velusamy, 1983, "X-ray and Microwave Observations of Active Regions," Solar Phys. 85, 267-283.
Webb, D.F., G.D. Holman, J.M. Davis and M.R. Kundu, 1986, "High-Spatial-Resolution Microwave and Soft X-ray Observations as Diagnostics of Solar Magnetic Loops", Astrophys. J., submitted
White, S.M., M.R. Kundu and P.D. Jackson, 1986, "Narrowband Radio Flares from Red Dwarf Stars, "Astrophys. J., submitted.
Willson,R.F., 1985, "VLA Observations of Solar Active Regions at Closely Spaced Frequencies: Evidence for Thermal Cyclotron Line Emission," Astrophys. J., 298, 911-917.
Willson, R.F. and K.R. Lang, 1986,"VLA Observations of Compact, Variable Sources on the Sun," Astrophys. J., in press.

COMPACT, VARIABLE, MOVING SOURCES OBSERVED ON THE SUN AT 2 CENTIMETERS WAVELENGTH*

KENNETH R. LANG and ROBERT F. WILLSON

Department of Physics and Astronomy

Tufts University

Medford, MA 02155

* To be published in Coronal and Prominence Plasmas, a NASA Workshop Proceedings, U.S. Government Printing Office, Washington, D.C. 1986.

COMPACT, VARIABLE, MOVING SOURCES OBSERVED ON THE SUN AT 2 CENTIMETERS WAVELENGTH

KENNETH R. LANG
ROBERT F. WILLSON

Department of Physics and Astronomy
Tufts University
Medford, MA 02155

INTRODUCTION

The high angular resolution provided by the Very Large Array (VLA) has permitted the spatial resolution of solar microwave sources and opened the way for comparisons with observations of similar angular resolution at optical and X-ray wavelengths. High-resolution VLA observations of solar active regions at relatively long wavelengths of 6 cm and 20 cm have, for example, led to the discovery of the microwave counterpart of the ubiquitous coronal loops that had previously only been observed by X-ray telescopes lofted above the Earth's atmosphere. The microwave emission of the coronal loops is attributed to the gyroresonant radiation and/or the bremsstrahlung of million-degree, thermal electrons trapped within the loops by strong magnetic fields; observations of this emission have provided valuable new insights into the nature of solar active regions and eruptions from the Sun and nearby stars [Kundu and Lang (1985); Lang (1986 a,b - this proceedings)].

In contrast, the short wavelength 2 cm emission of solar active regions is poorly understood. In spite of numerous VLA solar observations at 2 cm, there are only two published results [Lang, Willson and Gaizauskas (1983); Shevgaonkar and Kundu (1984)]. In both instances, compact (angular sizes $\theta \approx 15''$), highly polarized (degrees of circular polarization $\rho_c \approx 80\%$ to 90%) sources were found in regions of strong magnetic field (strength $H \approx 2{,}000$ G) above sunspots. The brightness temperatures of $T_B \approx 10^5$ K were characteristic of the electron temperature in the transition region.

Subsequent examination of the compact 2 cm sources in active regions indicated that they are variable over time scales of an hour or shorter. This probably explains the paucity of VLA results; synthesis maps averaged over 11 or 12 hours would not reveal several relatively-weak, time-variable sources.

To further complicate the matter, we have recently discovered compact, variable, highly-polarized 2 cm sources in regions of apparently-weak, photospheric magnetic field [Willson and Lang (1986)]. Our subsequent VLA observations have confirmed the existence of compact, variable 2 cm sources that are not associated with active regions, but these sources had no detectable circular polarization. In addition, both the unpolarized and polarized 2 cm sources were found to move laterally across the solar surface with velocities $V \approx 1$ km s^{-1}. In the next section we present observations of these compact, variable, moving sources. The concluding discussion mentions possible radiation mechanisms and implications for studies of the quiet Sun.

OBSERVATIONS

The VLA was used to observe the active region AR 4508 in the C configuration between 1530 and 2330 UT on June 4, 1984. The position of this region was N06 E57 at 1300 UT on this day. Follow-up observations were made between 1500 and 2300 UT on January 17, 1986 in the D configuration. In this case, a region of bright plage and relatively-weak magnetic fields (no sunspots) was observed; its position was S10 W62 at 1300 UT on this day.

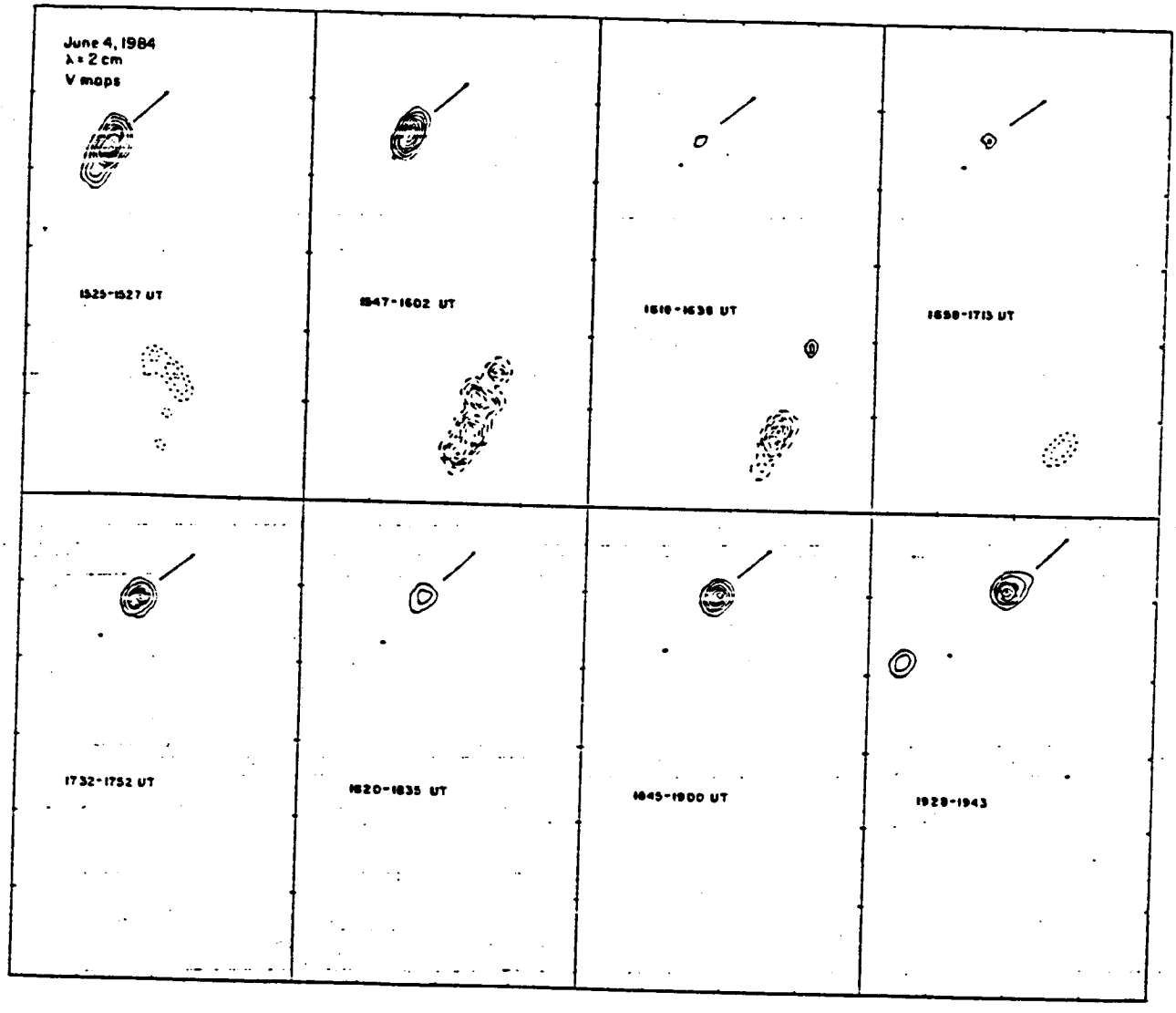

Figure 1. VLA synthesis maps of left circularly polarized (solid contours) and right circularly polarized (dashed contours) radiation at 2 cm wavelength. Here each box refers to the same area on the surface of the Sun, and the fiducial marks on the axes are separated by 10 arc-seconds. The northern source (top) varied over time scales of 30 minutes and moved laterally across the solar surface in the northwest direction a velocity of ~1 km s^{-1}. The southernmost source varied over a time scale of about 60 minutes, and moved laterally towards the southwest at a velocity of ~2 km s^{-1}. Here the contours mark levels of equal brightness with an outermost contour of 6.1×10^4 and a contour interval of 3.1×10^4 K.

As illustrated in Figure 1, the 2 cm maps on June 4 showed two compact ($\theta \approx 5''$), highly circularly polarized (ρ_c = 80 to 90%) sources that vary on time scales of 30 to 60 minutes. The left circularly polarized source (solid contours) varied in maximum brightness temperature from $T_B = 2.0 \times 10^5$ K to $T_B < 0.5 \times 10^5$ K. Here each box refers to the same area of the Sun, and the arrows illustrate systematic motion to the northwest with a total motion of about 15" in three hours. The left circularly polarized source was therefore moving laterally across the surface of the Sun with a velocity of $V \approx 1$ km s^{-1}. The right circularly polarized source (dashed contours) apparently moved towards the southwest at about twice this speed, but the motion is confused by the presence of more than one source.

Comparisons with Mt. Wilson magnetograms indicate that the two compact, variable, moving sources were located in regions of apprently-weak photospheric magnetic field ($H \lesssim 80$ G), and that they did not overlie sunspots. The high polarization of these sources is therefore somewhat enigmatic, for the polarization of thermal radiation requires strong magnetic fields of $H \approx 2{,}000$ G. We will return to this paradox in the discussion.

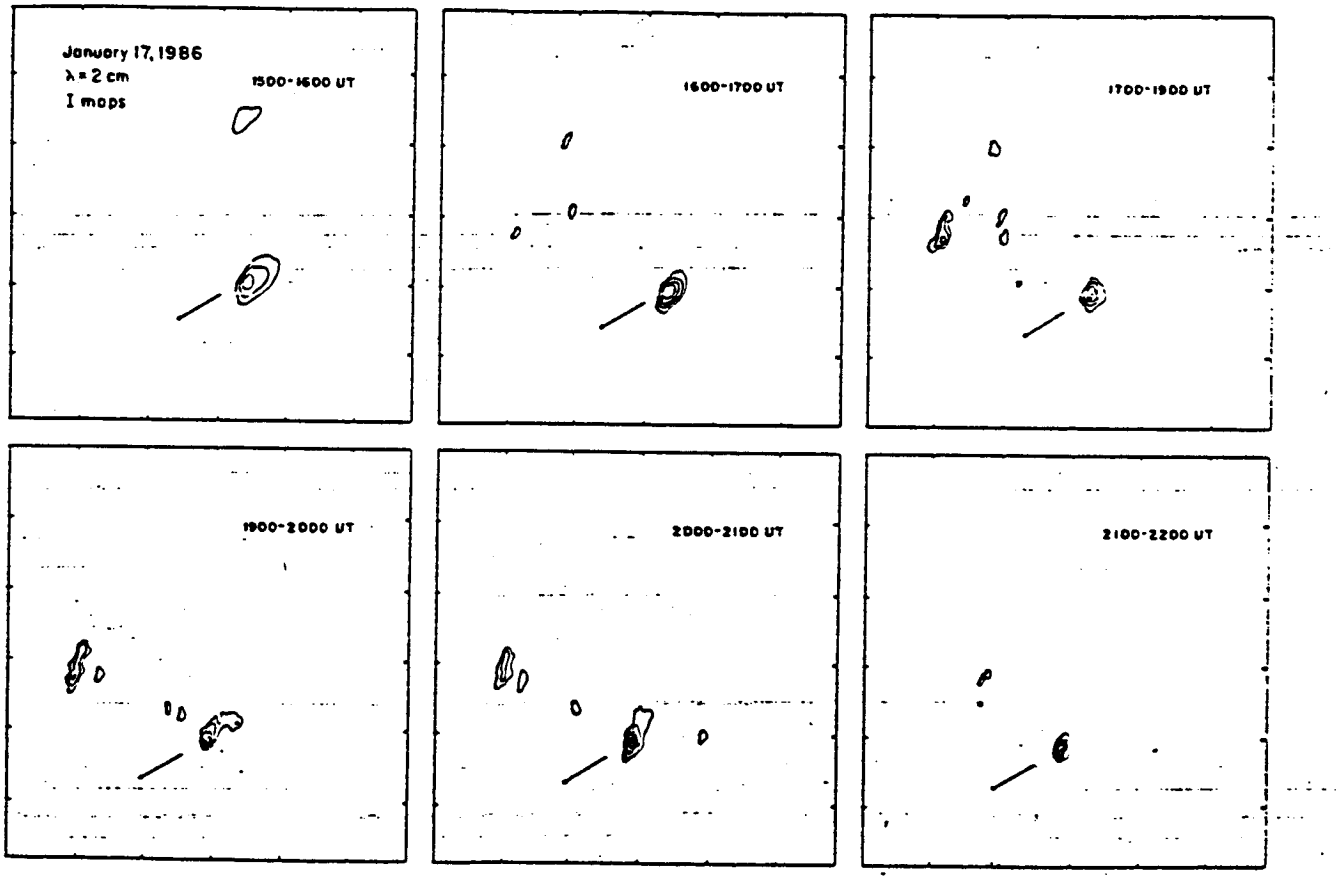

Figure 2. VLA synthesis map of the total intensity of the radiation at 2 cm wavelength. Here each box refers to the same area on the surface of the Sun, and the fiducial marks on the axes are separated by 60 arc-seconds. The southern source (bottom) increased slowly in brightness over a seven hour period while moving laterally across the solar surface in the southeast direction at a velocity of ~ 1 km s^{-1}. The northern source (top) varied over a time scale of 180 minutes, but showed no detectable lateral motion. Here the contours mark levels of equal brightness with an outermost contour of 5.2×10^4 K and a contour interval of 1.8×10^4 K.

Our confirming observations on January 17, 1986 revealed compact 2 cm sources with angular sizes $\theta \approx 25"$ and maximum brightness temperatures of $T_B \approx 2.0 \times 10^5$ K These sources were observed in plage regions with apparently-weak photospheric magnetic field and no sunspots, but in this case the compact sources had no detectable circular polarization ($\rho_c < 15\%$).

As illustrated in Figure 2, the compact unpolarized sources either varied substantially in intensity over time scales of hours (top sources) or slowly increased in brightness over a seven hour period (bottom source). Here each box refers to the same area on the surface of the Sun, and the arrows indicate a lateral motion at a velocity of $V \approx 1$ km s^{-1}. Curiously, the relatively-unvarying source exhibited this motion, but the variable one showed no detectable motion.

DISCUSSION

We have discovered previously-unobserved sources at 2 cm wavelength in regions of apparently-weak photospheric magnetic field. The brightness temperatures of $T_B \sim 10^5$ K are characteristic of the transition region. The angular sizes are $\theta \sim 5"$ to $25"$, and they vary in intensity over time-scales of 30 minutes to more than 180 minutes. We have observed at least two of these compact, variable 2-cm sources within the 3' field of view every time we have observed the Sun; extrapolating to the 30' - wide Sun, we would expect hundreds of them on the visible surface of the quiet Sun. The compact, variable sources can either be highly circularly polarized ($\rho_c \approx 90\%$) or they can exhibit no detectable circular polarization ($\rho_c < 15\%$).

The enigmatic presence of highly polarized sources in regions of apparently-weak photospheric magnetic field may be explained by any one of three hypothesis. First, the photospheric field may have strengths of up to 2,000 G in compact regions that are not readily detected by the photospheric magnetograms. Alternatively, the magnetic field in the transition region or the low corona may be amplified by currents to a strength above that in the underlying photosphere. If either of these hypothesis is true, then the high circular polarization of the 2 cm sources can be attributed to either thermal gyroradiation or the propagation of thermal bremsstrahlung in the presence of a magnetic field of strength $H \approx 2{,}000$ G. A third hypothesis, developed by Willson and Lang(1985), is that the compact 2 cm sources are due to nonthermal gyrosynchrotron radiation of mildly relativistic electrons in relatively weak magnetic fields of strength $H \approx 50$ G.

But what accounts for the variability and lateral motion of both the polarized and the unpolarized sources? The source variability might be due to a variable magnetic field that comes and goes within the transition region and low solar corona. Alternatively, the variations could be interpreted in terms of thermal electron density variations related to heating changes or to non-thermal electron density variations resulting from a variable acceleration mechanism. The lateral motion can be attributed to an upward expansion of dipolar loops; the 2-cm observations detect the apparent lateral motion of the loop legs.

Finally, we would like to point out certain resemblances between the compact, variable 2-cm sources and other phenomena reported in this proceeding. These sources are resolved (they are not points) with angular sizes comparable to those of small erupting filaments [Martin (1986 - this proceedings)] and the 20 cm observations of so-called coronal bright points [Habbal (1986 - this proceedings)]. The time scale of the variations and the lateral motions of the 2-cm sources are

comparable to those of the small erupting filaments. The brightness temperatures of the 2-cm sources are the same as those of the 20-cm ones. Comparisons with features seem at the He I, λ 10830 transition are very misleading, for there are so many of these features that the statistical significance of a correlation has to be very low.

ACKNOWLEDGEMENTS

Radio astronomical studies of the Sun at Tufts University are supported under grant AFOSR-83-0019 with the Air Force Office of Scientific Research (AFOSR) and contract N0014-86-K-0068 with the Office of Naval Research (ONR).

REFERENCES

Habbal, S., 1986, " Spatial and Temporal Observations of Coronal Bright Points" - this Proceedings.

Kundu, M.R. and K.R. Lang, 1985, "The Sun and Nearby Stars: Microwave Observations at High Resolution, " Science 228, 9-15

Kundu, M.R., 1986 a, "Coronal Plasmas on the Sun and Nearby Stars" - this Proceedings.

Lang, K.R., 1986a "Coronal Plasmas on the Sun and Nearby Stars"- this Proceedings.

Lang, K.R., 1986b, "Coronal Diagnostics - this proceedings.

Lang, K.R., R.F. Willson and V. Gaizauskas, 1983, " Very Large Array Observations of Solar Active Regions III. Multiple Wavelength Observations," Astrophysical J., 267, 455-464.

Martin, S., 1986, : Small Eruptive Filamentary Sources" - this Proceedings.

Shevgaonkar, R.K. and M.R. Kundu, 1984 "Three Dimensional Structures of two Solar Active Regions from VLA Observations at 2,6 and 20 cm. Centimeter Wavelength", Astrophy. J., 283, 413-420.

Willson, R.F. and K.R. Lang, 1986, "VLA Observations of Compact, Variable Sources on the Sun," Astrophysical Journal - to be published.

VLA OBSERVATIONS OF COMPACT, VARIABLE SOURCES ON THE SUN

ROBERT F. WILLSON AND KENNETH R. LANG

Department of Physics and Astronomy, Tufts University

Submitted to the Astrophysical Journal Letters

Received 1985 September 24

Revised 1986 January 22

ABSTRACT

Very Large Array observations of a solar active region at 2 cm wavelength have revealed a new class of compact, variable sources on the Sun. The compact sources vary on two different time scales of 10 to 20 seconds and 30 to 60 minutes . They are small (angular size θ = 5"), hot (brightness temperatures T_B = 0.5 to 3 x 10^5 K), and highly circularly polarized (degrees of circular polarization ρ_c = 80 to 90%). This emission originates in regions of low magnetic field strength H $\leq$ 80 G. The high circular polarization must nevertheless be associated with magnetic fields, and a plausible explanation for the source variability is variations in the magnetic fields on the two time scales. Alternatively, the variability might be attributed to a variable non-thermal electron density, perhaps resulting from a variable acceleration mechanism. The compact sources are attributed to gyrosynchrotron emission from mildly relativisitic electrons with a power law spectrum.

I. INTRODUCTION

The radiation mechanisms of quiescent (non-flaring) microwave emission from solar active regions at 6 cm and 20 cm wavelength are now well understood. This emission is attributed to the gyroresonant radiation and/or the bremsstrahlung of thermal electrons at the legs or apex of coronal loops (Lang, Willson, and Gaizauskas 1983; Lang and Willson 1983; Shevgaonkar and Kundu 1984; Kundu and Lang 1985). In contrast, the quiescent emission of solar active regions at 2 cm wavelength is poorly understood.

There are only two published reports of 2 cm VLA observations of solar active regions (Lang, Willson and Gaizauskas 1983; Shevgaonkar and Kundu 1984). Both papers report the presence of several (2 to 6) compact (angular sizes $\theta \lesssim 15"$), highly polarized (degrees of circular polarization $\rho_c \sim 80\%$ to 90%) sources at the feet of coronal loops and overlying sunspots. The brightness temperatures ($T_B \approx 10^5$ K) of these compact polarized sources suggests an origin in the transition region, while the high polarization is attributed to intense magnetic fields of strength $H \sim 2{,}000$ G.

The relationship of the compact, highly-polarized sources to the magnetic field geometry is controversial. Shevgaonkar and Kundu (1984) report the presence of two compact sources underlying larger 6 cm emission. This suggested that coronal loops diverge as they rise toward their apex, and contradicted loop models that assume a constant cross section (Rosner, Tucker and Vaiana 1978). In contrast, Lang, Willson and Gaizauskas (1983) find at least six compact 2 cm sources scattered over an area that is comparable to that of the 6 cm emission. They also notice that the 2 cm sources are not

found everywhere over sunspots, suggesting an origin in the low corona rather than the transition region where uniformly strong magnetic fields are expected above umbrae.

Previous VLA observations of compact, highly-polarized 2 cm sources were used to make synthesis maps over intervals of 11 to 12 hours. These maps revealed long-lasting sources that overlie sunspots in regions of strong magnetic field. Our recent VLA observations at 2 cm wavelength have been used to make snapshot synthesis maps for time intervals as short as 10 seconds. These maps indicate the presence of variable compact sources that vary over intervals of about 20 seconds and about 30 minutes. The variable sources originate in regions of low magnetic field strength $H \leq 80$ G, but they are highly circularly polarized. These observations are discussed in greater detail in Section II. The compact ($\theta \simeq 5"$), highly circularly polarized (ρ_c = 80-90%) sources have brightness temperatures T_B = 0.5 to 3 x 10^5 K, and they vary in brightness on two different time scales of 10 to 20 seconds and 30 to 60 minutes. In Section III we associate the high circular polarization with magnetic fields. Since the sources appear above regions of low magnetic field strength, the high circular polarization and high brightness temperatures cannot be explained by thermal radiation mechanisms. Here we explain the polarization and temperatures in terms of the non-thermal gyrosynchrotron emission from mildly relativistic electrons. The source variability is attributed to varying magnetic fields or a varying non-thermal electron density.

II. OBSERVATIONS

The VLA was used to observe the active region AR 4508 in the C configuration between 1530 and 2330 UT on June 4, 1984. The position of AR 4508 was N06 E57 at 1300 UT on this day. Wavelengths of 2.1 cm and 20.7 cm

were used for alternate 15 minute periods, followed by 5-minute observations of the calibration source PKS 0528 + 134. In all cases, the bandwidth was 12.5 MHz. In the C configuration the synthesized beamwidths are ≃ 1.2" and 1.7" at 2.1 and 20.7 cm, respectively. The data were sampled every 10s and were calibrated using the standard solar calibration procedures at the VLA. These data were then used to make synthesis maps of both the total intensity, I, and circular polarization , V, at each wavelength. These maps were finally CLEANED to produce images having a dynamic range of about 10:1.

The synthesis maps of total intensity at both wavelengths are shown in Figure 1. The 20.7 cm map was made using the data taken during the entire 8 hour observation period, whereas the 2 cm map refers to a shorter 15 minute interval beginning at 1547 UT. The most intense 20 cm emission is contained within an elongated looplike structure of ~ 2.5' in extent which has a peak brightness temperature of 1.0×10^6 K. There was no detectable 20 cm circular polarization to a limit of $\leq$ 10%. A comparison with Kitt Peak and Mt. Wilson magnetograms indicates that the extended 20 cm component lies along the magnetic neutral line in the western part of the active region. The weaker component lies ~30" to the east of a pair of sunspots.

In contrast, the 2 cm map shows two compact (θ ~ 5"), highly circularly polarized (ρ_c = 80-90%) sources that vary on time scales of 30 to 60 minutes Figure 2). Comparisons with Mt. Wilson magnetograms indicate that the two compact, variable sources appeared in regions of weak magnetic field with strengths $H \leq 80$ G, and that they did not overlie sunspots. The left circularly polarized sources (solid contours) varied in brightness temperature from $T_B = 2.0 \times 10^5$ K to $T_B \leq 0.5 \times 10^5$ K, while also moving systematically to the northwest with a total movement of 12" in three hours, or at a rate of about 0.8 km s^{-1} (1" = 725.3 km on the Sun). The right circulary

polarized source (dashed contours) ranged between 3.0 and 1.0 x 10^5 K.

Figure 3 shows 30 s snapshot maps of additional 2 cm compact sources with angular sizes $\theta \sim 4''$ and peak brightness temperatures of $T_B = 1.0$ to 3.0 x 10^5 K. These sources are denoted by A and B in Figure 1. They also appeared in regions of weak magnetic field ($H \leq 80$ G) and did not overlie sunspots. An examination of 10s snapshot maps indicates that sources A and B had respective lifetimes of 10 seconds and 20 seconds. The A source appeared at about 165740 and was unpolarized, whereas the B source appeared at 173130 and had a dipolar structure. Source B suggests the emergence of a small dipolar loop with a lifetime of 20 seconds and a temperature characteristic of the transition region.

III. DISCUSSION

The high degree of circular polarization of the compact, transient 2 cm sources is somewhat enigmatic. This polarization cannot be accounted for by propagation effects (thermal bremsstrahlung) or gyroresonant absorption. The compact, transient 2 cm sources are in regions of weak magnetic field ($H < 80$ G) and do not overlie sunspots. The circular polarization of these sources cannot be explained by propagation effects of the thermal bremsstrahlung, for magnetic fields of $H \sim 2{,}000$ G are required. Although gyroresonant absorption might account for the circular polarization, the weak magnetic field requires a very high harmonic of the gyrofrequency. The optical depth due to gyroresonant absorption is then negligibly small and the observed brightness temperatures $T_B \sim 10^5$ K cannot be accounted for by a plausible electron temperature. (The electron temperatures would be much too high.)

Conventional thermal radiation mechanisms like bremsstrahlung and gyroresonant, or cyclotron, radiation cannot explain the high circular polarization and high brightness temperature in the presence of weak photospheric

magnetic fields. However, non-thermal gyrosynchrotron radiation might explain the observations. This mechanism has been invoked to explain 6 cm sources of high brightness temperature in regions of weak magnetic fields (Webb et al. 1983; Chiuderi Drago and Melozzi 1984), as well as a filament-associated source with a high brightness temperature and steep radiation spectrum (Akhmedov et al. 1985).

Simplified expressions for the gyrosynchrotron emission from mildly relativistic electrons with both a thermal (Maxwellian) and non-thermal (power-law) energy distribution have been given by Dulk and Marsh (1982). For non-thermal electrons with a power-law energy distribution of index δ, the degre of circular polarization, ρ_c, of the radiation and the effective temperature, T_{eff}, of the radiating electrons are given by

$$\rho_c = 0.20 \times 10^{0.5\delta} 10^{1.93\cos\theta - 1.16\cos^2\theta} \left(\frac{\nu}{\nu_H}\right)^{-0.21-0.37\sin\theta} \qquad (1)$$

and

$$T_{eff} = 2.2 \times 10^9 10^{-0.31\delta} (\sin\theta)^{-0.36-0.06\delta} \left(\frac{\nu}{\nu_H}\right)^{0.50+0.085\delta} \qquad (2)$$

where θ is the angle between the line of sight and the direction of the magnetic field, the observing frequency is ν and the gyrofrequency $\nu_H = 2.8 \times 10^6$ H Hz. For an observing frequency of $\nu = 15.0 \times 10^9$ Hz, and a magnetic field strength of H = 50G, we have $\nu/\nu_H = 107.1$, and for $\theta = 20^o$ to 40^o we obtain:

$$\rho_c = 22\% \text{ to } 36\%$$

and

$$T_{eff} = 1.1 \times 10^{10} \text{ K to } 1.5 \times 10^{10} \text{ K}$$

for an energy spectral index of $\delta = 3$.

The high effective temperatures permit brightness temperatures $T_B \approx 10^5$ K under the optically thin conditions (optical depth $\tau \ll 1$) that occur when one is observing at such high harmonics, n, of the gyrofrequency. (For our case $\nu = n\nu_H = 2.8 \times 10^6$ nH = 15×10^9 Hz so that n = 107). In contrast, the effective temperature of thermal electrons is equal to the kinetic temperature of 10^5K to 10^6K, and the expected brightness temperatures are very much lower than those observed. For non-thermal electrons of density N_{nt} above some cut-off energy E_o, we have

$$T_B = \tau\, T_{eff} = HLN_{nt} \frac{c^2}{k\upsilon^2} \times \left(\frac{\eta_\upsilon}{HN_{nt}}\right) \qquad (3)$$

where E_o is assumed to be E_o = 10 keV = 1.6×10^{-8} ergs,

and

$$\frac{\eta_\upsilon}{HN_{nt}} = 3.3 \times 10^{-24} 10^{-0.52\delta} (\sin\theta)^{-0.43+0.65\delta} \left(\frac{\nu}{\nu_H}\right)^{1.22-0.90\delta} \qquad (4)$$

If the magnetic field strength H = 50 G and the dimension along the line of sight is L = 10^9 cm, then a non-thermal electron density of $N_{nt} = 5 \times 10^6$ cm^{-3} and $\theta = 20^o$ and $\theta = 20^o$ 40^o give

$\tau = 8.6 \times 10^{-6}$ to 3.0×10^{-5},

and

$T_B = 1.2 \times 10^5$ K to 3.3×10^5 K

These brightness temperatures are comparable to those observed.

The absence of non-thermal gyrosynchrotron radiation at 20 cm wavelength can be explained by the large optical depth in the overlying corona. With an electron temperature of $T_e = 10^6$ K and an electron density of $N_e = 5 \times 10^9$ cm^{-3}, the optical depth due to thermal bremsstrahlung at 20 cm is $\tau = 20$. In this case, the non-thermal gyrosynchrotron radiation would be completely absorbed at

20 cm. Because the optical depth scales as the square of the wavelength, the corona would be optically thin at 2 cm wavelength.

Because the compact 2 cm sources are transient with lifetimes as short as 10 seconds, continual acceleration of the electrons is not required. The energy loss by synchrotron radiation with a power-law electron energy distribution has a half-life, T, for the total emitted radiation given by

$$T \approx \frac{10^8}{H^2} \text{ seconds} \qquad (5)$$

A magnetic field of strength th H = 50 G, gives $T \approx 4 \times 10^4$ seconds or ~11 hours. But how are the electrons initially accelerated? Spicer (1979) and Shoub (1983) showed that large electric fields can be produced in the transition region as a result of the steep temperature gradient there. One possibility is that the electric fields become unstable and generate numerous non-thermal electrons. Spicer's calculations indicate that the number density of non-thermal electrons is $N_{nt} = 5 \times 10^6$ cm^{-3} for a thermal electron density of $N_e = 3 \times 10^9$ cm^{-3}. This is consistent with the number of nonthermal electrons required to account for the compact, transient 2 cm sources.

But what causes the variability of the observed emission? According to equation (3), the observed brightness temperature decreases with decreasing magnetic field strength and decreasing non-thermal electron density. We have observed an apparent emergence and disappearance of a dipolar magnetic field in one case. A plausible explanation for the source variability is therefore variations in the magnetic fields. Alternatively, the variability might be attributed to a variable non-thermal electron density, perhaps resulting from an variable acceleration mechanism.

Radio astronomical studies of the Sun at Tufts University are supported

under grant AFOSR-83-0019 with the Air Force Office of Scientific Research (AFOSR) and contract N0014-86-K-0068 with the Office of Naval Research (ONR). Comparisons of Very Large Array (VLA) and Solar Maximum Mission (SMM) data are supported by our NASA-SMM Guest Investigator grant NAG 5-501. The VLA is operated by Associated Universities Inc., under contract with the National Science Foundation.

REFERENCES

Akhmedov, Sh.B., Borovik, V.N., Gelfreikh, G.B., Bogod, V.M., Korzhavin, A.N., Petrov, Z.E., Kikij, V.N., Lang, K.R., and Willson, R.F. 1985, Ap. J. - to be published.

Chiuderi Drago, F., and Melozzi, M. 1984, Astr. Ap., 131, 103.

Dulk, G.A., and Marsh, K.A. 1982, Ap. J., 259, 350.

Kundu, M.R., and Lang, K.R. 1985, Science, 228, 9.

Lang, K.R. 1980, Astrophysical Formulae (2ed., New York: Springer Verlag).

Lang, K.R., and Willson, R.F. 1983, Adv. Space Res. 2, No. 11, 91 (COSPAR, Pergamon: Oxford).

Lang, K.R., Willson, R.F., and Gaizauskas, V. 1983, Ap. J., 267, 455.

Rosner, R., Tucker, W.H., and Vaiana, G.S. 1978, Ap. J., 283, 413.

Shevgaonkar, R.K., and Kundu, M.R. 1984, Ap. J., 283, 413.

Shoub, E.C. 1983, Ap. J., 266, 339.

Spicer, D.S. 1979, Solar Phys., 62, 295.

Webb, D.F., Davis, J.M., Kundu, M.R., and Velusamy, T. 1983, Solar Phys., 85, 267.

KENNETH R. LANG AND ROBERT F. WILLSON

Department of Physics and Astronomy

Robinson Hall

Tufts University

Medford, MA 02155

FIGURE LEGENDS

Fig. 1. VLA synthesis maps of total intensity, I, at 20.7 cm for eight hours of data and 2.1 cm (box) for 15 minutes of data (also see Figure 2). The points marked A and B denote the positions of compact, variable 2 cm sources with lifetimes of 10 to 20 seconds (see Figure 3). All of the compact 2 cm sources lie in regions of weak magnetic fields and do not overlie sunspots. The contours mark levels of equal brightness, and the fiducial marks on the axes are separated by 1' at 20 cm and 10" at 2 cm. The outermost contour and contour intervals are 4.5×10^5 K and 1.5×10^5 K at 20 cm and 6.1×10^4 K and 3.1×10^4 K at 2 cm.

Fig. 2. VLA synthesis maps of left circularly polarized (solid contours) and right circularly polarized (dashed contours) radiation at 2 cm wavelength. Each map begins at the UT time indicated. The map beginning at 1525 UT is for only 2 minutes of data, those beginning at 1618 and 1732 UT covered a 20 minute interval, and all of the other maps were for 15 minute intervals. The northern (top) source varied over time scales of 30 minutes, the southernmost (bottom) source had a lifetime of about 60 minutes, and the complex of sources just above the southernmost source lasted for about 30 minutes. Here the contours mark levels of equal brightness with an outermost contour of 6.1×10^4 K and a contour interval of 3.1×10^4 K. The fiducial marks on the axes are separated by 10".

Fig. 3. A series of 30 s snapshot maps of total intensity I (top) and circular polarization V (bottom). The maps reveal the presence of compact sources at 165740 and 173130 UT, respectively denoted by A and B in Figure 1. An examination of 10s snapshot maps indicates that compact sources A and B had respective lifetimes of 10 seconds and 20 seconds. Here the contour intervals mark levels

of equal brightness temperture, and the fiducial marks on the axes are separated by 10". The outermost contour and the contour interval are 6.1×10^4 K and 3.1×10^4 K for the I maps and 1.5×10^4 K for the V maps. The solid and dashed contours of the V maps respectively refer to positive and negative values of V.

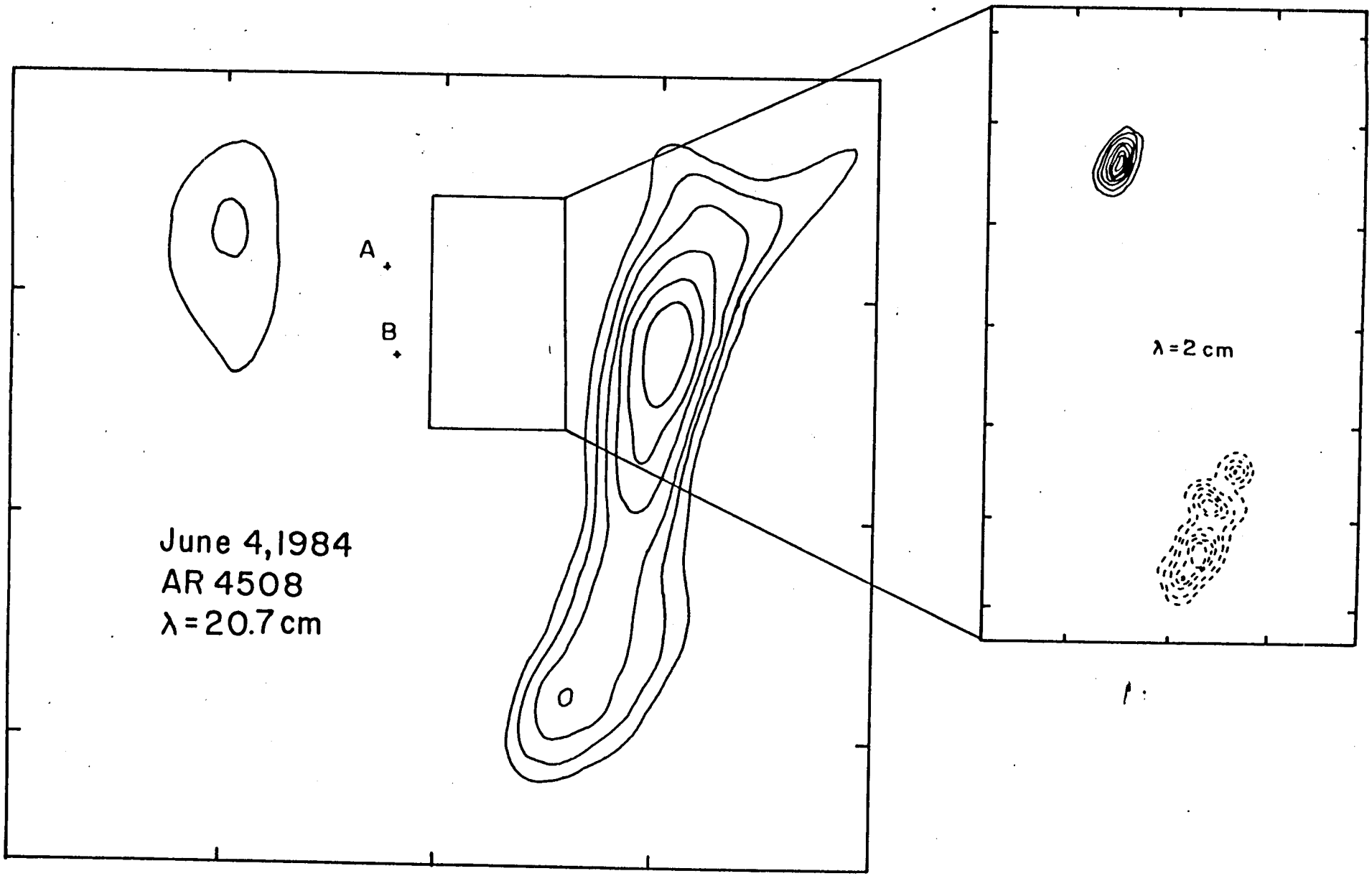

Fig. 1

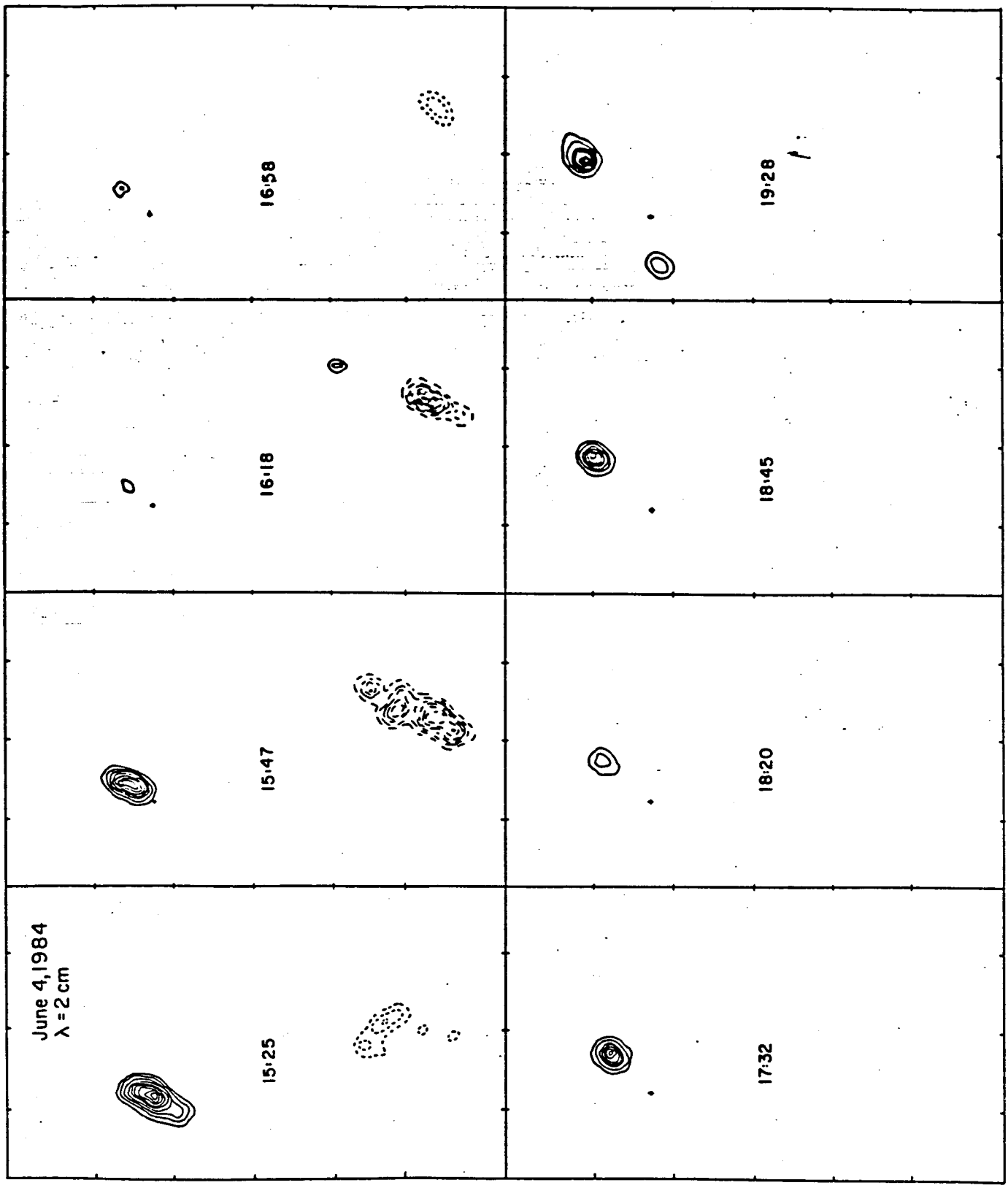

Fig. 2.

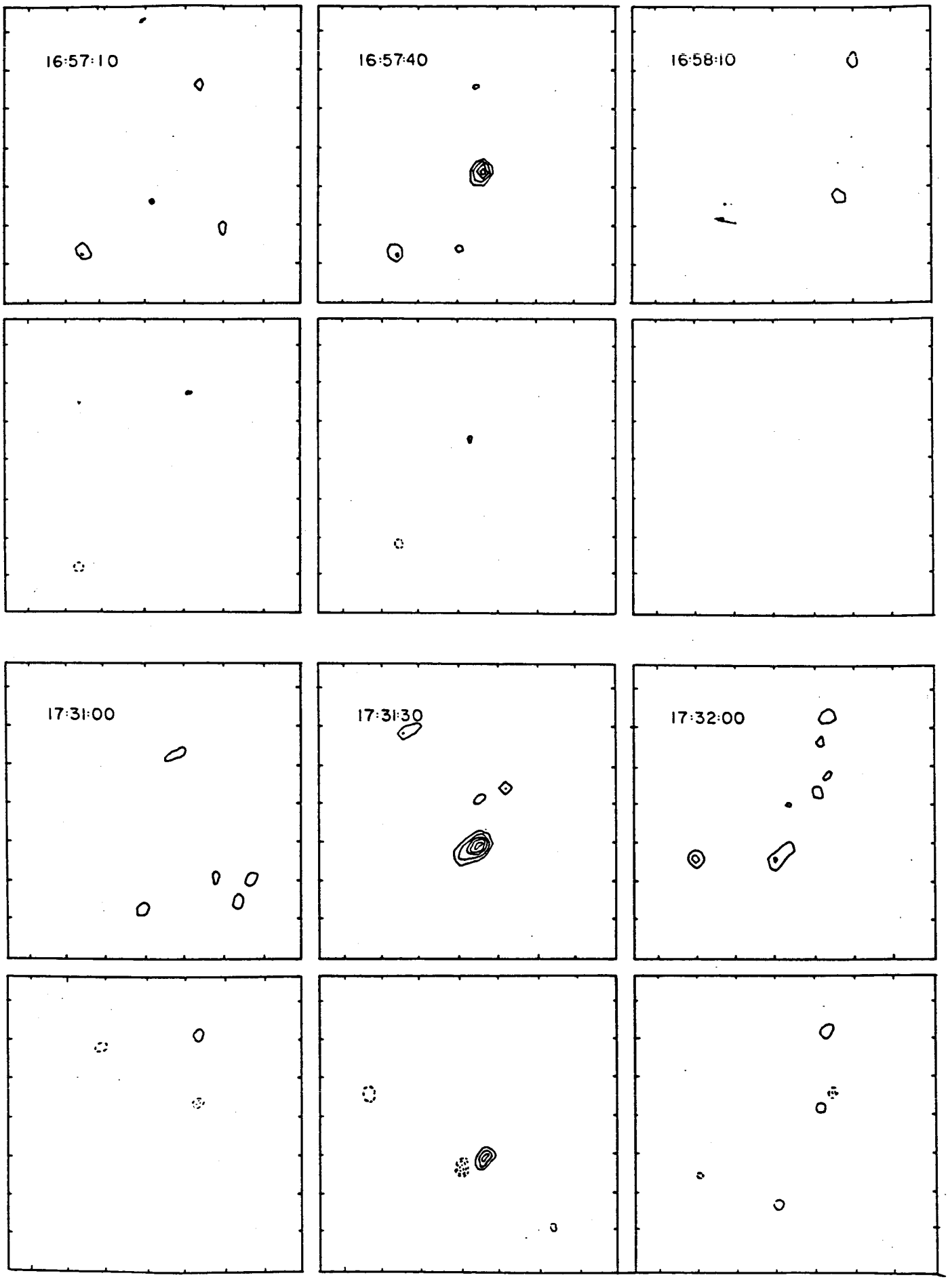

Fig. 3.

III. PAPERS TO BE PUBLISHED

SIMULTANEOUS SOLAR MAXIMUM MISSION AND VERY LARGE ARRAY OBSERVATIONS OF SOLAR ACTIVE REGIONS

Kenneth R. Lang and Robert F. Willson
Department of Physics and Astronomy
Tufts University

and

Kermit L. Smith and Keith T. Strong
Lockheed Palo Alto Research Laboratory
Palo Alto, California

ABSTRACT

We compare high-resolution images of the quiescent emission from two solar active regions at 20 cm (VLA) and soft X-ray (SMM-XRP) wavelengths. There are regions where the X-ray coronal loops are completely imaged at 20 cm wavelength. In other regions, the X-ray radiation is detected without detectable 20 cm radiation, and vice versa. The X-ray data were used to infer average electron temperatures $T_e \approx 3 \times 10^6$ K and average electron densities of $N_e \approx 2.5 \times 10^{10}$ cm^{-3} for the X-ray emitting plasma in the two active regions. Although the 20-cm brightness temperatures were always less than T_e, suggesting optically thin layers, both the thermal bremsstrahlung and the thermal gyroresonance radiation from the X-ray emitting plasma ought to be optically thick at 20 cm wavelength. Unexpectedly thin loops of widths $W = 4 \times 10^7$ cm are obtained if the observed optical depths are attributed to the thermal bremsstrahlung of this plasma. The low brightness temperatures can be explained if a higher, cooler plasma covers the hotter X-ray emitting plasma. Thermal gyroresonance radiation must account for the intense 20-cm radiation near and above sunspots where no X-ray radiation is detected. We next discuss the potential of additional 20-cm (VLA) and soft X-ray (SMM-XRP) comparisons.

I. INTRODUCTION

High-resolution observations with X-ray telescopes lofted above the atmosphere have transformed our understanding of the solar corona. The corona is now viewed as a highly inhomogeneous distribution of closed magnetic loops, that are anchored in the Sun, and open magnetic fields that extend out into interplanetary space [see Vaiana and Rosner (1978) for a review]. The hot, dense plasma that is trapped within coronal loops gives rise to intense X-ray radiation, and observations of X-ray spectral lines can be used to infer the electron temperature, electron density, and emission measure of this plasma.

The development of aperture synthesis telescopes like the Very Large Array (VLA) has permitted ground-based microwave observations of the solar corona with angular resolutions that are comparable to those of X-ray telescopes in space. The high-resolution microwave observations can uniquely specify the strength and structure of the coronal magnetic field. VLA synthesis maps of the total intensity, I, describe the two-dimensional distribution of source brightness, whereas synthesis maps of circular polarization, or Stokes parameter V, describe the two-dimensional structure of the longitudinal magnetic field [see Kundu and Lang (1985) for a review].

The microwave brightness temperature, T_B, of the quiescent, or non-flaring, corona is nearly equal to the coronal electron temperature, T_e, with $T_B \approx T_e \approx 10^6$ K. This suggests that the quiescent microwave emission is thermal. However, there are two possible thermal radiation mechanisms. They are thermal bremsstrahlung, or free-free emission, and thermal gyroresonance radiation, or cyclotron emission. In contrast, the quiescent X-ray emission of the solar corona is due solely to thermal bremsstrahlung.

In order to identify the dominant thermal radiation mechanism at microwave wavelengths, one needs to know the electron temperature, the electron density

and the magnetic field strength, as well as the thickness of the radiating layer, the scale length of the magnetic field, and the angle between the line of sight and the magnetic field. Thermal gyroresonance will generally dominate radiation at short centimeter wavelengths when the electron density is relatively low and the magnetic field is strong.

Early evidence for thermal gyroresonance radiation at coronal levels above sunspots was provided by comparing the soft X-ray and short centimeter-wavelength radiation of active regions (Kundu, Schmahl and Gerassimenko 1980; Pallavicini, Sakurai and Vaiana 1981). Bright microwave radiation was found in the strong magnetic fields above sunspots, but the X-ray observations indicated a relatively low electron density in these regions. This meant that the high microwave brightness temperatures above sunspots could not be due to thermal bremsstrahlung, but it could be explained by thermal gyroresonant radiation at the second or third harmonic of the gyrofrequency.

These early low-resolution comparisons were fully confirmed when high-resolution synthesis maps at 6 cm wavelength were compared with simultaneous soft X-ray images obtained with the X-ray Polychromator (XRP) aboard the Solar Maximum Mission (SMM) satellite (Chiuderi-Drago et al. 1982; Schmahl et al. 1982; Shibasaki et al. 1983; Strong, Alissandrakis and Kundu 1984). Soft X-ray spectral lines were used to determine the electron temperature and electron density of the X-ray emitting plasma that coincided with the 6 cm sunspot-associated sources. These parameters were then used to compute the bremsstrahlung brightness temperature at 6 cm wavelength. Because the computed value was much less than the observed brightness temperature, additional 6 cm opacity due to gyroresonance absorption above sunspots was required.

Thermal gyroresonance radiation at 6 cm wavelength in coronal regions above sunspots was additionally confirmed by the detection of circularly polarized

ring-shaped or horseshoe structures (Alissandrakis and Kundu 1982; Lang and Willson 1982). The highly-polarized (up to 100 percent) structures were predicted by the theory of cyclotron radiation in the curved magnetic fields above sunspots (Gel'freikh and Lubyshev 1979). Depressions in the 6 cm brightness temperature above sunspot umbrae have been attributed to cool material in these regions (Strong, Alissandrakis and Kundu 1984).

But what about the microwave counterpart of the intense X-ray sources? The brightest 6 cm sources are not usually associated with the brightest X-ray sources, and the detailed correspondence between the radiation at the two wavelengths is poor (Schmahl et al. 1982; Webb et al. 1983). But this result is not terribly surprising. It would be expected if the dominant radiation mechanisms are different in the two wavelength domains. Thermal bremsstrahlung is often too optically thin to be detected at 6 cm wavelength where gyroresonant radiation dominates. Different structures are observed at the two wavelengths because 6 cm gyroresonance absorption occurs in the strong magnetic fields above sunspots while the X-ray emission originates in coronal loops that stretch between sunspots of opposite magnetic polarity.

Yet, the hot temperatures, slow evolution and long lifetime of X-ray coronal loops make them ideal candidates for aperture synthesis techniques. Of course, low-lying loops have occasionally been detected at 6 cm wavelength (Strong, Allisandrakis and Kundu 1984, Webb et al. 1986), but radiation at this wavelength originates at relatively low heights and it is usually dominated by gyroresonance absorption. Higher levels are observed at 20 cm wavelength where the thermal bremsstrahlung of coronal loops can become optically thick. In fact, when VLA observations were extended to the longer 20 cm wavelength, quiescent, or non-flaring, loop-like coronal features were discovered (Lang, Willson and Rayrole 1982).

The 20-cm coronal loops strongly resemble their X-ray counterparts (Lang and Willson 1983, 1984). They have million-degree temperatures and stretch across

regions of opposite magnetic polarity in the underlying photosphere. The size and shape of the loops observed at 20 cm wavelength are also similar to those of arcades of X-ray coronal loops, with linear extents $L \approx 10^9$ to 10^{10} cm. In addition, the electron temperature and electron density inferred from X-ray observations of other loops are consistent with the idea that the 20-cm coronal loops are due to thermal radiation from the X-ray emitting plasma. All of these similarities suggest that the microwave counterpart of X-ray coronal loops can be observed in VLA synthesis maps at the longer 20 cm wavelength.

Numerous authors have now identified elongated, loop-like 20-cm features with coronal loops, but the exact radiation mechanism for the 20-cm emission remains controversial. A majority of authors attribute this radiation to the optically-thick thermal bremsstrahlung of a hot, dense plasma trapped within coronal magnetic loops that connect with underlying sunspots (Lang, Willson and Rayrole 1982; Dulk and Gary 1983; Lang, Willson and Gaizauskas 1983; Lang and Willson 1983, 1984; Gary and Hurford 1986; Holman 1986). Others reason that optically-thick thermal gyroresonance radiation may dominate the 20 cm emission of coronal loops (McConnell and Kundu 1983; Shevgaonkar and Kundu 1984). Both radiation mechanisms could play a role, with gyroresonance radiation becoming important at relatively high brightness temperatures or relatively low electron densities.

One can distinguish between the two thermal radiation mechanisms for 20-cm loops if the VLA synthesis maps are compared with simultaneous X-ray images. This has only been done in two instances. Chiuderi-Drago et al. (1982) used X-ray spectral lines from the SMM-XRP to infer the electron temperature and emission measure of the X-ray emitting plasma, concluding that one 20-cm source is the optically-thin bremsstrahlung of this plasma. The angular extent of the X-ray source was comparable to that of the 20-cm one, but the observations at both wavelengths were of relatively poor angular resolution. Another sunspot-associated 20-cm source had to be attributed to gyroresonance radiation, for there was no detectable X-ray

radiation from this region. Webb et al. (1986) used X-ray data taken during a recent rocket flight to conclude that one of several 20-cm features was due to optically-thick thermal bremsstrahlung associated with X-ray coronal loops. They noticed that the 20-cm radiation was concentrated at the tops of the X-ray loops and attributed this apparent concentration to absorption in a cool external plasma. However, such a concentration was not present in the data of Chiuderi-Drago et al. (1982).

Webb et al. (1986) concluded that complete X-ray loops could not be imaged at any single microwave wavelength, and that this conclusion differed from the interpretations of Lang, Willson and Rayrole (1982) and Lang and Willson (1983, 1984). Webb et al. (1986) ignored the substantial indirect evidence of numerous observers who have associated loop-like 20-cm features with coronal loops. Their generalization was also based upon a comparison of a single seven-hour 20-cm map with a single X-ray image made during a five-minute rocket flight. (As we have previously discussed, comparisons of X-ray maps with 6 cm data are largely irrelevant for the 6 cm radiation is usually due to a different radiation process in different parts of the active region.)

In this paper we present the first comparisons of high-resolution 20-cm maps (VLA) with simultaneous high-resolution X-ray images (SMM-XRP). These comparisons are given in §II. In one instance, all of the X-ray emitting plasma was detected at 20 cm wavelength, and additional 20-cm emission was observed near sunspots where no X-ray radiation was detected. However, the 20-cm radiation was concentrated at the apex of the more extensive X-ray coronal loops of another active region. In §III we discuss the absorption and radiation mechanisms for coronal loops at 20 cm wavelength. We next use X-ray measurements of electron temperature and electron density to place constraints on these mechanisms. The observed 20-cm features are then explained. Our results are

summarized in §IV where we also discuss the potential of future 20-cm (VLA) and soft X-ray (SMM-XRP) comparisons.

II. OBSERVATIONS

We have used the Very Large Array (VLA) and the X-ray Polychromator (XRP) aboard the Solar Maximum Mission (SMM) satellite to observe solar active regions AR 4508 and AR 4532 on 1984 June 4 and July 8, respectively. The VLA was in the C configuration on June 4 and in the hybrid C-D configuration on July 8. In both instances the signal wavelength was 20.7 cm (1446 MHz) and the bandwidths were 12.5 MHz. Active region AR 4508 was observed with the VLA for an 8 hour period between 1500 UT and 2300 UT on June 4; its position on the solar surface was 06° N and 57° E at 1300 UT on this day. Active region AR 4532 was observed for a 4.5 hour period between 1800 UT and 2300 UT on July 8; its position on the solar surface was 07° S and 18° E on this day. The Flat Crystal Spectrometer (FCS) of the SMM-XRP observed six prominent soft X-ray lines: OV III at 18.9 A, Ne IX at 13.4 A, Mg XI at 9.2 A, Si XIII at 6.7 A, S XV at 5.0 A and Fe XXV at 1.9 A. The FCS observed AR 4508 for a ? hour perod between ???? UT and ???? UT on June 4, and it observed AR 4532 for a ? hour period between ???? UT and ???? UT on July 8.

The half-power beamwidth of the individual VLA antennae was ~ 30' at 20 cm wavelength, and the synthesized maps constructed from up to 325 interferometer pairs had beamwidths of 12.6" x 15.5" in the C configuration and 12.6" x 36.0" in the C-D configuration. The June 4 data were calibrated by 5 minute observations of the calibrator source PKS 0528 + 134 every 35 minutes, while the July 8 data were similarly calibrated with the source PKS 0742 + 103. The flux density of PKS 0528 + 134 and PKS 0742 + 103 was 1.5 Jy and 3.3 Jy at 1446 MHz, respectively. The calibrated data for the entire observing period were used together with the standard CLEAN procedure to make synthesis maps of both the

total intensity, I, and the circular polarization, or Stokes parameter V. No solar bursts or flares were observed during these observations, and the synthesis maps therefore refer to the quiescent, or non-flaring, radio emission. There was no detectable circular polarization (V/I < 15%) for both active regions, suggesting that they were both optically thick to the extraordinary and ordinary modes of wave propagation at 20 cm wavelength.

The 14" collimated field of view of the FCS was rastered over a 7' x 7' field of view on June 4 and over a 4' x 4' field of view on July 8; in each case the pixel spacing was 9" x 9". X-ray images were obtained for each of the six spectral lines during the orbital day at a cadance of 410 s. All of the available data for each spectral line were then summed and averaged during each orbit to improve the statistical uncertainty on the count rate from each pixel. Significant emission was only detected from the three softest channels - O VIII, Ne IX and Mg XI. The peak formation temperatures for these lines are 3×10^6 K, 4×10^6 K and 7×10^6 K, respectively. The failure to detect emission in the harder, more energetic channels indicates that the active regions were stable and unperturbed by flaring activity during the periods of observation.

The XRP also produced a white-light image that showed the sunspots, making it possible to align the X-ray images with the sunspots to an accuracy of 10". The VLA maps of the total intensity, I, at 20 cm wavelength were aligned with Hα photographs of the same sunspots with a similar 10" accuracy. This enabled us to compare the soft X-ray and 20-cm data with the same field of view and angular scale.

As illustrated in Figure 1, the 20-cm radiation of AR 4508 is concentrated in the central regions of a more extensive system of X-ray loops. In this

instance, the 20-cm radiation was aligned along the magnetic neutral line (see Figure 2). There is a sharp drop in the intensity of the radio emission along the edges of the magnetic neutral line where there ought to be a sharp gradient in the magnetic field strength.

However, all of the X-ray emitting plasma of AR 4532 was detected at 20-cm wavelength, and additional 20-cm emission was observed near and above sunspots where no X-ray radiation was detected. As illustrated in Figure 3, intense X-ray radiation and intense 20-cm radiation were detected from coronal loops or arcades of loops that are connected with underlying sunspots. These loops were about 60" across or about 5×10^9 cm in linear extent. Both X-ray and 20-cm radiation were also emitted from regions of bright plage. In addition, Lang et al. (1986) have presented simultaneous SMM-VLA data in which an entire system of X-ray loops was completely imaged at 20 cm wavelength.

Thus, the same coronal loops are often detected at both 20-cm and X-ray wavelengths, with extra information at 20 cm near and above sunspots. Of course, the 20-cm coronal loops can also be limited to a smaller volume than their X-ray counterparts, but our SMM-VLA comparisons and other VLA observations suggest that this is not usually the case. The claim by Webb et al. (1986) that complete X-ray loops may never be imaged at any microwave wavelength can no longer be justified. We will therefore now turn our attention to the absorption and radiation mechanisms that account for the 20 cm-coronal loops.

III. DISCUSSION

Because the microwave brightness temperature, T_B, of the quiescent coronal loops is nearly equal to the electron temperature, T_e, the quiescent radiation

from 20-cm loops is most likely thermal. The two possible thermal radiation mechanisms at 20 cm wavelength are thermal bremsstrahlung, or free-free emission, and thermal gyroresonance radiation, or cyclotron emission. In order to identify the dominant thermal radiation mechanism at 20 cm wavelength, we will evaluate the electron temperture, T_e, and the electron density, N_e, using the X-ray radiation that is attributed to thermal bremsstrahlung alone.

As previously mentioned, the active regions were so quiescent that they were only detectable in the three softest X-ray channels (O VIII, Ne IX and Mg XI). Because the O VIII to Ne IX line intensity ratio is insensitive to temperature variations over the range typical of solar active regions, the ratios of the other two lines (O VIII to Mg XI and Ne IX to Mg XI) were used as temperature diagnostics. The temperatures inferred from the two ratios were averaged to obtain our estimate for the electron temperature.

An emission measure was inferred from the temperatures and the observed X-ray fluxes. The electron density was then calculated using a volume of 3×10^{27} cm^3, which equals the product of the FCS pixel area and a typical soft X-ray scale height of 3×10^9 cm.

The mean electron temperatures, T_e, and electron densities, N_e, for AR 4508 were determined for the areas marked A, B and C in Figure 4. These parameters are given in Table 1 together with the maximum observed brightness temperature, T_B, at 20 cm wavelength and the optical depth $\tau = T_B/T_e$. The mean T_e and N_e for AR 4532 were similarly inferred for the areas marked A, B, C and D in Figure 5; they are given in Table 5 together with the relevant T_B and τ.

The mean values for different areas were then combined to give average values of $T_e = 3.4 \pm 0.4 \times 10^6$ K and $N_e = 2.5 \pm 0.6 \times 10^{10}$ cm^{-3} for AR 4508 and $T_e = 3.2 \pm 0.4 \times 10^6$ K and $N_e = 2.4 \pm 0.6 \times 10^{10}$ cm^{-3} for AR 4532. Here the

uncertainties correspond to the maximum possible deviation that reproduces the flux in all the detected X-ray lines to within 1 standard deviation of the observed values. These values of T_e and N_e are typical values for quiescent coronal loops in active regions.

Within the uncertainties, the observed loops were isothermal. They also all had optical depths $\tau < 1$ (optically thin). We will therefore evaluate the loop width or thickness, W, that would give rise to optically-thin thermal bremsstrahlung at our observing frequency of $\nu = 1446$ MHz (20.75 cm). According to Lang (1980):

$$W = \frac{102\ \tau_{f-f} \nu^2\ T_e^{3}\ /2}{N_e^2\ \ln\ (4.7 \times 10^{10}\ T_e/\nu)}, \qquad (1)$$

or

$$W = \frac{2.13 \times 10^{20}\ \tau_{f-f}\ T_e^{3/2}}{N_e^2\ \ln\ (32.5\ T_e)}\ \text{cm},$$

where τ_{f-f} is the optical depth for bremsstrahlung. The N_e and T_e obtained from the X-ray observations have been substituted into equation (1) to provide the widths, W, given in Tables 1 and 2. The average value of W for both active regions is $W = 4 \times 10^7$ cm.

The 20 cm coronal loops are unexpectedly thin, for the inferred widths are at least an order of magnitude less than the expected width of X-ray coronal loops. To put it another way, typical X-ray scale heights of $W \sim 3 \times 10^9$ cm would produce optically-thick thermal bremsstrahlung at 20 cm wavelength, and the 20-cm brightness temperatures would be higher than those observed. For a plausible coronal loop thickness and the X-ray values of N_e and T_e, equation (1) would give $\tau_{f-f} > 1$ and $T_B \sim T_e$.

An appeal to the alternate gyroresonance emission mechanism will not help resolve this paradox. If the optical depth τ_{g-r} for gyroresonance absorption is less than unity, bremsstrahlung will dominate the radiation which should be optically thick, and if τ_{g-r} is greater than τ_{f-f} the radiation will still be optically thick.

However, for completeness, we will evaluate τ_{g-r} using the equation (Zheleznyakov 1970)

$$\tau_{g-r} = 0.052 \frac{n^{2n}}{2^{n+1} n!} \frac{N_e}{\nu} (1.7 \times 10^{-10} T_e)^{n-1} L_H (1 \pm \cos\alpha)^2 \sin^{2n-2}\alpha \quad (2)$$

where the magnetic scale length L_H has typical values of $L_H \sim 1 \times 10^9$ cm, the angle between the line of site and the direction of the magnetic field lines is α, and our observing frequency $\nu = 1446$ MHz and the harmonic n is related to ν through the relation

$$\nu = 2.8 \times 10^6 \text{ nH Hz}, \quad (3)$$

where the magnetic field strength is H. For typical values of H ~ 100 G at the apex of coronal loops (Willson 1985), we have n = 4. Then, collecting terms in equation (2), we have for $\alpha = 90°$:

$$\tau_{g-r} = 3.1 N_e (1.7 \times 10^{-10} T_e)^3 \text{ for } n = 4.$$

Our average X-ray values of $N_e \sim 2.5 \times 10^{10}$ cm^{-3} and $T_e \sim 3 \times 10^6$ K give $\tau_{g-r} \sim 10$ for n = 4.

Thus, we expect both the thermal gyroresonance radiation and the thermal bremsstrahlung to be optically thick for plausible loop widths and magnetic scale

lengths. This is consistent with the lack of any detectable circular polarization at 20 cm wavelength. The observed brightness temperature, T_B, at 20 cm wavelength should therefore be equal to the electron temperature with $T_B = T_e$, but the values of T_B are between two and five times smaller than T_e. To resolve this paradox, we call attention to an idea first proposed by Holman (1986).

In order to explain the restriction of one 20-cm loop to the apex of an X-ray loop, Holman argued that cooler material with $T_e \sim 10^5$ K exists either as a sheath around the loops or as part of an external medium. The 20-cm radiation emitted by the X-ray loops will be partly absorbed in the cooler, higher plasma, thereby reducing its brightness temperature. The higher, cooler material would, however, be invisible in X-rays because of its low temperature and relatively small emission measure.

If the cool plasma is part of an external medium that is more extensive than the X-ray loops, then we would expect the observed 20-cm loops to be co-spatial with the X-ray ones, but with a lowered brightness temperature. This is what is observed for AR 4532. When the cool plasma is part of a sheath around the X-ray loops, then the line of sight through the low-temperature plasma will be greatest at the loop edges and footpoints, and the observed 20-cm emission will be concentrated at the apex of the X-ray coronal loops. This is what is observed for AR 4508.

But what about the bright 20 cm radiation near and above sunspots? There is no detectable X-ray radiation in these regions, and this can be attributed to a low electron density, N_e. Because the optical depth for free-free absorption scales with N_e^2, while that for gyroresonance absorption scales with N_e, the low electron density favors gyroresonance absorption. The high magnetic field

strength above sunspots also favors this process. We therefore attribute the 20-cm radiation near and above sunspots to thermal gyroresonance radiation.

IV. SUMMARY

The quiescent, or non-flaring, X-ray radiation of solar active regions is attributed to thermal bremsstrahlung, but the quiescent microwave radiation may be due to either thermal bremsstrahlung or thermal gyroresonant radiation. In our introduction we reviewed evidence for thermal gyroresonance radiation at 6 cm wavelength in coronal regions above sunspots. This evidence includes comparisons of 6 cm VLA maps with simultaneous soft X-ray data, as well as the detection of highly circularly-polarized horseshoe structures above sunspots at 6 cm wavelength. Bright 6 cm sources are not expected to coincide with bright soft X-ray sources because their different radiation mechanisms dominate different parts of solar active regions.

Although the thermal bremsstrahlung of coronal loops is usually optically thin at 6 cm wavelength, it can become optically thick at the longer 20 cm wavelength where loop-like coronal structures are observed. These 20-cm coronal loops stretch between regions of opposite magnetic polarity in the underlying photosphere, and the temperatures, sizes and shapes of the 20-cm coronal loops resemble those of soft X-ray coronal loops.

In this paper we have compared high-resolution 20-cm maps (VLA) with simultaneous high-resolution X-ray images (SMM-XRP) of two active regions. The X-ray coronal loops in AR 4532 were completely imaged at 20 cm wavelength, while the 20-cm emission of AR 4508 was concentrated along the magnetic neutral line within more extended X-ray loops. The X-ray data were used to infer average

electron temperatures, T_e, and average electron densities, N_e, with $T_e = 3.2 \pm 0.4 \times 10^6$ K and $N_e = 2.5 \pm 0.6 \times 10^{10}$ cm^{-3} for AR 4532 and $T_e = 3.4 \pm 0.4 \times 10^6$ K and $N_e = 2.4 \pm 0.6 \times 10^{10}$ cm^{-3} for AR 4508.

The microwave brightness temperatures, T_B, at 20 cm wavelength were always less than the average electron temperature, with optical depths $\tau = T_e/T_B$ of $0.2 < \tau < 0.5$. Unexpectedly thin loops of widths $W = 4 \times 10^7$ cm are obtained if these optical depths are attributed to the thermal bremsstrahlung of the X-ray emitting plasma. In fact, the X-ray values of T_e and N_e indicate that both thermal bremsstrahlung and thermal gyroresonance radiation ought to be optically thick at 20 cm wavelength for plausible loop widths and magnetic scale heights. Optically thick radiation is also consistent with the lack of detectable circular polarization at 20 cm. Thermal gyroresonance radiation must account for the intense 20-cm radiation near and above sunspots where no X-ray radiation is detected.

The unexpectedly low values of T_B can be explained if the X-ray emitting coronal loops lie beneath a higher, cooler plasma. The hot, dense plasma in the X-ray coronal loops would emit optically thick radiation at 20 cm wavelength, but the brightness temperature of this radiation would be reduced during subsequent propagation through the cooler, absorbing plasma. The observations of AR 4532 can be explained if the cooler plasma extends across and beyond the X-ray loops, while the AR 4508 results might be explained by a cool sheath around the X-ray loops. This cooler material would not be detected at X-ray wavelengths because of its low temperature and relatively small emission measure.

The results given in this paper indicate that the structure and dominant radiation mechanisms in the low corona are much more complex and inhomogeneous

than was previously thought. Systems of coronal loops within a single active region apparently have different temperatures and different radiation mechanisms that can only be detected by observing at both X-ray and 20 cm wavelength. Future comparisons of high-resolution images at these two wavelengths will lead to detailed information about the plasma and magnetic structure of the low solar corona. Physical parameters such as electron temperature, electron density and magnetic field strength can be specified, and the detailed variation of these parameters within the coronal atmosphere can be determined. Such information will provide important constraints on theories and models of coronal loops as well as general theories for the structure and heating of solar active regions.

Radio astronomical studies of the Sun at Tufts University are supported under grant AFOSR-83-0019 with the Air Force Office of Scientific Research and Contract N000-14-86-K-0068 with the Office of Naval Research (ONR). Simultaneous VLA and Solar Maximum Mission (SMM) observations of the Sun are supported by NASA grant NAG 5-501. K.L.S. and K.T.S. are supported by NASA contract NAS 5-23758 and the Lockheed Independent Research Program. The XRP was built by a consortium of three groups: Lockheed Palo Alto Research Laboratory, Mullard Space Science Laboratory, and the Rutherford and Appleton Laboratories. The Very Large Array is operated by Associated Universities Inc., under contract with the National Science Foundation.

REFERENCES

Alissandrakis, C.E., and Kundu, M.R. 1982, Ap. J. (Letters) 253, L49.

Chiuderi-Drago, F., Bandiera, R., Falciani, R., Antonucci, E., Lang, K.R., Willson, R.F., Shibasaki, K. and Slottje, C. 1982, Solar Phys. 80, 71.

Dulk, G.A., and Gary, D.E. 1983, Astr. Ap. 124, 103.

Gary, D.E., and Hurford, G.J. 1986, "Multi-Frequency Observations of a Solar Active Region During a Partial Eclipse", B.B.S.O. 0259, submitted to Ap. J.

Gel'friekh, G.B., and Lubyshev, B.I. 1979, Sov. Astron. A.J. 23, 316.

Holman, G.D. 1986, "High-Spatial-Resolution Microwave and Related Observations as Diagnostics of Coronal Loops", to be published in Coronal And Prominence Plasmas.

Kundu, M.R., and Lang, K.R. 1985, Science 228, 9.

Kundu, M.R., Schmahl, E.J., and Gerassimenko, M. 1980, Astr. Ap. 82, 265.

Lang, K.R. 1980, Astrophysical Formulae (2nd Ed. New York: Springer Verlag).

Lang, K.R., and Willson, R.F. 1982, Ap. J. (Letters) 255, L111.

Lang, K.R., and Willson, R.F. 1983, Adv. Space Res. 2, No. 11, 91.

Lang, K.R., and Willson, R.F. 1984, Adv. Space Res. 4, No. 7, 105.

Lang, K.R., Willson, R.F., and Gaizauskas, V. 1983, Ap. J. 267, 455.

Lang, K.R., Willson, R.F., and Rayrole, J. 1982 Ap. J. 258, 384.

Lang, K.R., Willson, R.F., Smith, K.L. and Strong, K.T. 1986, "Physical Parameters of a Solar Active Region Inferred From A Thermal Cyclotron Line and Soft X-ray Spectral Lines", submitted to Ap. J.

McConnell, D., and Kundu, M.R. 1983, Ap. J. 269, 698.

Pallavicini, R., Sakurai, T., and Vaiana, G.S. 1981, Astr. Ap. 98, 316.

Schmahl, E.J., Kundu, M.R., Strong, K.T., Bentley, R.D., Smith, J.B., and Krall, K.R., 1982, Solar Phys. 80, 233.

Shevgaonkar, R.K, and Kundu, M.R. 1984, Ap. J. 283, 413

Shibasaki, K., Chiuderi-Drago, F., Melozzi, M., Slottje, C., and Antonucci, E. 1983, Solar Phys. 89, 307.

Strong, K.T., Alissadrakis, C.E., and Kundu, M.R. 1984, Ap. J. 277, 865.

Takakura, T., and Scalise, E. 1970, Solar Phys. 11, 434.

Vaiana, G.S., and Rosner, R. 1978, Ann. Rev. Astron. Ap. 16, 393.

Webb, D.F., Davis, J.M., Kundu, M.R., and Velusamy, T. 1983, Solar Phys. 85, 267.

Webb, D.F., Holman G.D., Davis, J.M., Kundu, M.R., and Shevgaonkar, R.K. 1986, "The Plasma and Magnetic Field Properties of Coronal Loops Observed at High Spatial Resolution", submitted to Ap. J.

Willson, R.F. 1985, Ap. J. 298, 911.

KENNETH R. LANG and ROBERT F. WILLSON:
Department of Physics and Astronomy
Robinson Hall
Tufts University
Medford, MA 02155

KERMIT L. SMITH and KEITH T. STRONG
Code 602.6
Bldg. 7-XRP
Goddard Space Flight Center
Greenbelt, MD 20771

Table 1. The mean electron temperature, T_e, mean electron density, N_e, maximum brightness temperature, T_B, at 20 cm wavelength, optical depth, τ, and the inferred loop width or thickness, W, for the regions marked A, B, and C in Figure 4 of AR 4508.

Region	T_e (°K)	N_e (cm^{-3})	T_B (°K)	τ	W (cm)
A	3.8×10^6	2.4×10^{10}	0.8×10^6	0.21	3×10^7
B	3.4×10^6	2.4×10^{10}	1.7×10^6	0.50	6×10^7
C	3.1×10^6	2.8×10^{10}	1.0×10^6	0.32	3×10^7
Average	3.4×10^6	2.5×10^{10}	1.2×10^6	0.34	4×10^7

Table 2. The mean electron temperature, T_e, mean electron density, N_e, maximum brightness temperature, T_B, optical depth, τ, and the inferred loop width or thickness, W, for the regions marked A, B, C and D in Figure 5 of AR 4532.

Region	T_e (°K)	N_e (cm^{-3})	T_B (°K)	τ	W (cm)
A	3.1×10^6	2.4×10^{10}	1.3×10^6	0.42	5×10^7
B	3.4×10^6	2.7×10^{10}	1.4×10^6	0.41	4×10^7
C	2.9×10^6	2.7×10^{10}	0.6×10^6	0.21	2×10^7
D	3.4×10^6	1.6×10^{10}	0.7×10^6	0.21	6×10^7
Average	3.2×10^6	2.4×10^{10}	1.0×10^6	0.31	4×10^7

FIGURE LEGENDS

Fig. 1. A comparison of a 20 cm VLA synthesis map of AR 4508 with SMM-XRP images in the O VIII (18.9 A) and Mg XI (9.2 A) lines at soft X-ray wavelength on June 4 1984. The field of view of all three images is the same, and the angular scale can be inferred from the 60" spacing between fiducial marks on the axes. The contours of the 20 cm map mark levels of equal brightness temperature corresponding to 0.4, 0.5, 0.6 ... 1.0 times the maximum brightness temperature of 1.7×10^6 K. The contours of the O VIII image correspond to ??, ?? and ?? counts per second above a background level of ?? counts per second with a maximum signal of ?? counts per second. The contours of the Mg XI image similarly correspond to ??, ?? and ?? counts per second above a background level of ?? counts per second and with a maximum signal of ?? counts per second.

Fig. 2. The 20 cm contours of equal brightness temperature (solid black lines) are superposed on a Kitt Peak National Observatory (KPNO) magnetogram of AR 4508 on 1984 June 4. The radio emission is concentrated along the magnetic neutral line that separates regions of negative (black) and positive (white) magnetic polarity. Sharp magnetic field gradients may exist along the neutral line. The KPNO magnetogram was kindly provided by Jack Harvey of the National Solar Observatory.

Fig. 3. A comparison of soft X-ray (SMM-XRP-left), Hα (SOON-middle) and 20 cm (VLA-right) images of AR 4532 on 1984 July 8. The field of view of all three images is the same, and the angular scale can be inferred from the 120" spacing between the fiducial marks on the axes. The contours of the 20 cm map mark levels of equal brightness temperature corresponding 0.4, 0.5, 0.6 ... 1.0 times the maximum brightness temperature of 1.4×10^6 K. The soft X-ray data were

taken in the O VIII line (18.9 A) with contours corresponding to ??, ?? and ?? counts per second above a background level of ?? counts per second with a maximum signal of ?? counts per second. Here the sunspots are denoted by small black dots with a circle around them.

Fig. 4. A soft X-ray map of AR 4508 taken in the Mg XI line (9.2 A) with contours corresponding to ??, ?? and ?? counts per second. The ratio of the O VIII and Mg XI line intensities were used to determine the mean electron temperatures in the regions mark A, B and C. These temperatures are given together with estimates of the mean electron density, 20-cm brightness temperature, optical depth and loop width in Table 1. There is no detectable soft X-ray radiation in the vicinity of the sunspots marked E and F, but these regions are associated with intense radiation at 20 cm wavelength (also see Figure 3).

Fig. 5. A soft X-ray map of AR 4532 taken in the O VIII line (18.9 A) with contours corresponding to ??, ?? and ?? counts per second. The ratio of the O VIII and Mg XI line intensities were used to determine the mean electron temperature in the regions marked A, B, C and D. These temperatures are given together with estimates of the mean electron density, 20-cm brightness temperature, optical depth and loop width in Table 2.

C-2

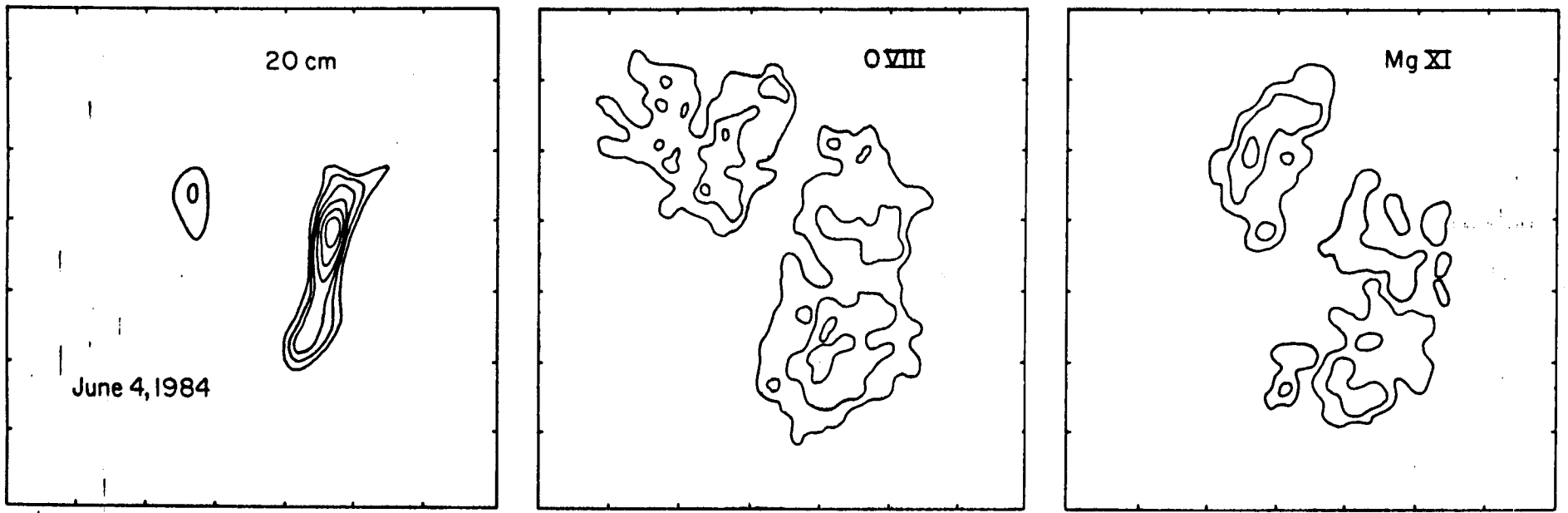

Fig. 1.

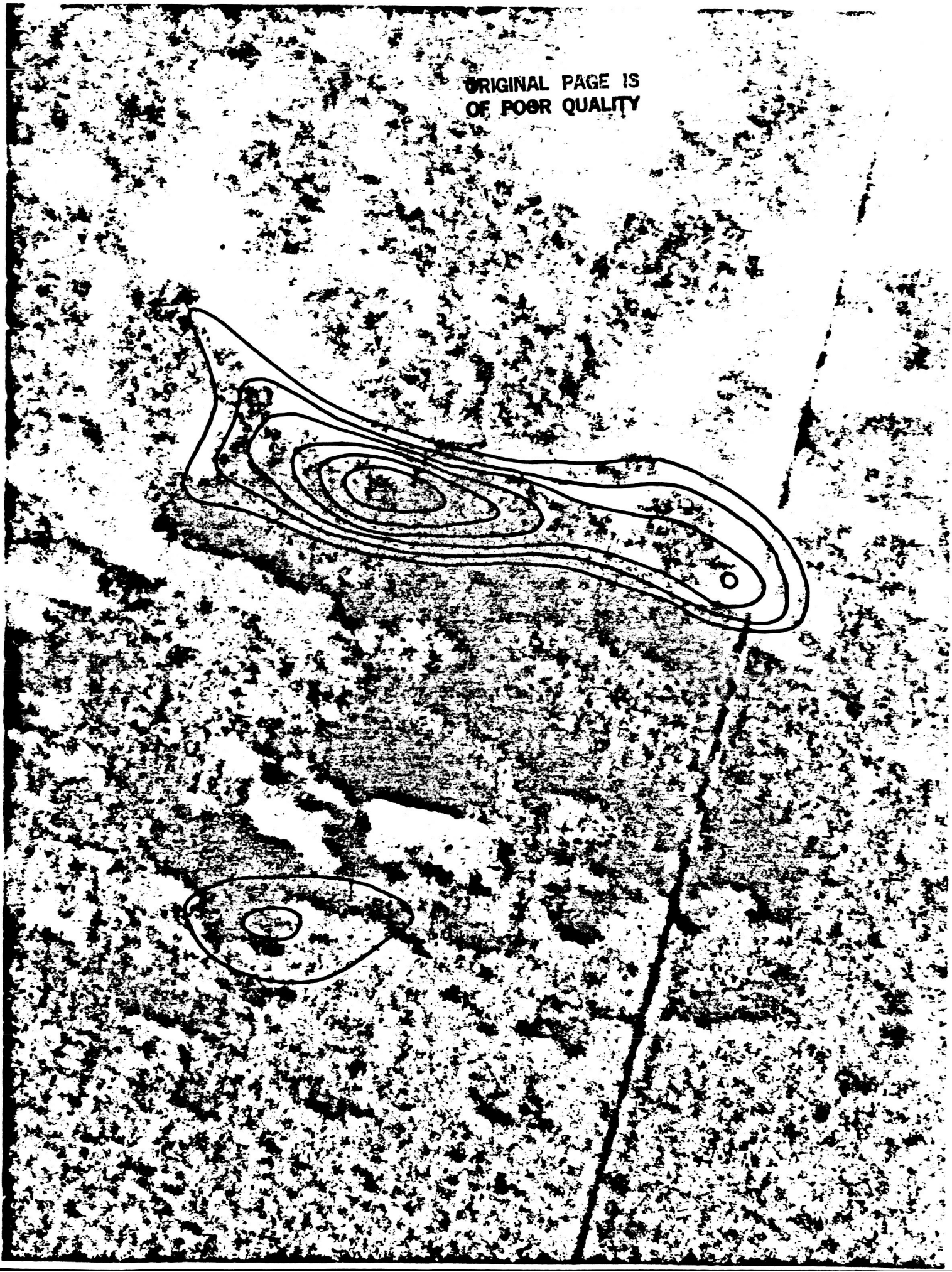
ORIGINAL PAGE IS
OF POOR QUALITY

ORIGINAL PAGE IS
OF POOR QUALITY

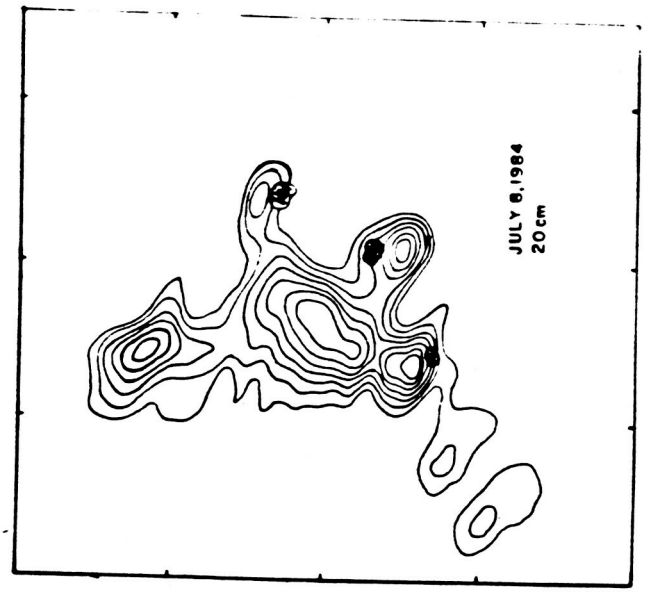

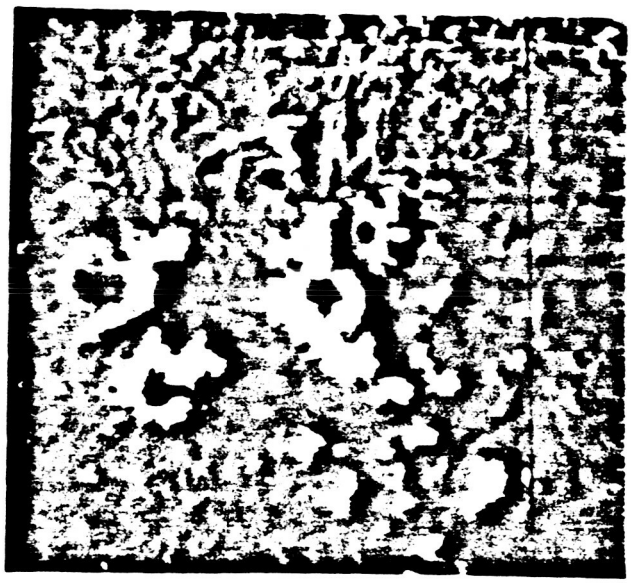

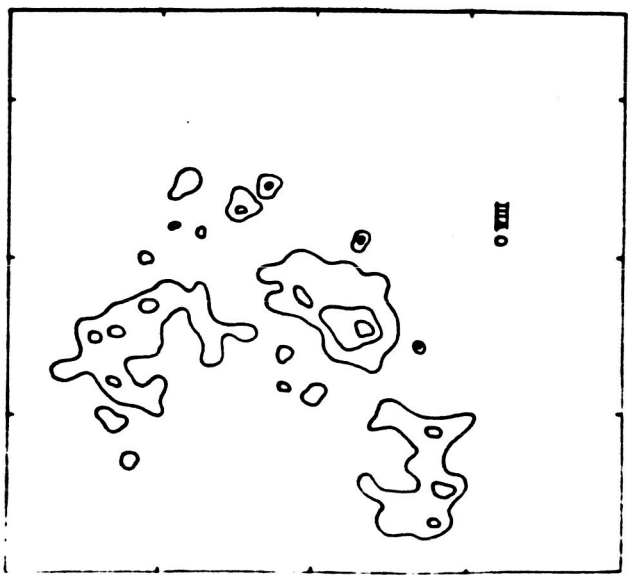

Fig. 3

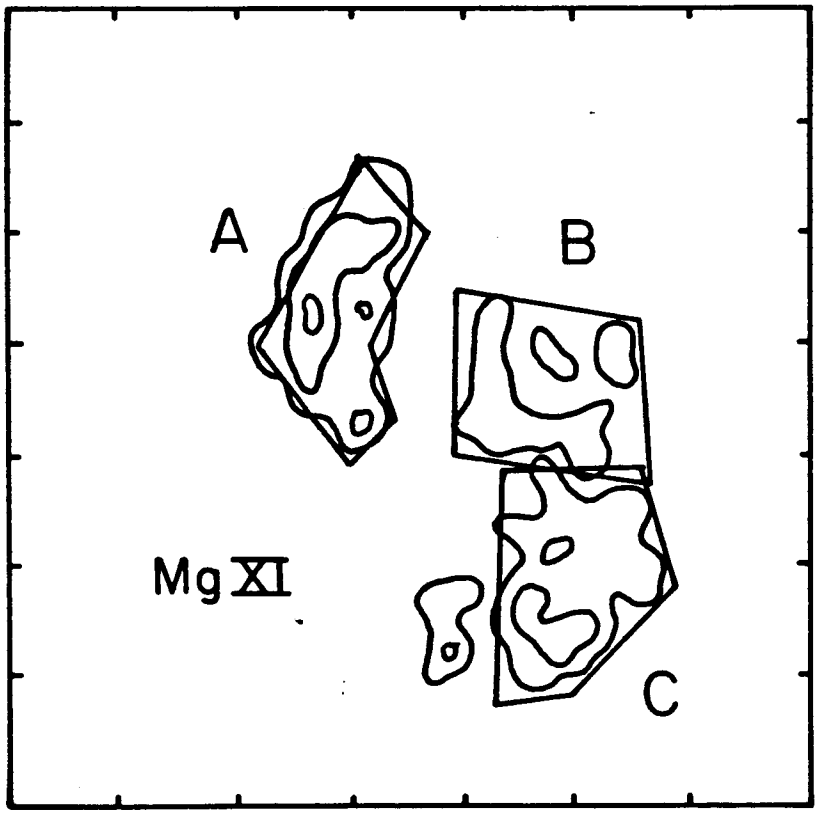

Fig. 4

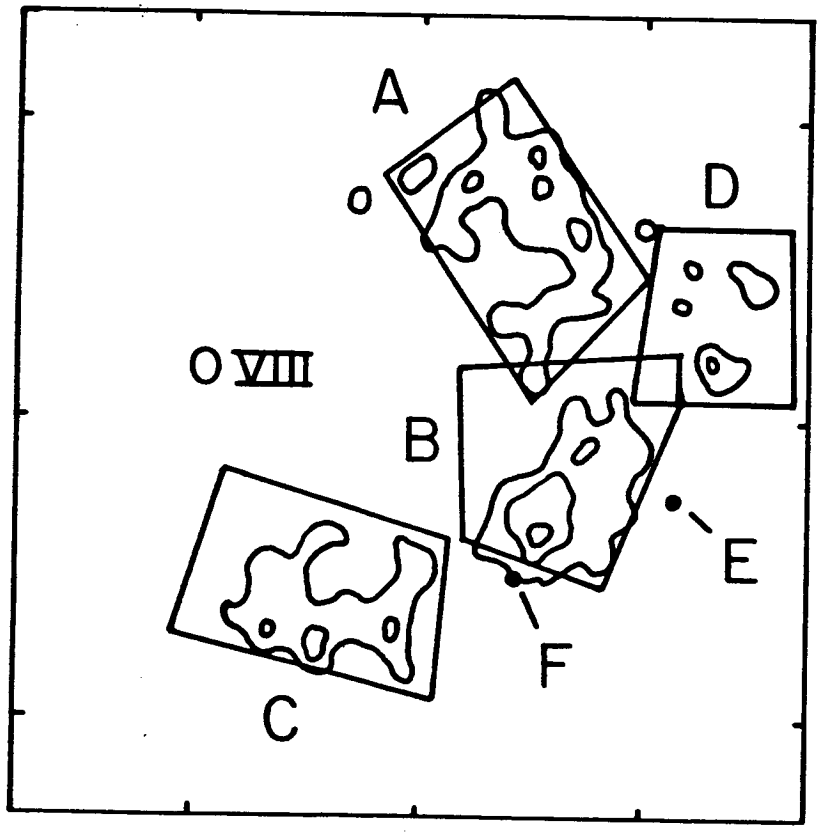

Fig 5

PHYSICAL PARAMETERS OF A SOLAR ACTIVE REGION INFERRED FROM A THERMAL CYCLOTRON LINE AND SOFT X-RAY SPECTRAL LINES

Kenneth R. Lang and Robert F. Willson
Department of Physics and Astronomy
Tufts University

and

Kermit L. Smith and Keith T. Strong
Lockheed Palo Alto Research Laboratory
Palo Alto, California

ABSTRACT

We present simultaneous high-resolution observations of coronal loops at 20 cm wavelength with the Very Large Array (VLA) and at soft X-ray wavelengths with the X-ray Polychromator (XRP) aboard the Solar Maximum Mission (SMM) satellite. The images at 20 cm and soft X-ray wavelengths have nearly identical sizes and ellipsoidal shapes, with a linear extent, L, of $L \approx 5 \times 10^9$ cm. Both the 20-cm and the X-ray emission stretch between and across regions of opposite magnetic polarity in the underlying photosphere. Complete X-ray coronal loops can therefore be imaged at 20 cm wavelength, and 20-cm VLA maps describe the radio wavelength counterpart of X-ray coronal loops. X-ray spectral lines were used to obtain values of electron temperature $T_e = 2.85 \pm 0.08 \times 10^6$ K and electron density $N_e = 1.8 \pm 0.3 \times 10^{10}$ cm^{-3} averaged over the emitting area. These parameters are used with plausible estimates for the loop thickness, magnetic scale height and magnetic field strength to show that the plasma is optically thick to both thermal bremsstrahlung and thermal gyroresonance radiation at 20 cm wavelength. The absence of detectable circular polarization is consistent with an optically thick plasma. The observed brightness temperature $T_B \approx T_e$. The VLA maps at 10 closely spaced frequencies between 1440 and 1720 MHz described the same coronal loops or arcades of loops. A plot of the maximum brightness temperature of these loops as a function of observing frequency exhibits a line-like feature with a central frequency of 1650 MHz and a half-width of 80 MHz. This spectral feature is attributed to a thermal cyclotron line, and it indicates that the optical depth of thermal gyroresonance radiation must be greater than that of thermal bremsstrahlung at these frequencies. The X-ray values for T_e and N_e are combined with plausible values of magnetic scale height and optical depth for gyroresonance absorption to show that the harmonic, n, of the gyrofrequency is $n = 4$. The central frequency and narrow width of the thermal cyclotron line are combined with this harmonic to show that the magnetic field strength, H, of the coronal loops is $H = 147 \pm 5$ G.

INTRODUCTION

Very Large Array (VLA) observations of solar active regions at 20-cm wavelength delineate loop-like features that are probably the radio wavelength counterpart of the coronal loops seen at X-ray wavelengths. The 20-cm coronal loops stretch across regions of opposite magnetic polarity, and they exhibit sizes, shapes and temperatures that are similar to those of X-ray coronal loops (Lang, Willson and Rayrole 1980; Lang, Willson and Gaizauskas 1983; Lang and Willson 1983, 1984). Because the radio brightness temperatures are nearly equal to the electron temperatures of coronal loops, the radio radiation is most likely due to a thermal radiation mechanism.

The two possible thermal processes are thermal bremsstrahlung, or free-free emission, and thermal gyroresonance radiation, or cyclotron emission. The electron temperatures and electron densities inferred from X-ray observations of coronal loops are consistent with optically thick thermal bremsstrahlung at 20-cm wavelength (Lang, Willson and Rayrole 1980), but these parameters can also be combined with plausible estimates of the coronal magnetic field strength to show that thermal gyroresonance radiation can also become optically thick at this wavelength (McConnell and Kundu 1983; Shevgaonkar and Kundu 1985).

When thermal gyroresonance dominates, one might detect individual cyclotron lines as narrow-band enhancements in the radio-wavelength spectra of coronal loops. Theoreticians have predicted that such thermal cyclotron lines might be observed if the radiation is emitted from relatively thin layers in the corona where the magnetic field is nearly constant (Syrovatskii and Kuznetsov 1980; Zheleznyakov and Zlotnik 1980; Kuznetsov and Syrovotskii 1981). The spectrum of a cyclotron line was subsequently observed at wavelengths near 20 cm when the apex of a coronal loop was resolved (Willson 1985). Observations of these lines provide an unusually accurate method of specifying the coronal magnetic field

strength. The central frequency of the line must be a harmonic of the gyrofrequency, and the narrow line width provides tight constraints on that frequency and the relevant magnetic field strength.

Although there have been rapid recent developments in the observations of 20-cm coronal loops, there have been relatively few comparisons of simultaneous 20-cm and soft X-ray observations. Such comparisons can help specify the dominant 20-cm radiation mechanism, while also establishing the physical parameters of the coronal plasma. X-ray spectral lines can, for example, be used to infer the electron temperature and electron density while the radio observations can uniquely specify the strength and structure of the magnetic field.

A single comparison of a five-minute X-ray image with a seven-hour VLA synthesis map at 20 cm wavelength led Webb et al. (1986) to conclude that complete loops cannot be imaged at this wavelength. Lang et al. (1986) subsequently compared high-resolution 20-cm maps (VLA) with simultaneous high-resolution soft X-ray images taken with the X-ray Polychromator (XRP) aboard the Solar Maximum Mission (SMM) satellite. They showed that complete X-ray coronal loops can be mapped at 20-cm wavelength and pointed out the potential advantages of comparing high resolution VLA and SMM-XRP data.

In this paper we provide another example in which the coronal radiation at 20-cm and X-ray wavelengths coincide. The observations are presented in §II where we also present radio-wavelength spectra that are attributed to a thermal cyclotron line. In §III we provide values for the electron density, electron temperature and magnetic field strength in these coronal loops and attribute the 20-cm radiation to thermal gyroresonance emission. The X-ray values of electron density and electron temperature are combined with the 20-cm brightness temperature and the cyclotron line to infer the harmonic of the gyrofrequency. Our results are summarized in §IV.

II. OBSERVATIONS

We have used the Very Large Array (VLA) and the X-ray Polychromator (XRP) aboard the Solar Maximum Mission (SMM) satellite to observe the solar active region AR 4663 on 1985 June 7. The VLA was used in the B configuration at 10 different wavelengths between 21.8 cm (1440 MHz) and 17.4 cm (1720 MHz) with bandwidths of 12.5 MHz during a 9 hour period between 1500 UT and 2400 UT on June 7, and the Flat Crystal Spectrometer (FCS) of the SMM-XRP observed six prominent soft X-ray lines (O VIII, Ne IX, Mg XI, Si XIII, S XV and Fe XXV) for a 4.7 hour period between 1500 UT and 1940 UT on June 7. The position of AR 4663 on the solar surface was 01° N and 65° E at 1300 UT on June 7.

The half-power beamwidth of the individual VLA antennae ranged between 26' and 31', and the synthesized maps constructed from up to 325 interferometer pairs had beamwidths between 3.0" x 3.5" and 3.6" x 4.2". The active region was observed with the VLA at successive pairs of wavelengths for 5 minutes each, so that all 10 wavelengths could be observed in 25 minutes. This sequence of observations was followed by successive 2 minute observations of the calibrator source PKS 0552 + 398 whose flux density was 1.7 Jy at 1465 MHz. The calibrated data for the 9 hour interval were used together with the standard CLEAN procedure to make synthesis maps of both the total intensity, I, and circular polarization or Stokes parameter V. No solar bursts or flares were observed during this interval, and the synthesis maps therefore refer to the quiescent, or non-flaring, radio emission. There was no detectable circular polarization ($V/I \leq 15\%$) suggesting that the region was optically thick to both the extraordinary and ordinary modes of wave propagation at 20-cm wavelength.

The 14" collimated field of view of the FCS was rastered over a 4' x 4' area with a pixel spacing of 9" x 9". X-ray images were obtained for each of the six spectral lines every 128 s during the orbital day. All of the available data for

each spectral line during each 1 hour orbit were then summed and averaged to improve the statistical uncertainty on the count rate from each pixel. Significant emission was detected in the three softest channels - O VIII, Ne IX and Mg XI. The peak formation temperatures for these lines are 3×10^6 K, 4×10^6 K and 7×10^6 K, respectively. The failure to detect emission in the harder, more energetic channels indicates that the active region was stable and unperturbed by flaring activity throughout the period of observation.

The XRP also produced a white-light image that showed the sunspots, making it possible to align the X-ray images with the sunspots to an accuracy of 10". The VLA maps of the total intensity, I, at 20-cm wavelength were aligned with Hα photographs of the same sunspots with a similar 10" accuracy. This enabled us to compare the soft X-ray and 20 cm data for the same field of view and angular scale.

As illustrated in Figure 1, the 20-cm (1480 MHz) radiation and the soft X-ray (O VIII) emission originated in the same area. Observations at both wavelengths apparently describe the same coronal loops or arcades of loops. They are about 60" across, which corresponds to a linear extent, L, of $L \approx 5 \times 10^9$ cm. Both the radio and the X-ray emission stretch between and across regions of opposite magnetic polarity seen in magnetograms of the underlying photosphere (see Figure 2).

As illustrated in Figure 3, the radio-wavelength coronal loops exhibited the same ellipsoidal shape and extent at 10 closely spaced frequencies ranging from between 1440 MHz (20.8 cm) and 1725 MHz (17.4 cm). The maximum brightness temperature of these loop-like structures varied by a factor of two (see Table 1), indicating that observations at a single wavelength may give a misleading representation of the brightness temperature and optical depth.

The maximum brightness temperatures are plotted as a function of observing

frequency in Figure 4. This spectrum contains a line-like feature with a central frequency, ν, of $\nu = 1650$ MHz and a full-width-to-half-maximum, $\Delta\nu$, of $\Delta\nu = 80$ MHz. As discussed in more detail in the next section, we attribute this feature to a thermal cyclotron line and use it to obtain an accurate estimate of the coronal magnetic field strength.

III. DISCUSSION

In order to identify the dominant thermal radiation mechanism at 20-cm wavelength, one needs to know the electron temperature, electron density, and the magnetic field strength. The X-ray data were therefore used to infer the mean electron temperature, T_e, and the mean electron density, N_e, for the regions marked A, B, C and D in Figure 5. As previously mentioned, the active region was so quiescent that it was only detectable in the three softest X-ray channels (O VIII, Ne IX and Mg XI). Because the O VIII to Ne IX line intensity ratio is insensitive to temperature variations over the temperature range typical of solar active regions, the ratios of the other two lines (O VIII to Mg XI and Ne IX to Mg XI) were used as temperature diagnostics.

An emission measure was inferred from the temperature and the observed X-ray fluxes. The electron density was then calculated using a volume of 3×10^{27} cm^3, which equals the product of the FCS pixel area and a typical soft X-ray scale height of 3×10^9 cm.

The mean temperatures and densities are given in Table 2. We obtain average values of $T_e = 2.85 \pm 0.08 \times 10^6$ K and $N_e = 1.8 \pm 0.3 \times 10^{10}$ cm^{-3} when averaged over all the coronal loops or arcades of loops. Here the uncertainties correspond to the maximum possible deviation that reproduces the flux in all the detected X-ray lines to within 1 standard deviation of the observed values. The inferred values of electron temperature and electron density are typical of those of

quiescent coronal active region loops. Within the uncertainties, the observed loops were isothermal and isobaric, but there was a statistically-uncertain tendency for a hotter temperature at the loop apex.

We may use the parameters derived from X-ray observations to estimate the optical depth and brightness temperture of the X-ray emitting plasma at radio wavelengths. Assuming an isothermal source of electron temperature, T_e, and optical depth, τ, the observed radio brightness temperature, T_B, will be given by

$$T_B = \tau\, T_e \qquad \text{for } \tau \ll 1 \text{ (optically thin)}$$

and

$$T_B = [\, 1 - \exp(-\tau)\,]\, T_e \qquad \text{for } \tau \gg 1 \text{ (optically thick).} \tag{1}$$

The free-free optical depth, τ_{f-f}, for an isothermal loop with electron temperature, T_e, and width or thickness, W, is (Lang, 1980)

$$\tau_{f-f} = 9.8 \times 10^{-3} \frac{N_e^2 W}{\nu^2\, T_e^{3/2}} \ln\left(4.7 \times 10^{10} \frac{T_e}{\nu}\right), \tag{2}$$

where ν is the observing frequency in Hz and N_e is the electron density in cm^{-3}. Using $\nu = 1.65 \times 10^9$ Hz, corresponding to the center of our line-like feature, together with the X-ray values of $T_e = 2.85 \times 10^6$ K and $N_e = 1.8 \times 10^{10}$ cm^{-3} and a typical loop thickness of $W = 1 \times 10^9$ cm in equation (2), we obtain $\tau_{f-f} \approx 4$. The plasma is therefore optically thick to thermal bremsstrahlung at this frequency, and the brightness temperature $T_B \approx 3 \times 10^6$ K inferred from equation (1) is consistent with that observed at this frequency. However, the optical depth will be only slightly greater at lower frequencies, and we would not expect the

dramatic changes in brightness temperature shown in figure 4.

We must therefore examine the alternative possibility of thermal gyroresonance radiation. The optical depth, τ_{g-r}, due to gyroresonance absorption is given by (Zheleznyakov 1970):

$$\tau_{g-r} = 2\pi^2 \frac{n^{2n}}{2^{n+1} n!} \frac{\nu_p^2}{c\nu} \left(\frac{kT_e}{mc^2} \right)^{n-1} L_H \ (1 \pm \cos\alpha)^2 \sin^{2n-2}\alpha \qquad (3)$$

where $n = 1, 2, 3, \ldots$ is the harmonic number, the plasma frequency $\nu_p = 8.9 \times 10^3 N_e^{1/2}$ Hz, the velocity of light $c = 2.9979 \times 10^{10}$ cm s^{-1}, Boltzmann's constant $k = 1.38 \times 10^{-16}$ erg $^oK^{-1}$, the electron mass $m = 9.1 \times 10^{-28}$ g, the scale height of the magnetic field is L_H, and α is the angle between the line of sight and the direction of the magnetic field lines. Collecting terms, we obtain

$$\tau_{g-r} = 0.052 \frac{n^{2n}}{2^{n+1} n!} \frac{N_e}{\nu} (1.7 \times 10^{-10} T_e)^{n-1} L_H \ (1 \pm \cos\alpha)^2 \sin^{2n-2}\alpha \qquad (4)$$

The harmonic n is related to the observing frequency ν and the magnetic field strength H through the relation

$$\nu = 2.8 \times 10^6 \ nH \ \text{Hz} \qquad (5)$$

In order for gyroresonance absorption to dominate free-free absorption at our reference frequency $\nu = 1.65 \times 10^9$ Hz, the layers must be optically thick with

$\tau_{g-r} > \tau_{f-f} \approx 4$. We will adopt $\tau_{g-r} \approx 6$ and determine the harmonic number, n. If we assume a magnetic scale height $L_H = 1 \times 10^9$ cm and $\alpha = 65°$, the solar longitude of AR 4663, then we may use these parameters together with the X-ray values of $N_e = 1.8 \times 10^{10}$ cm^{-3} and $T_e = 2.85 \times 10^6$ K in equation (4) to obtain n = 4.

To put it another way, the fourth harmonic of the gyrofrequency becomes optically thick to gyroresonance absorption with $T_B \approx T_e$ and $\tau_{g-r} \gtrsim \tau_{f-f}$. We can use equation (6) with n = 4 and $\nu = 1.65 \times 10^9$ Hz to obtain a magnetic field strength of H = 147 G. This is consistent with model calculations of the spectrum of another thermal cyclotron line in which n = 4 or possibly n = 5, with H = 145 G or possibly H = 119 G (Willson 1985), but in the case presented here, we do not have to make ad hoc assumptions about N_e and T_e.

But these are general arguments based upon homogeneous, isothermal models. When Table 1 and Figure 4 are examined in greater detail, we notice that inhomogeneities are required. For example, the 20-cm brightness temperture, T_B, is usually lower than the electron temperature, T_e, suggesting that the radio emission from the hot, optically-thick loops is partially absorbed in a cooler external plasma. In addition, the T_B at 1650 MHz is greater than T_e, suggesting a thin, hot gyroresonance layer similar to that proposed by Willson (1985). The detailed radio spectrum is probably due to a mixture of hot and cool loops whose average properties are inferred from X-ray observations. In any event, a key aspect of the use of thermal cyclotron lines as a coronal diagnostic is the accuracy with case, a change ΔH of only 5 G would shift the line center frequency by 56 MHz. Because the line half width is only 80 MHz, we can conclude that we know H to a precision of better than 5 G and conservatively estimate that H = 147 ± 5 G.

Here we should point out that individual cyclotron lines are observed near the apex of coronal loops where the magnetic field is relatively constant and a steep temperature gradient may exist. Neutral currents might also play a role, leading to intense radio emission from a relatively thin layer near the loop apex. The

field strength decreases uniformly with height. The cyclotron lines from loop legs will, however, exhibit a great deal of spatial structure if the loops are thin enough (Holman and Kundu 1986). Observations of thin loops at an oblique angle with wavelengths $\lambda \approx 6$ cm should lead to the spatial resolution of cyclotron-emitting layers along the loop legs, while observations of the loop apex at $\lambda \approx 20$ cm can resolve cyclotron lines in this region. Both techniques can provide a powerful diagnostic of the magnetic and thermal properties of coronal loops.

IV. SUMMARY

Simultaneous high-resolution observations of AR 4663 with the VLA and the SMM-XRP indicate that the radiation at 20-cm and soft X-ray wavelengths originates from the same region, and that 20-cm VLA maps can image X-ray coronal loops. The X-ray spectral lines were used to infer an average electron temperature of $T_e = 2.85 \pm 0.08 \times 10^6$ K and an average electron density of $N_e = 1.8 \pm 0.3 \times 10^{10}$ c These parameters were used to show that the layers emitting 20-cm radiation can be cm^{-3}. optically thick to either thermal bremsstrahlung or thermal gyroresonance radiation, depending upon unknown but plausible values of loop thickness, magnetic scale height and magnetic field strength.

The absence of circular polarization suggests that these coronal loops are optically thick at wavelengths near 20 cm, and the detection of a line-like feature in the radio spectrum indicates that gyroresonance absorption exceeds free-free absorption. This feature is attributed to a thermal cyclotron line. The X-ray values for T_e and N_e were combined with plausible values for gyroresonant optical depth and the magnetic scale height to show that the 20-cm radiation is at the fourth harmonic of the gyrofrequency. The central frequency and relatively narrow width of the thermal cyclotron line were combined with this harmonic to infer a magnetic field strength, H, of $H = 147 \pm 5$ G at the apex of these coronal loops.

Radio astronomical studies of the Sun at Tufts University are supported under grant AFOSR-83-0019 with the Air Force Office of Scientific Research and contract N00014-86-K-0068 with the Office of Naval Research (ONR). Simultaneous VLA and Solar Maximum Mission (SMM) observations of the Sun are supported by NASA grant NAG 5-501. K.L.S. and K.T.S. are supported by NASA contract NAS 5-23758 and the Lockheed Independent Research Program. The XPP was built by a consortium of three groups: Lockheed Palo Alto Research Laboratory, Mullard Space Science Laboratory, and the Rutherford and Appleton Laboratories. The Very Large Array is operated by Associated Universities Inc., under contract with the National Science Foundation.

REFERENCES

Holman, G.O., and Kundu, M.R. 1985, Ap. J. 292, 291.

Kuznetsov, V.S., and Syrovatskii, S.I. 1981, Solar Phys. 69, 391.

Lang, K.R. 1980, Astrophysical Formulae (2nd ed., New York: Springer-Verlag), p.47.

Lang, K.R., and Willson, R.F. 1983, Adv. Space Res. 2, No. 11, 91.

Lang, K.R., and Willson, R.F. 1984, Adv. Space Res. 4, No. 7, 105.

Lang, K.R., and Willson, R.F. and Gaizauskas, V. 1983, Ap. J. 267, 455.

Lang, K.R., Willson, R.F., and Rayrole, J. 1982, Ap. J. 258, 384.

Lang, K.R., Willson, R.F., Smith, K.L., and Strong, K.T. 1986, "Simultaneous Solar Maximum Mission and Very Large Array Observations of Solar Active Regions," submitted to Ap. J..

McConnell, D., and Kundu, M.R. 1983, Ap. J. 269, 698.

Shevgaonkar, R.K., and Kundu, M.R. 1984, Ap. J. 283, 413.

Syrovatskii, S.I., and Kuznetsov, V.D. 1980, in IAU Symposium 86, Radio Physics of the Sun, ed. M.R. Kundu and T.E. Gergely (Dordrecht: Reidel), p. 109.

Webb, D.F., Holman, G.D., Davis, J.M., Kundu, M.R., and Shevgaonkar, R.K. 1986, "The Plasma and Magnetic Field Properties of Coronal Loops Observed at High Spatial Resolution", submitted to Ap. J..

Willson, R.F. 1985, Ap. J. 298, 911.

Zheleznyakov, V.V. 1970, Radio Emission of the Sun and Planets (New York: Pergamon Press), p. 454.

Zheleznyakov, V.V., and Zlotnik, E. Ya. 1980, in IAU Symposium 86 Radio Physics of the Sun, ed. M.R. Kundu and T. Gergely (Dordrecht: Reidel). p. 87.

KENNETH R. LANG and ROBERT F. WILLSON
Department of Physics and Astronomy,
Robinson Hall,
Tufts University,
Medford, MA 02155

KERMIT L. SMITH and KEITH T. STRONG
Code 602.6,
Bldg. 7 - XRP,
Goddard Space Flight Center,
Greenbelt, MD 20771

Table 1. Maximum brightness temperatures, T_{Bmax}, of the coronal loops within AR 4336 at different radio frequencies.

Frequency (MHz)	T_{Bmax} (°K)	Frequency (MHz)	T_{Bmax} (°K)
1440	1.7×10^6	1620	2.8×10
1480	1.9×10^6	1658	3.8×10^6
1515	2.0×10^6	1690	2.4×10^6
1558	2.3×10^6	1705	2.0×10^6
1585	2.2×10^6	1725	1.8×10^6

Table 2. The mean electron temperature, T_e, and the mean electron density, N_e, for the regions marked A, B, C and D in Figure 5. Values averaged over all four regions are given at the bottom of each column.

Region	Te (°K)	N_e (cm^{-3})
A	2.87×10^6	1.8×10^{10}
B	2.92×10^6	2.2×10^{10}
C	2.93×10^6	1.4×10^{10}
D	2.69×10^6	1.8×10^{10}
Average	2.85×10^6	1.8×10^{10}

FIGURE LEGENDS

Fig. 1. A comparison of 20 cm (VLA-left), soft X-ray (SMM-XRP-center) and Hα (SOON-right) images of AR 4663 on 1985 June 7. The field of view of all three images is identical, and the identical angular scale can be inferred from the 60" spacing between fiducial marks on the axes. The contours of the 20 cm map mark levels of equal brightness temperature corresponding to 0.2, 0.4,...1.0 times the maximum brightness temperature of 1.8×10^6 K. The soft X-ray data were taken in the O VIII line (18.9 Å) with contours corresponding to , , and counts per second above a background level of counts per second with a maximum signal of counts per second.

Fig. 2. The 20 cm contours of equal brightness temperature (solid black lines) are superposed on a Kitt Peak National Observatory (KPNO) magnetogram of AR 4663 on 1985 June 7. The black magnetogram features indicate regions of negative magnetic polarity with magnetic fields pointed in towards the Sun, while the white magnetogram areas are regions of positive magnetic polarity with magnetic field lines pointed out towards the observer. The KPNO magnetogram is coutesy of Jack Harvey of the National Solar Observatory.

Fig. 3. VLA synthesis maps of the total intensity, I, of AR 4663 at 10 closely spaced frequencies during a 9 hour period on 1985 June 7. The synthesized beamwidth was about 3" x 4", and the spacing between fiducial marks on the axes is 60". The map contours mark levels of equal brightness temperature, with an outermost contour of 7.6×10^5 K and a contour interval of 3.8×10^5 K. The maximum brightness temperatures are given in Table 1 and plotted in Figure 4.

Fig. 4. The maximum brightness temperature of the coronal loops of AR 4663 at 10 closely spaced frequencies on 1985 June 7. The maximum temperatures were inferred from the 9-hour synthesis maps shown in Figure 3, and the error bars correspond to the peak-to-peak fluctuations in the background temperature of the synthesis maps.

Fig. 5. A soft X-ray map of AR 4663 taken in the O VIII line (18.9 Å) with contours corresponding to , and counts per second. The ratio of the O VIII and Mg XI line intensities were used to determine the mean electron temperature in the regions marked A, B, C and D. These temperatures are given together with estimates for the mean electron density in Table 2.

ORIGINAL PAGE IS
OF POOR QUALITY

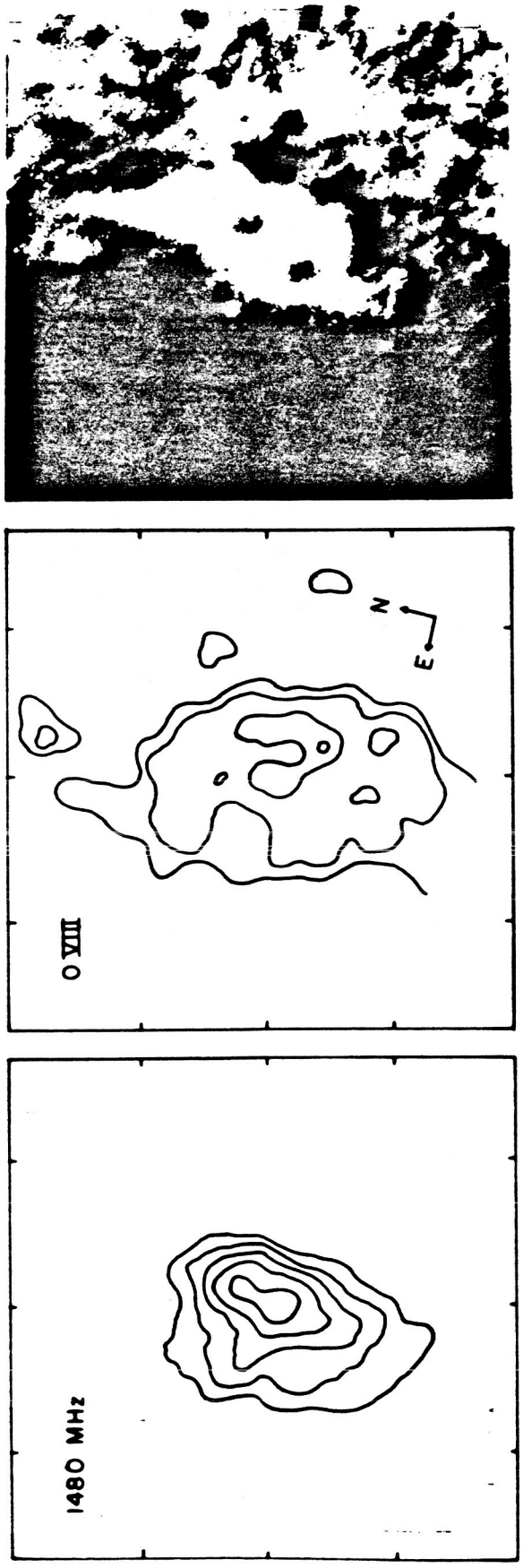

Fig. 1

ORIGINAL PAGE IS
OF POOR QUALITY

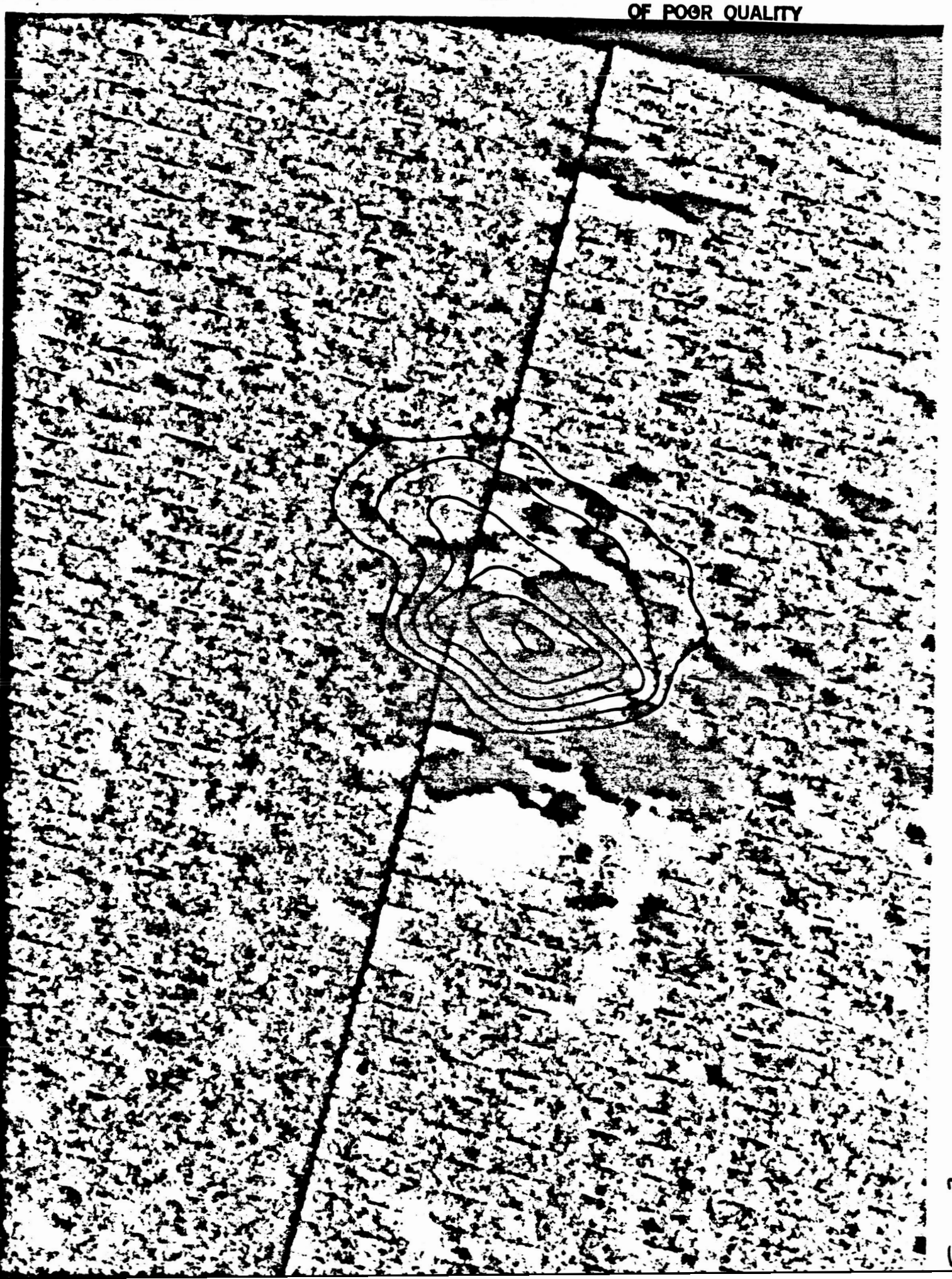

Fig. 2

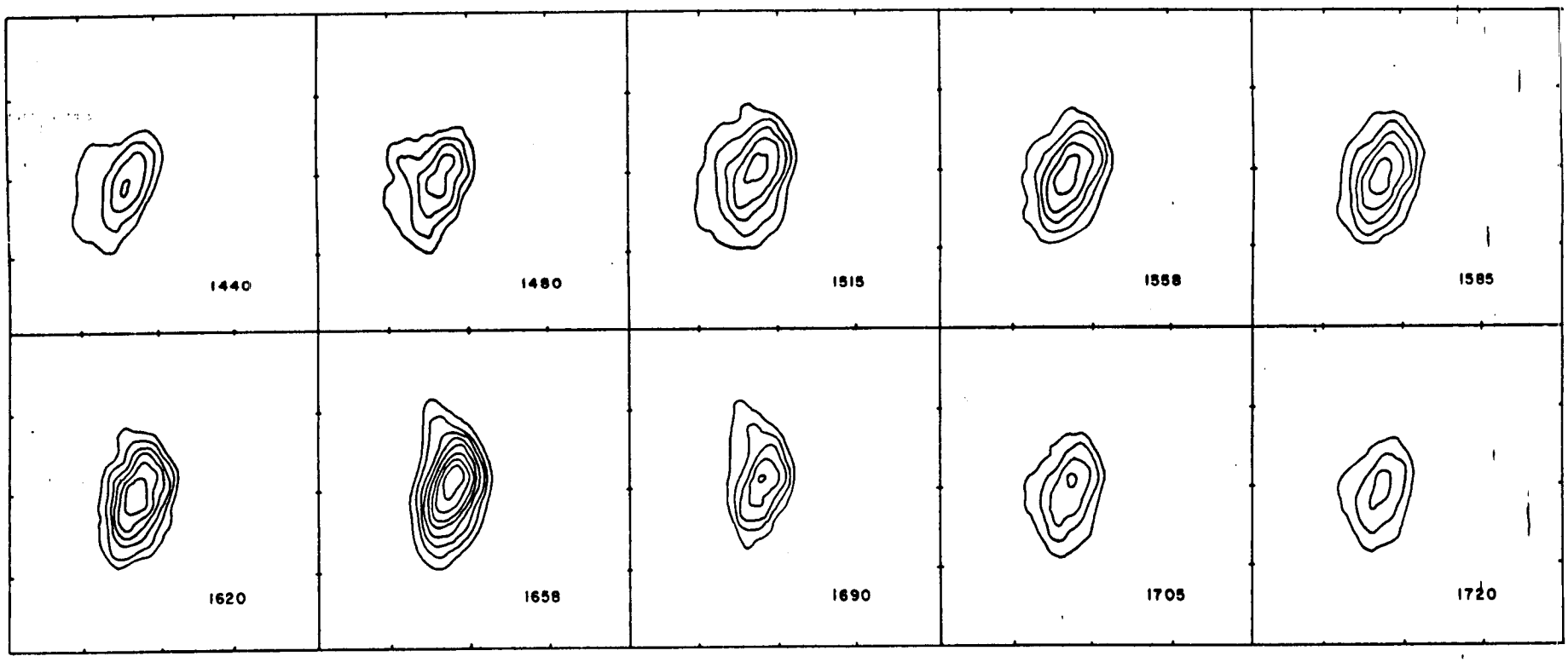

Fig 3

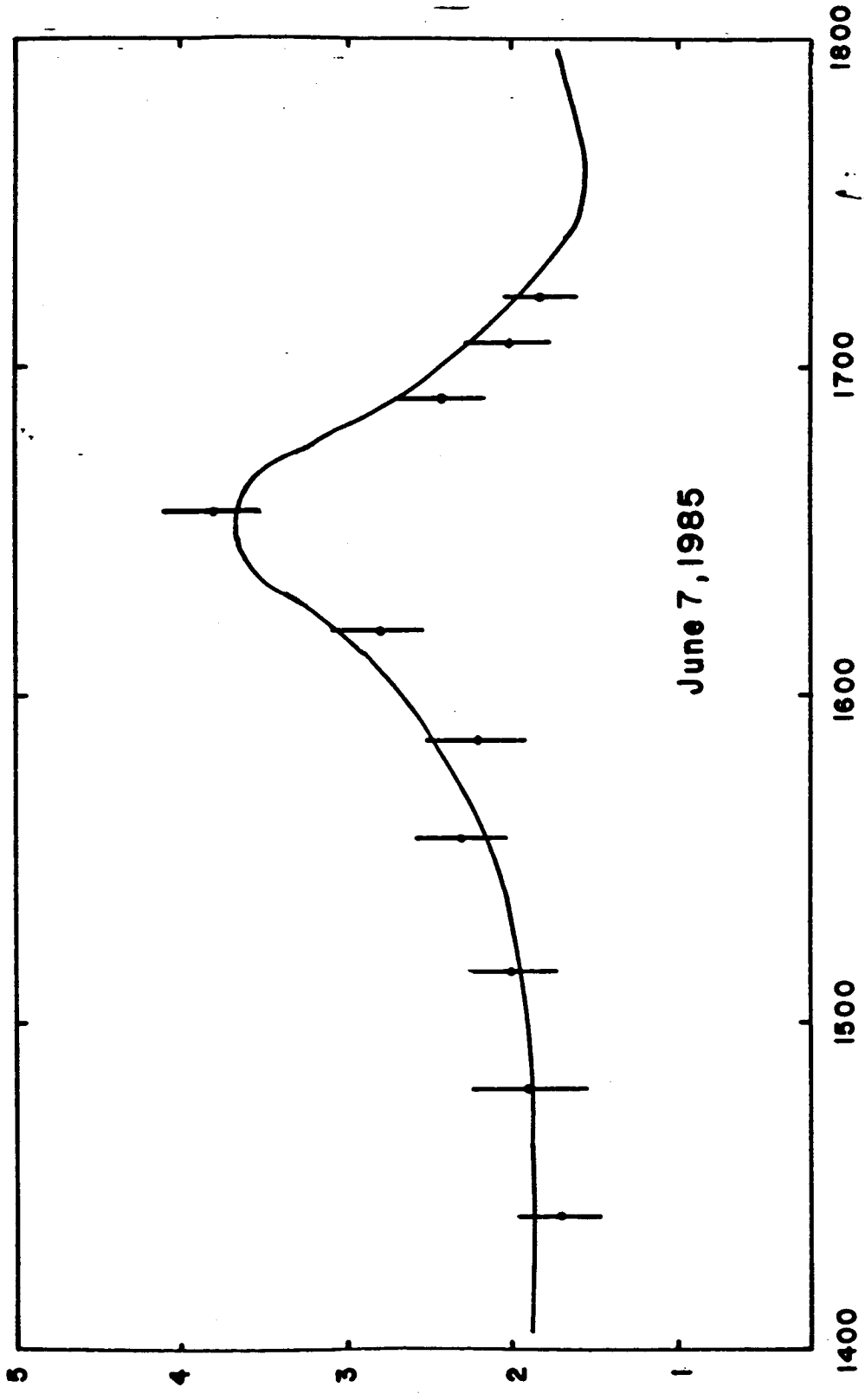
BRIGHTNESS TEMPERATURE (10^6K)
5
4
3
2
1
1400
1500
1600
1700
1800
FREQUENCY (MHz)
June 7, 1985

Fig. 4

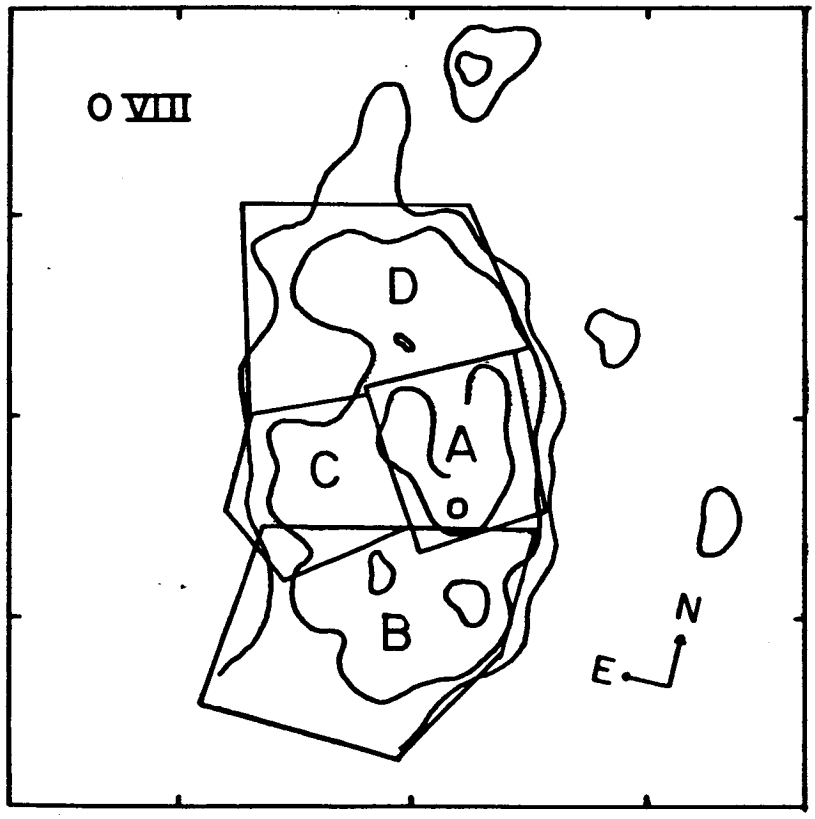

Fig 5.

VLA OBSERVATIONS OF A SOLAR NOISE STORM

KENNETH R. LANG AND ROBERT F. WILLSON

Department of Physics and Astronomy

Tufts University

ABSTRACT

We present the first Very Large Array (VLA) observations of the Sun at 92 cm wavelength (328 MHz). A solar noise storm, which lasted at least 3 hours, was detected at this wavelength and resolved with an angular resolution of 9". Snapshot maps of successive storm peaks indicate an elongated source with a persistant unchanging shape whose half-power angular size was 40" x 120". This result is not inconsistent with previous observations of a decrease in source size at increasing frequency, but it does indicate a previously unsuspected complexity to noise storm structure. The observed noise storm consisted of burst-like spikes superimposed on a slowly varying background. Both of these storm components were 95 ± 5% right-hand circularly polarized. This polarization is consistent with the ordinary mode of wave propagation in coronal magnetic fields that are connected to the dominant, leading sunspot of the associated active region. If the storm source lies radially above this sunspot, the source has a height, h, of $h = 0.30 \pm 0.30\ R_\odot = 2.0 \pm 0.2 \times 10^{10}$ cm above the photosphere. This result is consistent with an average storm height that decreases with increasing frequency. Ionospheric refraction will produce a noontime position shift, $\Delta\theta_I$, of $\Delta\theta_I \approx 15"$ at 92 cm wavelength. Greater position shifts can be expected at larger hour angles, but these shifts can be removed by frequent observations of a nearby calibrator source. An electron density of $N_e = 1.4 \times 10^9$ cm^{-3} is inferred for $h = 0.3\ R_\odot$, suggesting a dense plasma trapped in coronal loops. The plasma radiation also requires magnetic field strengths $H \ll 100$ G at $h = 0.3\ R_\odot$. A long-duration soft X-ray event had a similar time profile to that of the noise storm, but the onset of the X-ray emission preceded that of the radio radiation by 30 minutes This suggests a disturbance moving outwards at a velocity of $v \approx 100$ km s^{-1}.

During the first two hours, the noise storm consisted of two compact sources, each 40" in angular diameter and separated by 120". An angular size of 40" would be expected if the waves that excite the storm source move at the velocity of light for a duration of 0.1 s. Future VLA observations may distinguish between the sources of Type I bursts and the slowly-varying background, resolving both of them for the first time. The VLA can also test and constrain theoretical models in which newly-emerging magnetic flux arises in regions of strong, pre-existing coronal fields, thereby initiating and maintaining solar noise storms. The second harmonic of the storm plasma frequency can potentially be detected by the VLA for the first time. Future VLA observations at 92 cm wavelength will also provide new information about the middle corona in which open and closed magnetic field lines coexist, thereby providing new clues to the origin of coronal transients, decimetric bursts, and possibly even the solar wind.

I. INTRODUCTION

Noise storms are the most common phenomenon observed on the Sun at decimetric and metric wavelengths (see Elgaroy 1977 and Kai, Melrose and Susaki 1985 for reviews). Here we will present a brief synopsis of their properties, thereby providing a perspective for our subsequent observations and discussion.

The noise storms consist of a slowly-varying, wide-band continuum radiation with superimposed short-lived, narrow-band bursts. The background continuum, which is usually observed between 50 and 350 MHz, normally continues for a few hours and sometimes lasts for days. The noise storms are clearly associated with solar active regions, but there is no clear-cut association with solar flares.

Literally thousands of storm bursts are emitted, each with a bandwidth between 2 and 10 MHz and a duration of 0.1 to 2s. These bursts have been designated Type I bursts in order to distinguish them from other types of solar bursts. They are superimposed upon a continuum that is not thought to be composed of numerous bursts.

Both the background continuum and the bursts are strongly circularly polarized (up to 100%), usually with the same sense and degree of polarization. This polarization is attributed to coronal magnetic fields that connect with underlying sunspots. The sense of circular polarization usually corresponds to the ordinary mode of wave propagation in the magnetic field of the nearest leading spot; right-handed circular polarization therefore corresponds to negative magnetic polarity with the magnetic field lines pointed in towards the Sun.

It is thought that noise storms are some kind of plasma radiation emitted at the plasma frequency, and this is consistent with circular polarization in the ordinary mode. The emission originates in the lower solar corona at altitudes of between 0.1 and 0.5R. (solar radii) above the photosphere. Radiation at lower frequencies originates at higher altitudes where the electron density and plasma frequency are smaller than those at lower altitudes. The inferred electron density at a given altitude is greater than that of the quiet corona at this altitude, suggesting an origin in closed magnetic loops (coronal loops) that contain a high-density plasma.

Noise storms therefore appear to be due to plasma radiation at different altitudes within coronal loops. This radiation is triggered by some event, and then continues to be emitted for hours at a fixed altitude for each frequency. As we shall subsequently see, there is controversy over the cause of both the initial triggering and the continued excitation of solar noise storms. Very Large Array (VLA) observations will provide new insights that may resolve these controversies.

II. OBSERVATIONS

a) Time Profile

The VLA was used to observe the solar active region AR 4732 in the A configuration between 1300 UT and 2400 UT on 29 May 1986. The position of AR 4731 was on 0N 40W on this day. The array was divided into two subarrays with 12 antennas operating at 92 cm wavelength (328 MHz) with a 3.12 MHz bandwidth and 15 antennas operating at 21 cm wavelength (1420 MHz) with a 12.5 MHz

bandwidth. The beamwidth of the individual antennae at 21 cm was 31.5' and included the active region AR 4731 located at 6S 50W at 1300 UT on 29 May. The individual antennae had beamwidths of 138' at 92 cm, which includes the entire visible disk of the Sun, but AR 4731 and AR 4732 were the only active regions on the visible solar surface during our observations.

All four Stokes parameters were sampled every 6.67s, and the data were calibrated by observing 3C 84 every 30 minutes. The flux density of 3C 84 was assumed to be 32.0 Jy and 8.0 Jy at 21 cm and 92 cm, respectively.

As illustrated in Figure 1, a noise storm was detected at 92 cm between about 1930 UT and 2400 UT. No noise storm was detected at 21 cm, but this is not surprising for plasma radiation at this wavelength would be absorbed in the overlying solar atmosphere. The 92 cm noise storm consisted of numerous burst-like spikes superimposed on slowly-varying emission.

The burst-like spikes are analogous to Type I bursts, but the observed data have relatively long integration times that probably integrate the emission of several Type I bursts or chains of bursts. The slowly-varying emission resembles the background continuum of a typical noise storm. Both the burst-like spikes and the slowly-varying background emission were 95 ± 5% right-hand circularly polarized.

b) Source Size and Brightness Temperature

Observations of noise storms with the Culgoora radioheliograph at two frequencies (80 and 160 MHz) and with the Clark Lake facility at several frequencies between 20 and 65 MHz suggest that the higher frequency radiation

originates in more compact sources (Gergely and Kundu 1975; Stewart 1976; McLean 1981). This downward trend in source size with increasing frequency was also suggested by a small sample of storm sources observed with the Culgoora instrument at 80, 160 and 327 MHz (Sheridan, et al. 1983). Characteristic half-power angular sizes of $\theta \sim 6'$, $3'$ and $1.5'$ were respectively obtained at 80, 160 and 327 MHz.

However, storm sources are also often unresolved with even the largest radio telescopes, and the telescope beamwidths exhibit a disturbingly similar downward trend with increasing frequency. There have been no systematic high-resolution investigations of the size and shape of solar noise storms because of the poor resolving power of the existing radio telescopes. But now the VLA can provide angular resolutions that are more than an order of magnitude better than those of previous observations. Angular resolutions as great as $5''$ can be obtained with the VLA at 92 cm wavelength (328 MHz). By way of comparison, the Culgoora and Nancay instruments had respective beamwidths of $\sim 2'$ and $\sim 1.3'$ at 160 MHz.

The VLA also has the capability of making snapshot maps at time intervals as short as 3 s. As an example, Figure 2 shows VLA snapshot maps of successive peaks in the emission of the 92 cm noise storm shown in Figure 1 (peaks 3, 4, 5, and 6 and 7). This storm originates in an elongated source that has a persistant, unchanging shape with a half-power angular size of about 40" x 120". For comparison, the tapered beamwidth of 9" x 9" is shown as a black dot.

Although this result is not inconsistent with previous observations of a decrease in source size at higher frequencies, it suggests that complex source

structure will be revealed at high resolution. Such complexity may well rule out the simple model in which noise storms originate within a conical column (diverging magnetic fields) whose size increases with height (McLean 1973, 1981).

The largest peak brightness temperature, T_B, of the sources shown in Figure 2 was $T_B = 1.6 \times 10^7$ K. This is at least an order of magnitude lower than the brightness temperatures observed at lower frequencies for other noise storms (T_B 10^8 to 10^9 K at 160 MHz). Several plausible explanations might account for the lower T_B observed at 92 cm, including the ability of the VLA to detect weak noise storms, a reduced signal caused by integrating over several short-lived bursts, partial absorption in the overlying solar atmosphere, and a drop in the intrinsic source spectrum at high frequencies.

c) Circular Polarization and Magnetic Structure

The strong circular polarization of the 92 cm noise storm can be attributed to coronal magnetic fields that connect regions of opposite magnetic polarity in the underlying photosphere. Moreover, the sense of circular polarization should correspond with that of the ordinary mode expected from plasma radiation in a strong magnetic field (Dulk and Nelson 1973; Stewart 1985). Right-handed circular polarization is therefore associated with negative magnetic polarity in which the magnetic field is directed away from the observer and into the Sun. Left-handed circular polarization is similarly associated with positive magnetic polarity in which the magnetic field is directed towards the observer. By way of contrast, solar microwave radiation at the shorter 6 cm wavelength often exhibits the opposite behavior, with circular polarization in the extraordinary mode

expected from thermal cyclotron radiation in the legs of low-lying coronal loops (Lang and Willson 1982; Kundu and Lang 1985).

Because our observed storm was 95 ± 5% right-hand circularly polarized, it should originate in coronal magnetic fields that are connected with the dark, negative-polarity magnetogram features shown in Figure 3. Because the noise storm projects radially downward to the more central active region (AR 4732), the storm source is most likely associated with magnetic fields that connect to the dark dominant, leading spot of AR 4732.

As a matter of fact, noise storms are usually related to the dominant, leading sunspot of the associated active region. If this applies to our observations, then we can conclude that the observed radiation is polarized in the ordinary mode of the magneto-ionic theory and that it is probably due to plasma radiation.

Thus, the storm source is most likely plasma radiation in magnetic fields connected to the dark, leading spot of AR 4372. As illustrated in Figure 3, the angular size and distance of the noise storm are nevertheless larger than the angular separation of the leading and trailing spots of AR 4372. If the storm originates in closed magnetic loops, then they may not be solely connected to the bipolar AR 4372. Large-scale magnetic fields may instead connect the leading spots of the two active regions AR 4371 and AR 4372. A similar model has been proposed by Kai and Sheridan (1974) for other noise storms. However, our observations cannot by themselves rule out the possibility of open magnetic field lines that extend out into the interplanetary medium.

d) Source Height, Electron Density and Ionspheric Refraction

The height of a noise storm can be found if we assume that it lies radially above the associated sunspot. Under this assumption, the average observed heights, h, at 160 MHz and 80 MHz were h = 0.4 $R_\odot$ and h = 0.8 $R_\odot$ above the photosphere (Stewart 1976). Noise storms at the higher frequencies of 327 MHz and 408 MHz have estimated heights of h = 0.2 $R_\odot$ and h = 0.1 $R_\odot$, respectively (Sheridan, et al. 1983; Clavelier 1967).

Thus, the average height of the noise storm source decreases with increasing frequency. Our observations support this conclusion. The angular displacement of the noise storm from its associated spot is $\Delta\theta = 2.3'$ (when corrected for ionospheric refraction mentioned subsequently), and this displacement corresponds to a radial height of $h = 2.0 \pm 0.2 \times 10^{10}$ cm = 0.30 ± 0.03 $R_\odot$.

But this downward trend in height with increasing observing frequency is a quite general characteristic of solar radio emission. Higher frequencies usually arise closer to the solar surface because emission at frequency ν can arise only from regions where the electron plasma frequency $\nu_p = 8.9 \times 10^3$ $N_e^{1/2}$ Hz is equal to or lower than ν. Because the electron density, N_e, decreases as a function of height in the corona, ν_p also decreases with height and the lower frequencies must thus arise from greater heights.

It is the long-lived nature of noise storms that is the surprising thing. Storm radiation at frequency ν apparently originates in a relatively thin layer at a fixed height that corresponds to the local plasma frequency ν_p; and the height and relevant electron density remain relatively constant for hours. Moreover, the electron density at the measured height is larger than that inferred for the quiet coronal atmosphere. If we assume $\nu = \nu_p$, then our

observations at $\nu = 328$ MHz give an electron density of $N_e = 1.4 \times 10^9$ cm^{-3} at a height of $h = 2.0 \times 10^{10}$ cm above the photosphere. This electron density is an order of magnitude larger than that inferred from eclipse observations of the quiet corona and coronal active regions (Newkirk 1961; Saito 1970), and it supports previous observations of noise storms that indicated enhanced electron densities at a given height in the corona (Stewart 1976). Both the enhanced electron density and the long-lived nature of noise storms suggest that they originate in a dense plasma that is trapped within coronal loops. In fact, our observed electron density of $N_e = 1.4 \times 10^9$ cm^{-3} is comparable to that inferred from soft X-ray observations of coronal loops.

Refraction in the Earth's ionsphere will lead to a shift in source position and an error in height determination. This shift is smallest at source transit and largest near the horizon. It is also relatively large at sunrise and at times of increased solar activity.

In order to estimate refraction effects at 92 cm (328 MHz), we will build upon previous work at lower frequencies and note that the position shift is proportional to the inverse square of the observing frequency. When theoretical formulae given by Komesaroff (1960) are combined with measurements of the ionospheric electron density, Stewart and McLean (1982) obtain a noontime ionospheric shift of $\Delta\theta_I = 60''$ to the south at 160 MHz. Assuming that the refraction scales as the inverse square of the frequency, this corresponds to a noontime ionospheric shift of $\Delta\theta_I = 15''$ at 328 MHz. Greater position shifts can be expected at larger hour angles.

By way of comparison, Erikson (1984) determined the r.m.s. uncertainty, $\Delta\sigma_I$, in determining the positions of sources in night-time maps at frequencies

between 30 and 80 MHz. He found $\Delta\sigma_I = 60''$ at 80 MHz and noted that this could be extrapolated to the $\Delta\sigma_I = 1''$ at 600 MHz reported by Spoelstra (1983). Our noontime ionospheric shift of $\Delta\theta_I = 15''$ at 332 MHz therefore corresponds to $\Delta\theta_I = 4\Delta\sigma_I$ when previous results are scaled by the inverse square of the observing frequency.

When measuring the source height, we have corrected the observed shift for $\Delta\theta_I$, and note that the uncertainties in height correspond to a shift uncertainty of $\Delta\theta_I$. There will also be uncertainties in source size due to fluctuations in the ionospheric electron density that produce random position shifts. However, these size uncertainties are expected to be smaller than the synthesized VLA beamwidth of 5" to 10" at 92 cm, and they therefore do not need to be taken into account. Moreover, the systematic position shift $\Delta\theta_I$ can be automatically removed from future VLA data by frequent observations of a nearby calibration source.

III. DISCUSSION

a) Radiation and Excitation Mechanisms

Our observations are consistent with the idea that noise storms are due to plasma radiation with polarization in the ordinary mode. The plasma is constrained by coronal magnetic fields that connect to the dominant, leading spot of the associated active region. At our observing frequency of $\nu = 328$ MHz, we infer an electron density of $N_e = 1.4 \times 10^9$ cm^{-3} for the height $h = 2.0 \times 10^{10}$ cm from the condition that $\nu = \nu_p$, where the plasma frequency $\nu_p = 8.9 \times 10^3 N_e^{1/2}$ Hz.

The plasma radiation will dominate over thermal cyclotron radiation when $\nu = \nu_p >> \nu_H$, where the gyrofrequency $\nu_H = 2.8 \times 10^6 H$ Hz and H is the magnetic field strength in Gauss. Thus, we have $H << 100$ G in the storm source at a height of $h = 2.0 \times 10^{10}$ cm above the photosphere. The condition for suppression of the extraordinary mode of wave propagation, with the resultant escape of the ordinary mode, similarly requires $H << 100$ G at this height.

But what process triggers the onset of the solar noise storm, and what mechanism continues to excite this radiation in a relatively-small coronal volume for hours and even days? Some upward travelling disturbance probably excites plasma waves that are converted into electromagnetic radiation at the local plasma frequency. Because the electron density decreases with increasing height, this would account for the apparent decrease in its radiation frequency at higher altitudes. Of course, a magnetic field is required to explain the high circular polarization of the radiation, and upwardly-diverging magnetic field lines may account for the increase in source size with height.

There is, however, no generally accepted explanation for the initiating and driving mechanisms for solar noise storms. These mechanisms are probably related to magnetic evolution at coronal levels in the atmosphere above active regions. Noise storm durations of hours or several days are, for example, comparable to the time scales of coronal evolution, but much longer than the short-lived Hα flares and microwave bursts. A central ingredient of recent noise storm theories has therefore been the emergence of new magnetic flux in regions of strong, pre-existing coronal magnetic fields.

McLean (1981) has, for example, presented a model in which new dipolar magnetic structures emerge and move out through pre-existing ones, thereby initiating solar noise storms. Emerging magnetic flux in existing active regions has also been used to explain the association of noise storms with the sector structure of the interplanetary magnetic field (Stewart 1985). Newly-emerging magnetic fields might drive shocks or generate waves that move out into the corona where they initiate and maintain noise storms (Spicer, Benz and Huba 1981; Benz and Wentzel 1980).

But is there any direct observational evidence for an association between noise storms and newly-emerging magnetic flux? Noise storms have been related to eruptive prominences seen on the solar limb (McLean 1973), and the onset of three noise storms has been related to erupting filaments and coronal transients in conjunction with long-duration (hours) soft X-ray events (Webb and Kundu 1978). More recently, Lantos et al. (1981) have demonstrated a strong similarity between the time profiles of a noise storm at 169 MHz and a soft X-ray event of long duration (about one hour). In this case, the X-ray and radio events started at about the same time, and the radio noise storm was located in one leg of a white-light coronal transient observed with the Solar Maximum Mission Coronagraph/Polarimeter (SMM-C/P).

As illustrated in Figure 4, a long-duration soft X-ray event was also associated with the noise storm on 29 May 1986. The similar time profiles of the X-ray and radio emission suggest a physical link between the sources of the two types of radiation. In this case, the onset of the X-ray emission preceded that of the 92 cm radiation by about 30 m, suggesting that the noise

storm was triggered by a disturbance moving outwards from the source of X-ray radiation. If we assume that the sources of radiation at the two spectral regions are separated by a distance of $d = 0.3R_\odot = 2 \times 10^{10}$ cm, then the disturbance is moving outwards at a velocity of $v \sim 100$ km s^{-1}. This speed is probably higher than the local Alfven velocity, suggesting that the disturbance is a shock wave.

Information about the actual initiation and excitation of the noise storm will be obtained by observing the lowest possible level, or highest possible frequency. In fact, the 92 cm (or 328 MHz) VLA observations refer to one of the lowest levels that noise storms have been observed, and the high-resolution data provide some intriguing information about storm excitation. As illustrated in Figure 5, both the onset and the first maximum of the 92 cm noise storm consisted of two compact sources, each about 40" in angular diameter and separated by 120". These sources became gradually hotter during the course of three hours, increasing in brightness temperature from 2.4×10^6 K to 3.8×10^6 K.

An angular diameter of 40" corresponds to a linear size, L, of $L \sim 3 \times 10^9$ cm at the Sun's distance. Waves moving at the velocity of light would cross this dimension in a time, t, of $t = 0.1$ s. Because nothing can move faster than the velocity of light, the duration of an exciting source with this size must be $t \geq 0.1$ s. This is precisely the observed limit to the duration of individual Type I bursts! For instance, the duration of Type I

bursts at 318 MHz is 0.1 s $\leq$ t $\leq$ 0.5 s with an average value of t = 0.2 s (Elgaroy 1977). The VLA has therefore most probably resolved the intrinsic structure of the individual burst emitter even though individual bursts were not resolved in time. This emitter is probably the source of both the slowly-varying emission and the Type I bursts, for there was no substantial change in source structure for two hours.

b) Future VLA Potential

The VLA can potentially resolve noise storm sources with an angular resoltuion of 5" at 92 cm wavelength. Snapshot synthesis maps can be made with this resolution for intervals as short as 3 s, which is comparable to the duration of chains of Type I bursts. The observing bandwidth, $\Delta\nu$, can be comparable to that of Type I bursts ($\Delta\nu \sim 6$ MHz), and an improvement in VLA integration time to 0.1 s would permit observations of individual Type I bursts. Such an improvement would also benefit related VLA studies of flare stars and solar bursts at microwave wavelengths.

The VLA can probably distinguish between the two principal components of noise storms with the present integration time, thereby resolving the sources of Type I bursts and the background continuum for the first time. Future VLA observations will therefore probably determine if the two sources have comparable or different sizes, and if one of them resides within the other. Storm source sizes of 40" are expected if the waves within these sources move at the velocity of light with a duration of 0.1 s. Because the VLA has already been used to resolve storm sources with this size, it will detect individual emitters rather than the effects of scattering in the solar atmosphere.

Future VLA studies of the time profile, height and structure of noise storms will also provide new insights to their triggering and excitation mechanisms. VLA synthesis maps of circular polarization will delineate the magnetic field topology at the site of energy release. Radial extrapolations down to the photosphere may confirm the hypothesis that the noise storm sources are connected with sunspots whose magnetic polarity indicated circular polarization in the ordinary mode. This has only been convincingly demonstrated for a few small sources at lower frequencies (Dulk and Nelson 1973). Comparisons with ground-based optical observations of erupting filaments and satellite observations of soft X-ray events and coronal transients may confirm sugestions of a link between noise storms and these phenomena.

Both the fundamental and the second harmonic of the plasma frequency might be detected if an intense noise storm is observed with both the VLA and a smaller patrol-type solar radio telescope. The fundamental plasma radiation is all that has been previously observed, primarily because of the low brightness temperature of the harmonic. The large collecting area and high angular resolution of the VLA will vastly imporve detection thresholds. For instance, the fundamental noise storm radiation might be detected at 164 MHz with a typical brightness temperature of 10^9 K. The predicted brightness temperature of the second harmonic at 328 MHz would be about 5×10^6 K for a 40" source (Benz and Wentzel 1980). The VLA could easily detect such a signal.

In fact, we have already detected a noise storm with a comparable brightness temperature, but the absense of this event in Sagamore Hill observations at higher frequencies indicates that it is the fundamental of an

intrinsically-weak noise storm. Nevertheless, there is strong future potential for the VLA detection of the second harmonic of a strong noise storm. This would provide important constraints to theoretical explanations of noise storms.

Another potentially-rewarding result of future 92 cm VLA observations will be new information on the middle corona that is blocked from view by the occulting disks of coronagraphs. In the low corona detected at 6 cm and 20 cm wavelength, magnetism dominates plasma motion and the VLA detects the microwave counterpart of coronal loops (Kundu and Lang 1985). In the outer corona, however, the solar wind drags the solar magnetic field out into interplanetary space. The 92 cm VLA observations will refer to a region located between the field-dominated low corona and the plasma-dominated outer corona. We call this region the middle corona. It is expected to contain large-scale coronal loops whose magnetic field lines connect different active regions and open magnetic regions whose magnetic field lines are drawn out into interplanetary space.

Future 92 cm VLA observations of open and closed magnetic regions in the middle corona may resolve uncertainties over the origin of coronal transients or mass ejections in which loop-shaped, magnetically confined plasma rises and expands outwards into the solar wind. They will also provide information about the unknown origin of various kinds of decimetric bursts including those of Type I, III and IV. Future VLA studies of the middle corona may even provide new clues to the unknown source of the solar wind.

c) Acknowledgements

We thank the staff of the Very Large Array, and in particular, Durga Bagri and Rey Gonzalez, for help with the observations. Radio astronomical studies of the Sun at Tufts University are supported under grant AFOSR-83-0019 with the Air Force Office of Scientific Research and contract N00014-86-K-0068 with the Office of Naval Research (ONR). Our simultaneous VLA and Solar Maximum Mission (SMM) observations of the Sun are supported by NASA grant NAG 5-501. Collaborative long-wavelength solar observations by Tufts University and the Observatoire de Paris are supported by National Science Foundation (NSF) grant INT-8602285. The Very Large Array is operated by Associated Universities, Inc., under contract with the National Science Foundation.

KENNETH R. LANG and ROBERT F. WILLSON

Department of Physics and Astronomy

Robinson Hall

Tufts University

Medford, MA 02155

REFERENCES

Benz, A.O., and Wentzel, D.G. 1981, Astr. Ap. 94, 100.

Clavelier, B. 1967, Ann. d'Ap. 30, 895.

Dulk, G.A., and Nelson, G.J. 1973, Proc. Astr. Soc. Austr. 2, 211.

Elgaroy, O. 1977, Solar Noise Storms (New York: Pergamon Press).

Erickson, W.C. 1984, J. Astrophys. Astr. 5, 55.

Gergely, T.E., and Kundu, M.R. 1975, Solar Phys. 41, 163.

Kai, K., Melrose, D.B., and Suski, S., 1985, "Storms", in Solar Radiophysics, eds. D.J. McLean and N.R. Labrum (New York: Cambridge University Press) pp. 415-441.

Kai, K., and Sheridan, K.V. 1974, Solar Phys. 35, 181.

Komesaroff, M.M. 1960, Austr. J. Phys. 13, 153.

Kundu, M.R., and Lang, K.R. 1985, Science 228, 9.

Lang, K.R., and Willson, R.F. 1982, Ap. J. (Letters) 255, L111.

Lantos, P., Kerdraon, A., Rapley, C.G. and Bentley, R.D. 1981, Astr. Ap. 101, 33.

McLean, D.J. 1973, Proc. Astr. Soc. Austr. 2, 222.

McLean, D.J. 1981, Proc. Astr. Soc. Austr. 4, 132.

Newkirk, G. Jr. 1961, Ap. J. 133, 983.

Saito, K. 1970, Ann. Tokyo Astr. Obs. 12, 53.

Sheridan, K.V., Labrum, N.R., Payten, W.J., Nelson, G.J., and Hill, E.R. 1983, Solar Phys. 83, 167.

Spicer, D.S., Benz, A.O., and Huba, J.D. 1982, Astr. Ap. 105, 221.

Spoelstra, T.A.T. 1983, Astr. Ap. 120, 313.

Stewart, R.T. 1976, Solar Phys. 50, 437.

Stewart, R.T. 1985, Solar Phys. 96, 381.

Stewart, R.T., and McLean, D.J. 1982, Proc. Astr. Soc. Austr. 4, 386.

Webb, D.F., and Kundu, M.R. 1978, Solar Phys. 57, 154.

FIGURE LEGENDS

Fig. 1. The time profile of a solar noise storm observed with one interferometer pair of the Very Large Array (VLA) at 92 cm wavelength. The separation of the two antennae was 0.8 km, providing an angular resolution of 240" at 92 cm during source transit. Here the data have been smoothed over 33.3 s. Spike-like bursts are superimposed upon a slowly-varying background; both of these components were 95 ± 5% right-hand circularly polarized. VLA snapshot maps of the spikes denoted by 3, 4, 5, 6 and 7 are presented in Figure 2, and VLA maps covering the longer intervals denoted by 1 and 2 are shown in Figure 4.

Fig. 2. Very Large Array snapshot maps of successive peaks in a solar noise storm at 92 cm wavelength. These peaks are denoted by 3, 4, 5, 6 and 7 in Figure 1. The snapshot maps, each lasting 13 s or 30 s, show no substantial change in the shape or size of the storm source over a period of two hours. Here the synthesized beamwidth is denoted by the black dot, and the fiducial marks on the axes are separated by 100". The contours mark levels of equal brightness temperature, T_B, with an outermost contour of $T_B = 3.8 \times 10^6$ K, a contour interval of 2.5×10^6 K and a peak brightness temperature of $T_B = 1.6 \times 10^7$ K.

Fig. 3. A Very Large Array (VLA) synthesis map of a solar storm at 92 cm wavelength is superimposed on a Kitt Peak National Observatory (KPNO) magnetogram taken on the same day. The VLA map covered the one hour time interval between 2300 and 2400 UT; its synthesized beamwidth is denoted by the black spot. The contours mark levels of equal brightness temperature, T_B, with an outermost contour of $T_B = 1.0 \times 10^6$ K and a contour interval of 7.2 x

10^5 K. Dark areas on the magnetogram correspond to negative magnetic polarity with the magnetic field lines pointing in towards the Sun; whereas light magnetogram areas correspond to outward regions of positive magnetic polarity. Two dipolar regions are shown on the magnetogram - AR 4731 near the limb and AR 4732. The 92 cm source is attributed to plasma radiation in the ordinary mode of wave propagation along magnetic field lines connected to the dark negative spot of AR 4732. The angular displacement between this spot and the 92 cm source corresponds to a radial altitude of $0.2R_\odot$ above the photosphere. The magnetogram was kindly provided by Jack Harvey of the National Solar Observatory.

Fig. 4. A comparison of the 92 cm VLA time profile of a solar noise storm (top) with the soft X-ray emission detected by the GOES satellite (bottom). The X-ray emission precedes the 92 cm radiation by about 30 m. If we assume that the noise storm is excited by a disturbance that originates during the soft X-ray event, then that disturbance must travel outwards at a velocity of $v \sim 100$ km s^{-1} if it moves across the distance of $d \sim 0.2\ R_\odot$ in 30 m.

Fig. 5. Very Large Array (VLA) synthesis maps for a one hour interval that includes the beginning of a solar noise storm (left) and for the subsequent one hour interval that inclues the first maximum peak in the noise storm (right). These two intervals are respectively denoted by 1 and 2 in Figure 1. Both the onset and early excitation of the 92 cm noise storm consist of two sources with angular diameters of 40" and an angular separation of 120". Emission between the two sources became more intense later in the noise storm (see Figures 2 and 3). The he fiducial marks on the axes are separated by 100", and the contours mark levels of equal brightness temperature T_B, with an outermost contour of $T_B = 1.0 \times 10^6$ K and a contour interval of 7.2×10^5 K.

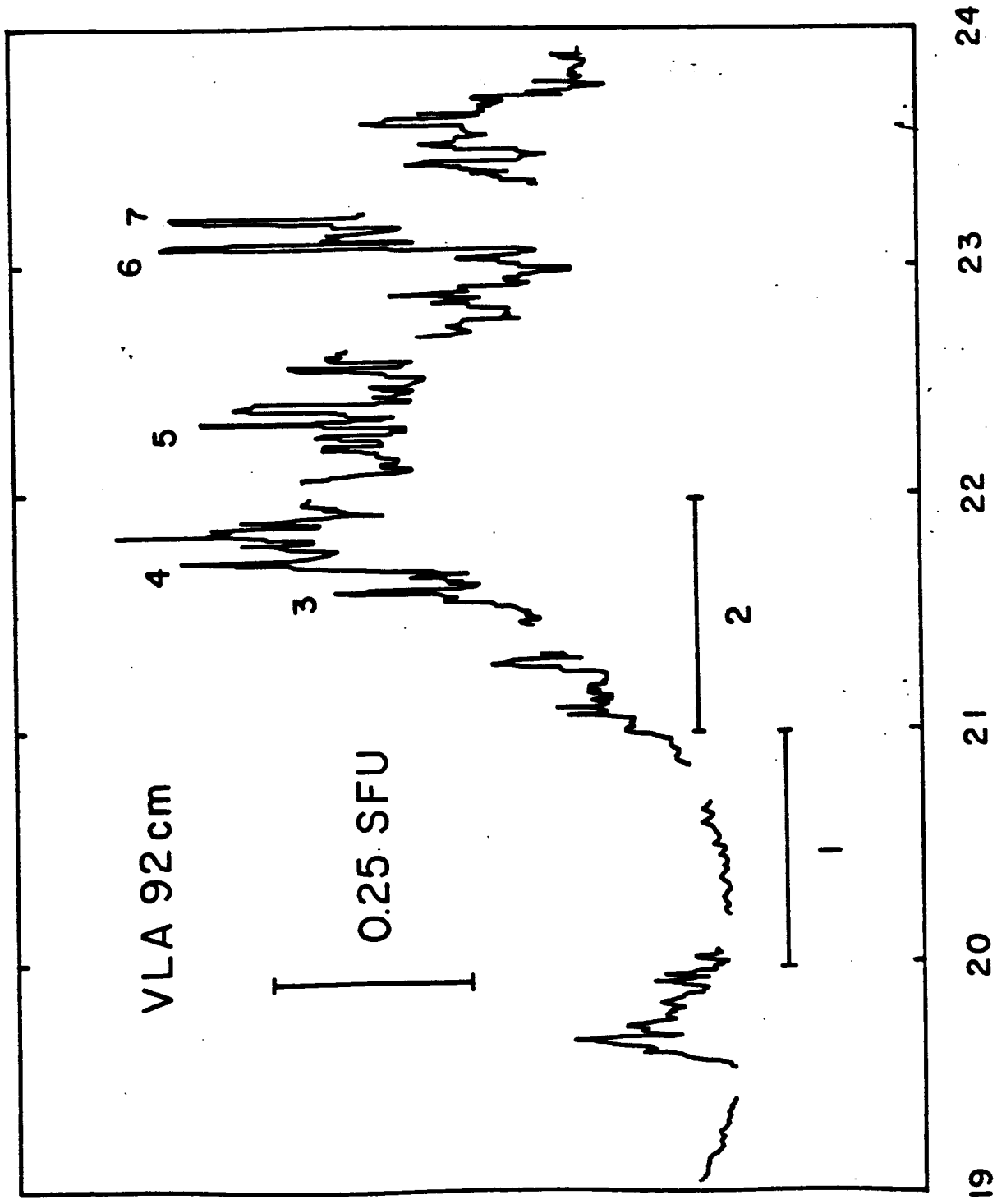

Fig. 1.

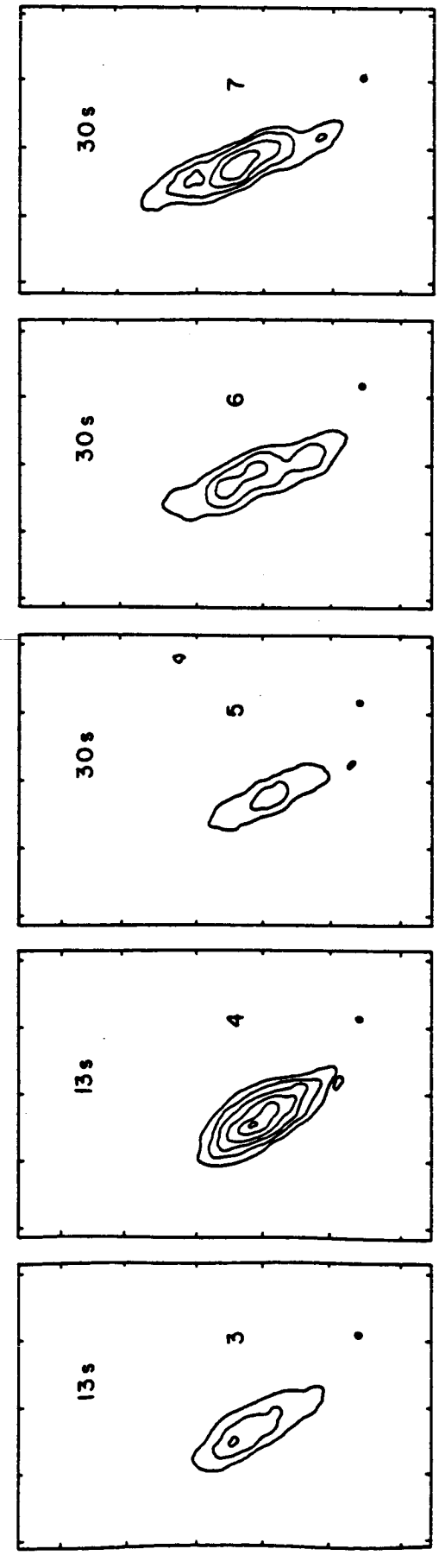

Fig. 2

ORIGINAL PAGE IS
OF POOR QUALITY

Fig. 3

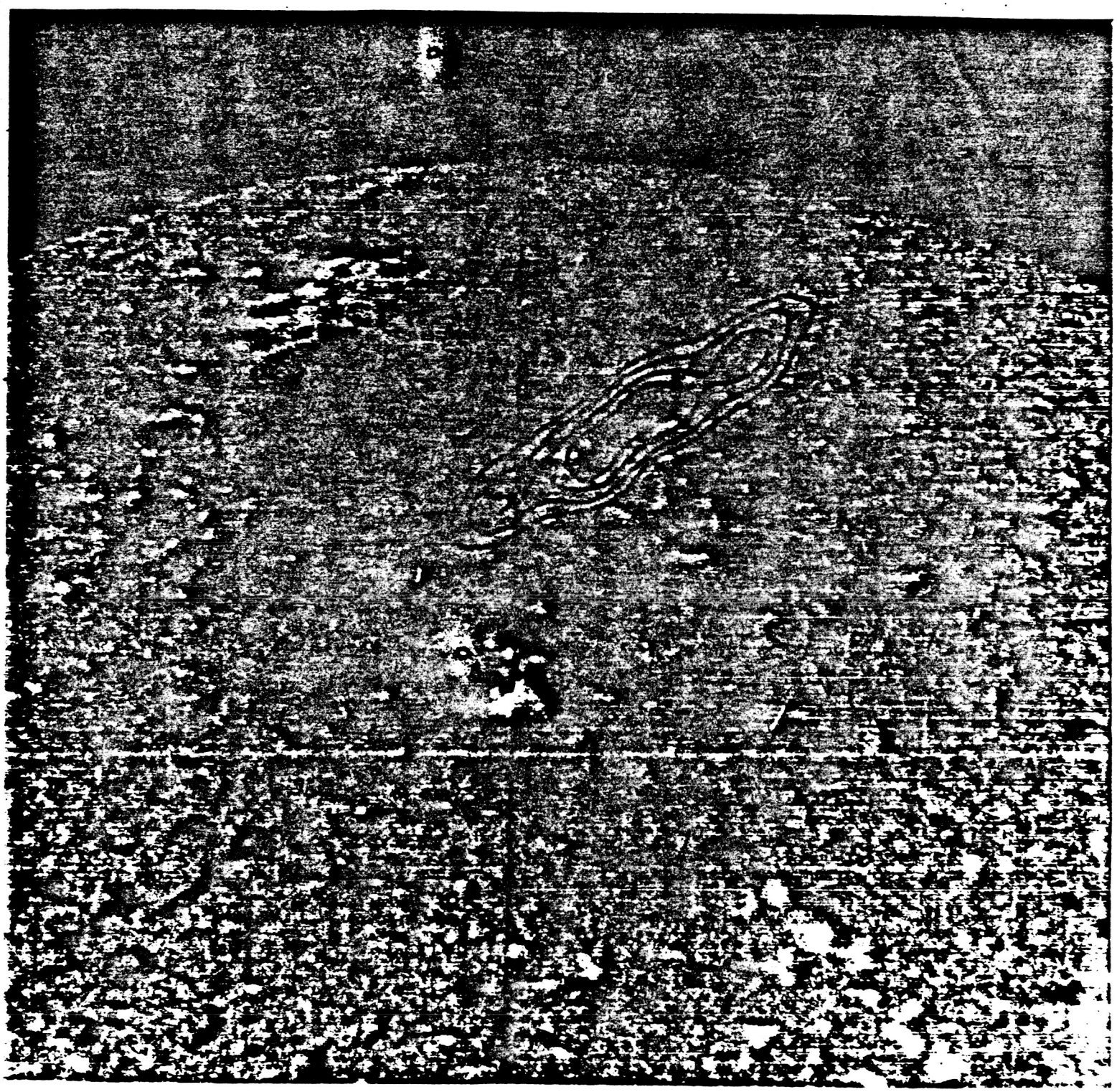

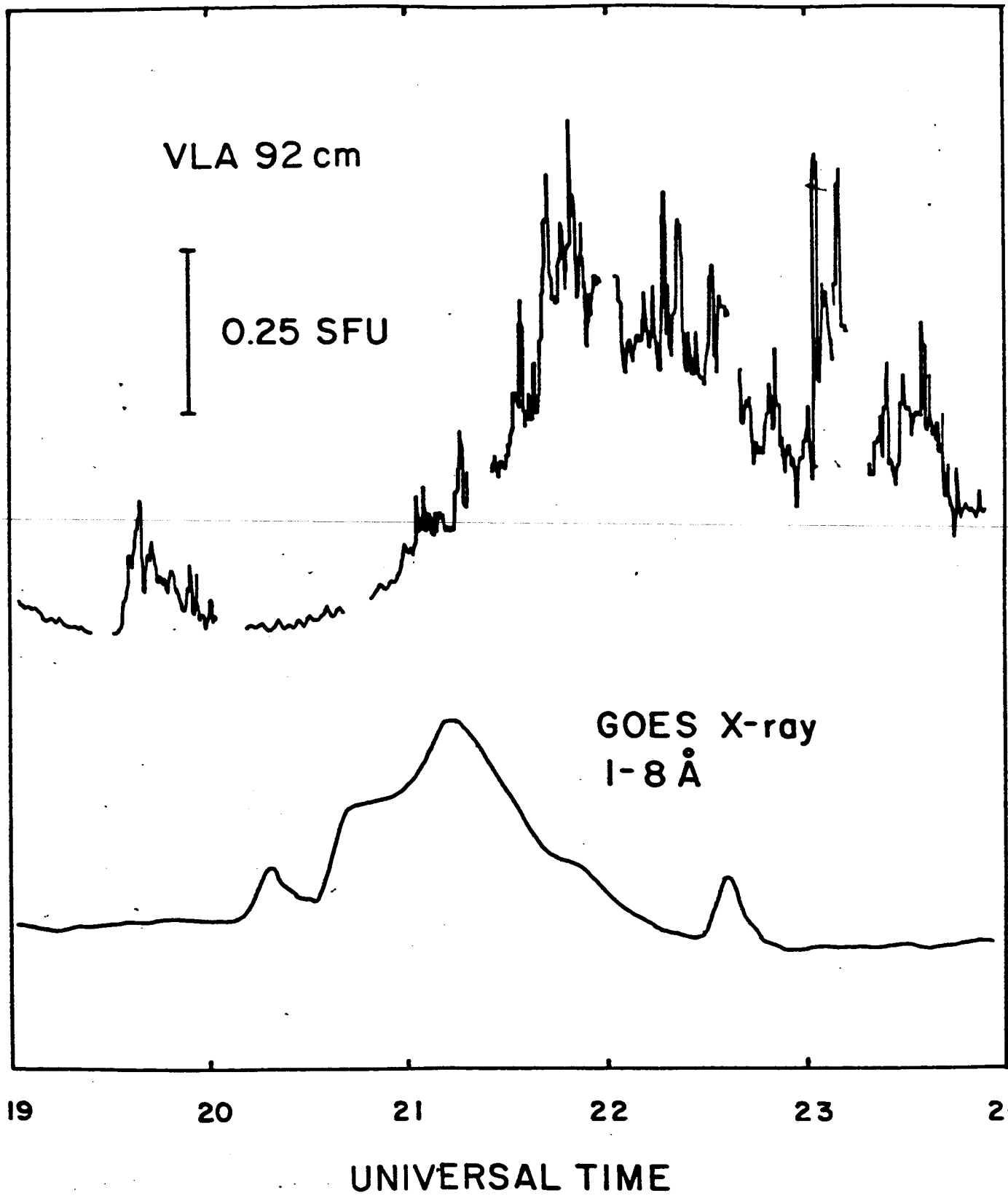

Fig. 4

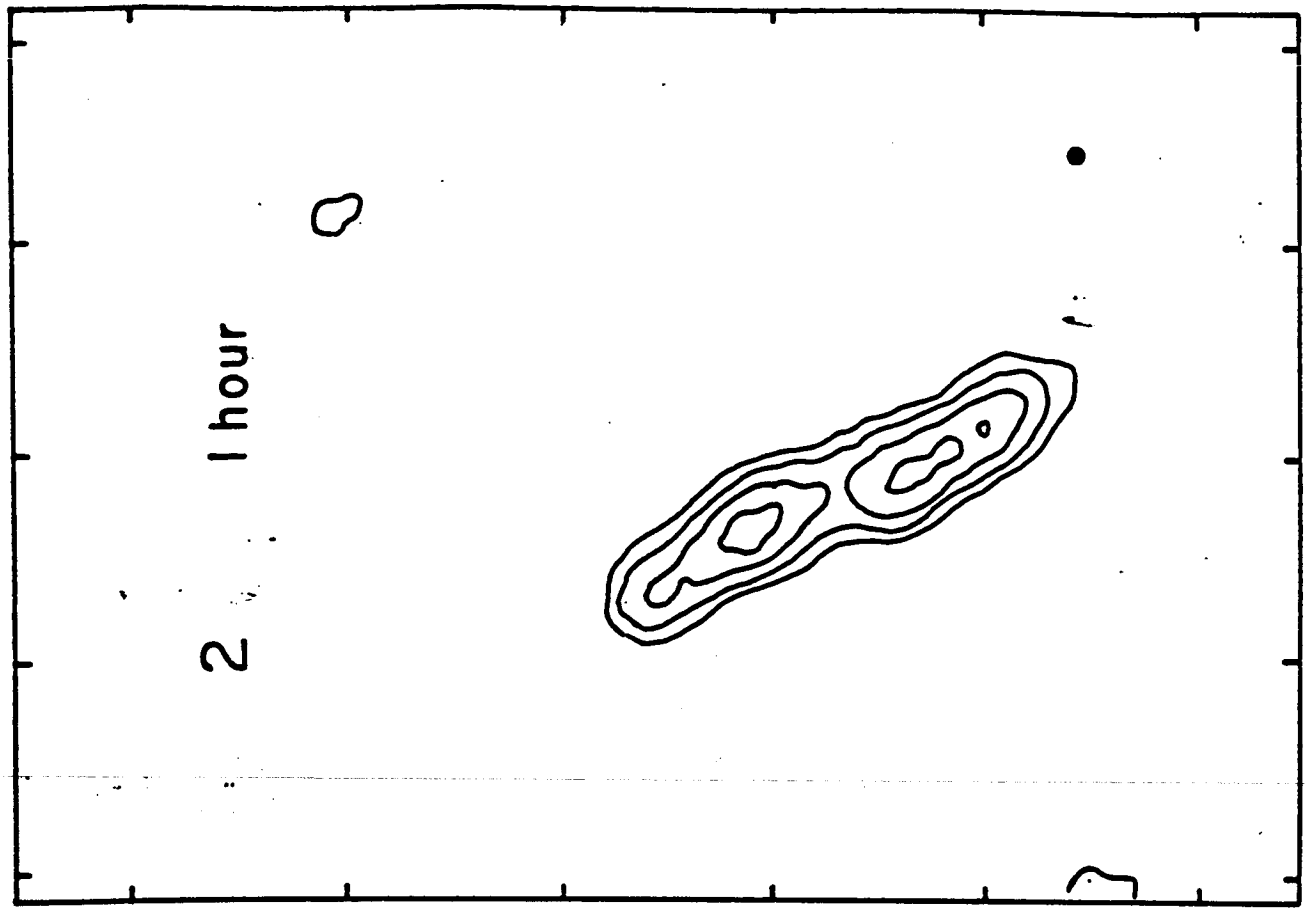

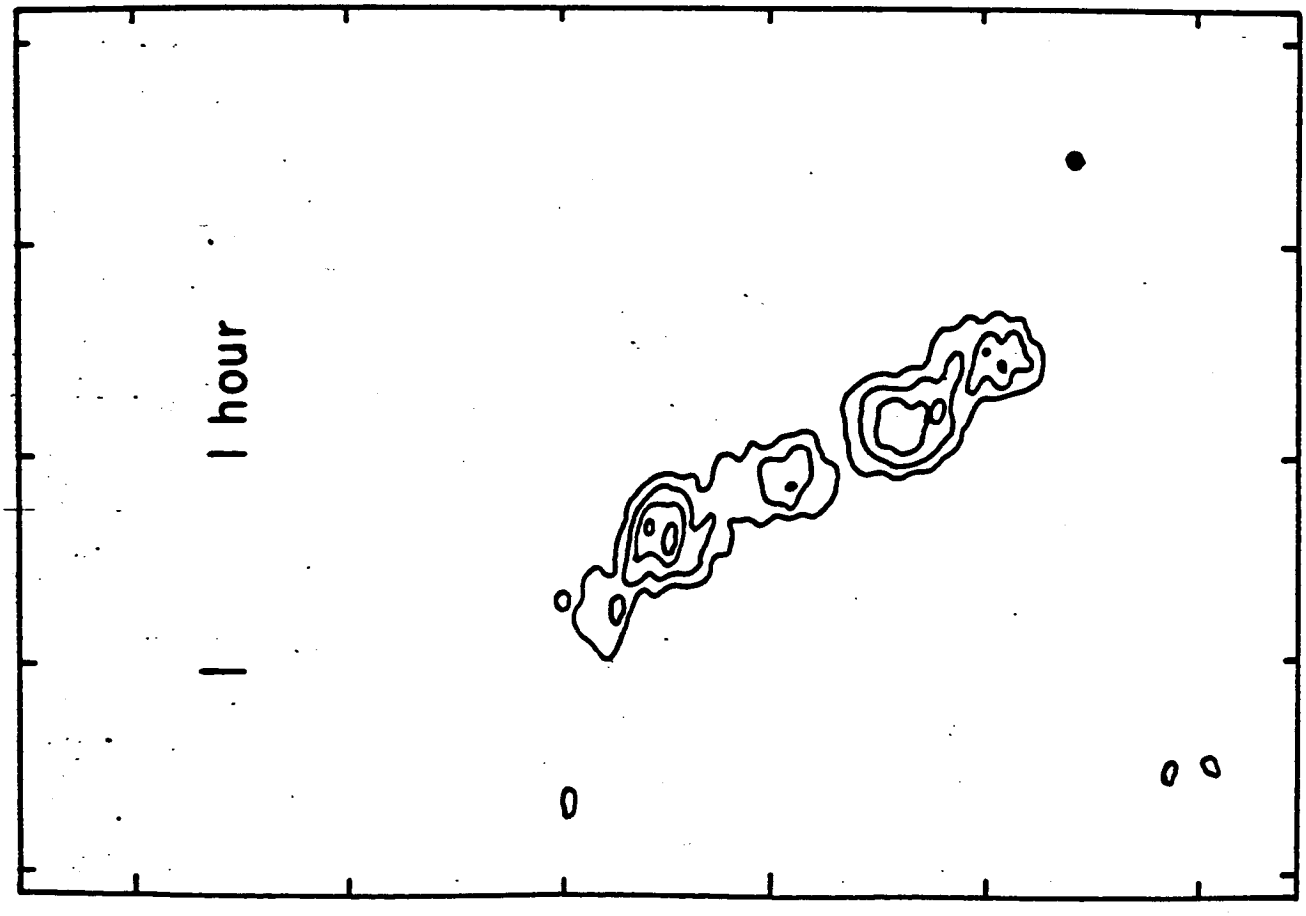

Fig. 5

V. LECTURES AT PROFESSIONAL MEETINGS.

The Principal Investigator, Kenneth R. Lang, gave an invited talk entitled "Microwave Emission from the Sun and Nearby Stars" at the Tokyo Astronomical Observatory in November, 1985. This was followed by three lectures in April, 1986 at the NASA Workshop on Coronal and Prominence Plasmas held at the Airlie Conference Center in Warrenton, Virginia. These lectures, which are reproduced in Sections III E, III F, and III G, will be published in the Workshop Proceedings. They are entitled "Coronal Diagnostics", "Coronal Plasmas on the Sun and Nearby Stars" and "Compact, Variable, Moving Sources Observed on the Sun at 2 Centimeters Wavelength".

During the period 20 to 26 June, 1986, Lang attended the Committee of European Radio Astronomers (CESRA) Workshop on Radio Continua During Solar Flares held at Aubigney-Sur-Nere, France. The workshop was divided into six sessions: acceleration processes, particle storage, emission processes, radio pulsations, cyclotron masers-spikes, and hard X-ray bursts. Lang attended all of the sessions, presenting a paper entitled "VLA Observations of Coronal Loops at 20 cm and 92 cm Wavelength" at the session on emission processes. He also presented a paper on "Radio Emission from Flare Stars" during the session on cyclotron masers-spikes."

Lang next attended the XXVI meeting of the Committee on Space Research (COSPAR) held at Toulouse, France from 28 June to 10 July 1986. He presented a paper entitled "Solar Burst Precursors and Energy Build Up At Microwave Wavelength during Symposium 5 on Synopsis of the Solar Maximum Analysis. This paper, which is reproduced in Section III D, will be published in the appropriate volume of Advances in Space Research.

VI. FUNDING AND FUTURE PROSPECTS

This ongoing research is funded by NASA Grant NAG 5-501 in the amount of $25,000 from 1 February 1985 to 31 March 1986 and $28,245 from 1 April 1986 to 31 March 1987. We spent the initial $25,000 allocation by 31 March 1986 and compeleted all of the proposed research for the period from 1 February 1985 to 31 March 1986. The second $28,245 allocation is expected to be spent by 31 March 1987 when all of the proposed research from 1 April 1986 to 31 March 1987 will be completed.

Our future research will be the subject of a $48,180 proposal to the next round of the Solar Maximum Mission Guest Investigator Program. This will be a one-year proposal for the period between 1 April 1987 and 31 March 1988. During this period we will emphasize visits to the Goddard Space Flight Center for collaborative comparisons of existing soft X-ray (XRP) data with existing VLA observations of coronal loops. The existing VLA data are listed in Table 1 at the end of this section. These future comparisons of existing XRP and VLA data are a natural extension of the work discussed in Sections IV-I and IV-J.

Our future research will also involve unique observations of the inner solar corona at decimetric wavelengths (10 cm to 100 cm). New technological developments at the Very Large Array and the Nancay Radioheliograph will make it possible to observe this region with hitherto unavailable resolution in space, time and frequency. The Very Large Array (VLA) will be used at 20 cm wavelength where it can be used to infer the physical properties of coronal loops. This is a natural extension of the work reported in Sections II B, III D, III E, and III F. The VLA will also be used at the longer wavelength of 92 cm where it will detect larger-scale coronal features. This is a natural extension of the first VLA solar observation at 92 cm wavelength that was reported in Section III K. The 20 cm observations can be compared with

simultaneous Solar Maximum Mission (SMM) XRP observations, while the 92 cm data may be compared with SMM C/P data that refer to the outer solar corona. The high temporal (20 msec) and frequency (five bands of variable spacing) of the Nancay Radioheliograph may additionally detect the signatures of pulsating and/or coherent burst mechanisms. It will be used at several wavelengths near 92 cm and 183 cm.

The combined results of our forthcoming SMM Guest Investigator proposal will specify the three-dimensional structure of both quiescent active regions and solar bursts. Large-scale quiet Sun features such as coronal holes, filament cavities and magnetically weak regions will also be observed, helping to resolve uncertainties over the temperature, density and magnetic structure in the low solar corona. The proposed observations will provide valuable new insights to the driving mechanisms and initiating source for decimetric bursts that currently remain a mystery. They may also resolve uncertainties over the origin of coronal transients or mass ejections in which loop-shaped, magnetically confined plasma rises and expands outwards into the solar wind. The combined SMM, VLA and Nancay data may, for example, tell if mass ejections are initiated by erupting filaments, rising loops or magnetic reconnection in the low corona.

Table 1. Existing Very Large Array (VLA) observations of coronal loops that may be compared with existing Solar Maximum Mission (SMM) XRP observations of the same active regions.

DATE	ACTIVE REGION	COORDINATES	GROUP*	TYPE**	BURST TIME
May 5, 1979	McM. 15999	N00 W22	K	B,Q	
May 16, 1981	AR 3106/7	N12 E14	K	Q	
May 17, 1981	AR 3106/7	N12 E01	K	Q	
May 18, 1981	AR 3106/7	N12 W13	K	Q	
May 19, 1981	AR 3106/7	N12 W26	K	Q	
June 13, 1981	AR 3159	S26 E44	LW	Q	
June 14, 1981	AR 3159	S26 E32	LW	Q	
June 15, 1981	AR 3159	S26 E19	LW	Q	
June 16, 1981	AR 3159	S26 E07	LW	Q	
July 12, 1982	AR 3804	N13 E35	LW	Q	
				B	1531-1532
				B	1905-1909
				B	1905-2007
July 13, 1982	AR 3804	N13 E21	LW	Q	
July 19, 1982	AR 3804	N09 W64	LW	Q	
			LW	B	1841-1843
July 20, 1982	AR 3804	N11 W77	LW	Q	
				B	2149-2151
				B	2310-2312
July 28, 1982	AR 3828	N06 E27	LW	Q	
March 6, 1983	—	S16 W13	K	Q	
March 7, 1983	—	S14 W21	K	Q	
May 1, 1983	AR 4154	S14 W24	K	Q	
May 2, 1983	AR 4165	?	K	Q	
May 2, 1983	AR 4154	S14 W37	K	Q	
Jan. 28, 1984	AR 4398	N14 W11	LW	Q	
Jan. 28, 1984	AR 4398	N14 W24	LW	Q,	B 1820-1850
May 30, 1984	AR 4500		GH	Q	
June 4, 1984	AR 4508	N06 E57	LW	Q	
July 8, 1984	AR 4532	S07 E18	LW	Q	
July 14, 1984	AR 4537	S06 E12	LW	Q	
July 15, 1984	AR 4539	S09 W23	LW	Q	
June 7, 1985	AR 4663	N01 E65	LW	Q	
June 7, 1985	AR 4663	N01 E52	LW	Q	

*K denotes observations by Kundu's group, GH delineates an eclipse observation by Gary and Hurford, and LW describes the VLA observations of coronal loops by Lang and Willson.

**Q denotes a quiescent, or non-flaring, coronal loop and B denotes a bursting one.